Science of the Total Environment 950 (2024) 175280

Contents lists available at ScienceDirect

Science of the Total Environment

journal homepage: www.elsevier.com/locate/scitotenv

Impacts of atmospheric particulate matter deposition on phytoplankton: A review

Vignesh Thiagarajan [a], Theodora Nah [a,*], Xiaying Xin [b,**]

[a] School of Energy and Environment and State Key Laboratory of Marine Pollution, City University of Hong Kong, Hong Kong
[b] Beaty Water Research Centre, Department of Civil Engineering, Queen's University, Kingston, Ontario K7L 3N6, Canada

HIGHLIGHTS

- Impacts of various classes of atmospheric species on phytoplankton were reviewed.
- Marine ecosystems received greater attention than freshwater ecosystems.
- Atmospheric deposition to surface waters exerts different effects on phytoplankton.
- Positive effects on phytoplankton reported for N, P, and Fe.
- Toxic effects on phytoplankton by other trace metals (Cu, Al, and Zn).

GRAPHICAL ABSTRACT

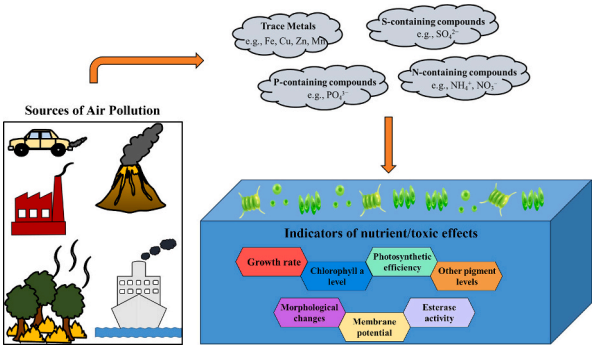

ARTICLE INFO

Editor: Fernando Pacheco

Keywords:
Atmospheric deposition
Nitrogen
Phosphorus
Phytoplankton
Sulfur
Trace metals

ABSTRACT

In many rapidly urbanizing and industrializing countries, atmospheric pollution causes severe environmental problems and compromises the health of humans and ecosystems. Atmospheric emissions, which encompass gases and particulate matter, can be transported back to the earth's surface through atmospheric deposition. Atmospheric deposition supplies chemical species that can serve as nutrients and/or toxins to aquatic ecosystems, resulting in wide-ranging responses of aquatic organisms. Among the aquatic organisms, phytoplankton is the basis of the aquatic food web and is a key player in global primary production. Atmospheric deposition alters nutrient availability and thus influences phytoplankton species abundance and composition. This review provides a comprehensive overview of the physiological responses of phytoplankton resulting from the atmospheric deposition of trace metals, nitrogen-containing compounds, phosphorus-containing compounds, and sulfur-containing compounds in particulate matter into aquatic ecosystems. Knowledge gaps and critical areas for future studies are also discussed.

* Correspondence to: T. Nah, School of Energy and Environment and State Key Laboratory of Marine Pollution, City University of Hong Kong, Kowloon, Hong Kong.
** Correspondence to: X. Xin, Beaty Water Research Centre, Department of Civil Engineering, Queen's University, Kingston, Ontario K7L 3N6, Canada.
E-mail addresses: theodora.nah@cityu.edu.hk (T. Nah), x.xin@queensu.ca (X. Xin).

https://doi.org/10.1016/j.scitotenv.2024.175280
Received 16 May 2024; Received in revised form 1 August 2024; Accepted 2 August 2024
Available online 8 August 2024

1. Introduction

Air pollution is known to have adverse effects on human and ecosystem health. Air pollutants are a complex mixture of gases and particulate matter (PM) that constantly interact with each other and other atmospheric constituents (Seinfeld and Pandis, 2016). Common gas-phase air pollutants include nitrogen oxides (NO_x), sulfur dioxide (SO_2), carbon monoxide (CO), ammonia (NH_3), volatile organic compounds (VOCs), and ozone (O_3). PM, defined as solid particles or liquid droplets suspended in the air, are emitted directly into the atmosphere or formed through complex atmospheric chemical reactions. The PM composition comprises nitrate (NO_3^-), sulfate (SO_4^{2-}), ammonium (NH_4^+), trace metals, as well as elemental and organic forms of carbon (C) (Fuzzi et al., 2015).

Atmospheric deposition is the primary process through which atmospheric gases and PM enter aquatic ecosystems (e.g., lakes, rivers, and oceans). Although atmospheric deposition introduces a variety of essential nutrients into aquatic ecosystems, it also poses a major threat to these ecosystems since it can cause acidification, eutrophication, and bioaccumulation of toxic substances (Greaver et al., 2012; Grennfelt and Hultberg, 1986). The volume and composition of chemical species deposited determine whether their effects on the aquatic ecosystem will be beneficial or detrimental. The toxic potential of the deposited chemical species is governed by its properties, including its inherent toxicity, environmental persistence, interaction with other chemical species, bioaccumulation, and transformation after its deposition into water (Swackhamer et al., 2004). On the other hand, the nutritional role of a chemical species is determined by the nutrient limitation conditions and demand of the aquatic ecosystem (Thomas and Cebrian, 2008).

The monitoring of air pollutant emissions, concentrations in ambient air, and deposition are typically performed separately from the monitoring of the health of aquatic ecosystems. This has led to gaps in our understanding on how the deposition of air pollutants affects aquatic ecosystems. Establishing stronger links between atmospheric deposition and its effects on aquatic ecosystems can help fill these knowledge gaps (Wright et al., 2018). This can be achieved by investigating the impacts of atmospheric deposition on bioindicators. Bioindicators are organisms, species, or biological communities that are used to assess the quality of the environment based on their presence, abundance, and physical conditions in natural ecosystems or through toxicity testing in the laboratory (Da Silva Souza et al., 2014). Phytoplankton is a ubiquitous bioindicator that is commonly used to provide insights into the impacts of pollutants and nutrients in aquatic ecosystems (Zaghloul et al., 2020). Phytoplankton are photosynthetic, microscopic plants that form the basis of the aquatic food chain. Phytoplankton communities are highly diverse and include tens of thousands of species. They are responsible for most of the Earth's primary productivity and rely on nutrients in open waters to survive (Maberly et al., 2022). The nutrients in the shortest supply relative to cellular requirements limit primary productivity in the aquatic ecosystem. Nutrients such as nitrogen (N) and phosphorus (P) are typically recognized as growth-limiting nutrients in aquatic ecosystems (Mahowald et al., 2018; Rabalais, 2002). However, when these nutrients are in excess, phytoplankton biomass and productivity may change to the point where they have a variety of ecological consequences. Phytoplankton communities respond to changes in nutrient levels by adjusting species composition, either decreasing the abundance of sensitive taxa or increasing the abundance of tolerant taxa (Carstensen and Heiskanen, 2007). Their ability to respond to changes in nutrients (and toxins) make phytoplankton a good bioindicator for investigations of the impacts of atmospheric deposition on the health and productivity of the aquatic ecosystem.

Atmospheric deposition introduces a variety of chemical species into aquatic ecosystems. The introduction of these chemical species will impact biogeochemical cycles and alter the primary productivity of aquatic ecosystems. While there have been previous reviews on the impacts of atmospheric deposition on phytoplankton, they tend to focus on specific topics and/or a single class of chemical species. For instance, Hessen (2013) focused on the effects of inorganic N deposition on the productivity of phytoplankton in lakes. Mahowald et al. (2018) focused on PM metal deposition and its short-term impacts on marine biota, while Yang et al. (2019) examined the effects of PM copper (Cu) on marine phytoplankton. A recent review by Zak et al. (2021) summarized the direct and indirect ecotoxicological effects of SO_4^{2-} on freshwater aquatic organisms. While some reviews have collectively focused on the impacts of two or more classes of compounds (e.g., N, P, and iron (Fe)) on marine productivity (Jickells and Moore, 2015; Kanakidou et al., 2018), they did not consider the roles and impacts of other ubiquitous atmospheric chemical species, such as other trace metals, and S-containing compounds on phytoplankton. Moreover, those reviews focused mainly on the biogeochemical cycling of the atmospheric chemical species, instead of the physiological responses underlying their nutritional and/or toxic effects on phytoplankton.

This review aims to provide a comprehensive summary of the depositional effects of different ubiquitous atmospheric PM chemical species (trace metals, N-containing compounds, P-containing compounds, and S-containing compounds) on phytoplankton in oceans and lakes. It discusses in detail the various physiological responses of phytoplankton when they are exposed to the forementioned chemical species. All the chemical species discussed in this review are important classes of atmospheric PM chemical species that are commonly deposited into aquatic ecosystems, especially in coastal zones where the ocean, atmosphere, and land meet. The review is organized as follows: Section 2 summarizes how atmospheric PM are typically classified and discusses the classes of ubiquitous chemical species in atmospheric PM that will be the focus of this review. Included in this section are discussions about their major emission sources and previously reported ambient concentrations. Section 3 discusses the different factors governing the atmospheric deposition process and summarizes the deposition fluxes reported for the forementioned chemical species. Section 4 discusses the physiological effects of phytoplankton when they are exposed to these classes of chemical species during deposition. Lastly, Section 5 discusses current knowledge gaps and suggests future studies that can be done to address these gaps.

2. Atmospheric PM

Anthropogenic activities and natural processes emit different compounds in the form of gases and PM into the atmosphere. Important anthropogenic sources include the transportation, industrial, and domestic sectors, almost all of which utilize combustion processes for energy generation. Important non-combustion-related anthropogenic sources include road dust and PM generated during the wear and tear of vehicle parts (Piscitello et al., 2021; Thorpe and Harrison, 2008). Important natural sources include emissions from volcanoes, wildfires, wind-blown minerals, sea sprays, and trace gas emissions from soils and oceans (Fuzzi et al., 2015). Regardless of the nature of their sources (anthropogenic or natural), atmospheric PM can be categorized as either primary or secondary. Primary PM are released directly into the atmosphere from a source, whereas secondary PM are formed in the atmosphere from chemical reactions.

Vehicular emissions constitute a major anthropogenic PM source in urban areas (Fuzzi et al., 2015; Karagulian et al., 2015; Molina, 2021). Although vehicular exhaust emissions have long been recognized as the main source of PM (Pant and Harrison, 2013; Platt et al., 2017), non-exhaust vehicular emissions arising from the abrasion of brakes and tires, road surface wear and resuspension of road dust also contribute substantially to PM (Harrison et al., 2012; Thorpe and Harrison, 2008; Zhang et al., 2020). Biomass burning is another major contributor to atmospheric PM. Anthropogenic activities are responsible for around 90 % of biomass burning and include slash-and-burn agriculture, open burning of agricultural waste, and domestic wood burning for cooking and heating (Bhattarai et al., 2019). Mineral dust, which can originate

from anthropogenic (e.g., agriculture, deforestation, traffic on dirt roads) and natural (e.g., desert storms) sources, is another important contributor to PM. Particularly during dust storms, large amounts of mineral dust are released into the atmosphere (Miller-Schulze et al., 2015).

One of the most important factors affecting how long PM remains in the atmosphere and how much is deposited into water bodies is its aerodynamic size. The aerodynamic size of PM can range from <1 μm to larger than 100 μm. Coarse PM ($PM_{10–2.5}$) have aerodynamic diameters of 2.5 to 10 μm, while fine PM ($PM_{2.5}$) have aerodynamic diameters smaller than 2.5 μm. The atmospheric residence time of $PM_{10–2.5}$ is short, ranging from minutes to hours, and their transport distances typically range from 1 to 10 km (Zeb et al., 2022). PM larger than 10 μm are also present in the atmosphere, but they have shorter residence times due to their larger size and rapid removal. Compared to $PM_{10–2.5}$, $PM_{2.5}$ remains airborne for extended periods (days to weeks) and can be transported over longer distances before their deposition.

Trace metals, NO_3^-, NH_4^+, SO_4^{2-}, and phosphates (PO_4^{3-}) are commonly identified chemical species in PM. Trace metals account for a relatively small portion of PM (typically <1 %). Still, they are ecologically interesting due to their biological importance and nutritional (or toxic) characteristics (Mukhtar and Limbeck, 2013). NH_4^+, NO_3^-, and SO_4^{2-} are the three most abundant inorganic constituents of $PM_{2.5}$ (Pöschl, 2005), and they are produced by multiphase reactions involving gas-phase NH_3, NO_x, and SO_2, respectively (Seinfeld and Pandis, 2016). At environmentally relevant concentrations, NO_3^- promotes metabolism and growth in increasingly N-enriched waters rather than directly causing toxicity (Glibert et al., 2016). SO_4^{2-} influences the biogeochemical processes of C, N, and P in addition to potentially inducing toxic effects on some aquatic species (Zak et al., 2021). PO_4^{3-}, a growth-limiting nutrient in marine ecosystems, is essential for phytoplankton growth (Lin et al., 2016). The main sources, concentrations, and distribution of these PM constituents are discussed below.

2.1. Trace metals

Different technical terms have been used to define trace metal species in PM, cloud water, rainwater, and seawater. Thus, Meskhidze et al. (2019) recommended that the atmospheric and oceanic science communities adopt consistent definitions based on operationally determined forms of trace metals. Trace metals retained by a 0.2 μm membrane filter and gravitationally settled are referred to as particulate trace metals. Trace metals that penetrate a 0.2 μm membrane filter, those that penetrate a 0.02 μm membrane filter, and those that penetrate a 0.2 μm but are retained by a 0.02 μm membrane filter are referred to as dissolved, soluble, and colloidal trace metals, respectively (Al-Abadleh et al., 2022). Trace metals in PM originate from both natural and anthropogenic sources. Large concentrations of Cu, Fe, aluminum (Al), cadmium (Cd), cobalt (Co), lead (Pb), manganese (Mn), nickel (Ni), and zinc (Zn) originate from natural sources, which are dominated by volcanic emissions, wildfires, and wind-borne mineral dust (Hoffmann et al., 2012; Isley and Taylor, 2020; Prospero et al., 2002). Large concentrations of arsenic (As), chromium (Cr), Mn, Pb, selenium (Se), and vanadium (V) originate from anthropogenic sources, which include fossil fuel combustion, vehicular non-exhaust emissions (e.g., Zn), and dust dispersion from metal processing (Lazo et al., 2019; Maciejczyk et al., 2021; Nawrot et al., 2020). Measurements from the Global Atmospheric Passive Sampling (GAPS) and GAPS Megacities (GAPS-MC) networks showed that the highest concentrations of total trace metals were found in Mendoza Province, Argentina (82.7 μg m^{-3}), followed by New Delhi, India (51 μg m^{-3}), while the lowest concentrations (0.425 μg m^{-3}) were found in Pallas, Finland (Mastin et al., 2023). Fe and Al are the most abundant trace metals in atmospheric PM, with average concentrations of 4.63 μg m^{-3} and 3.4 μg m^{-3}, respectively, due to their prevalence in the Earth's crust and soil resuspension in rural areas (Mahowald et al., 2018; Mastin et al., 2023). This is followed by non-crustal trace metals such as Zn and Pb, which are mostly emitted from urban anthropogenic activities (Hien et al., 2022; Liu et al., 2020a).

Trace metals in PM are mostly emitted into the atmosphere in water-insoluble, particulate forms, which subsequently undergo atmospheric processing (e.g., acid processing, metal-organic complexation reactions, photoreduction) to convert them to water-soluble (dissolved, soluble, colloid) forms (Chen and Grassian, 2013). There are differences in the size distribution and water-soluble fractions of trace metals in PM from anthropogenic and natural sources. Trace metals originating from natural sources are mostly present in coarse PM and have low solubility, while trace metals from anthropogenic sources are usually in fine PM and have higher solubility (Jiang et al., 2014; Yang et al., 2023). The mass concentrations of water-soluble metals are usually higher in fine PM than in coarse PM. This is due to the large quantities of acidic inorganic species that promote acid processing and organic species that serve as organic ligands present in fine PM that enhance metal solubility (Fang et al., 2017; Tao and Murphy, 2019; Yang et al., 2023). Factors that influence the solubility of metals in aquatic waters include source composition (Aguilar-Islas et al., 2010; Buck et al., 2010), metal mineralogy (Journet et al., 2008), atmospheric deposition processes (wet vs. dry deposition) (Srinivas and Sarin, 2013), PM aging during long-distance transport, and in-cloud dissolution during which PM form cloud condensation nuclei and dissolve into the liquid phase (Bianco et al., 2017). The geochemical processes involved in the atmospheric deposition of trace metals to surface waters vary. Dry deposition occurs continuously, with the PM deposition rates governed by PM size and the solubility of trace metals influenced by the interaction of PM with surface waters. In contrast, wet deposition removes trace metals that are more prevalent in $PM_{2.5}$ and exhibit higher solubility. This is due to the low pH of rainwater, which can solubilize trace metals before they reach the water surface, making the dissolved fractions of trace metals readily available to phytoplankton. The solubility of trace metals in wet deposition is governed by the interaction between PM and rainwater (Chester et al., 1999).

2.2. N-containing compounds

Inorganic NH_4^+ makes up a substantial fraction of N-containing compounds in fine PM. It is usually present in the forms of ammonium nitrate (NH_4NO_3) and ammonium sulfate ($(NH_4)_2SO_4$) in fine PM. NH_4NO_3 and $(NH_4)_2SO_4$ are formed from multiphase reactions of NH_3 with nitric acid (HNO_3) and sulfuric acid (H_2SO_4), respectively (Seinfeld and Pandis, 2016). $(NH_4)_2SO_4$ and NH_4NO_3 account for 20 to 80 % of fine PM (Zhang et al., 2007). Agricultural activities such as fertilizer application, livestock waste, and biomass burning account for over 80 % of the global emissions of NH_3 (Van Damme et al., 2021). Regions with intensive agriculture, such as the Indo-Gangetic plains in India, the North China Plain in China, the US Midwest, and pastoral lands in Europe, have been identified as hotspots of NH_3 emissions (Nair and Yu, 2020). In urban areas where agricultural activities are mostly absent, non-agricultural sources such as vehicular exhaust, power plants, and industries contribute to NH_3 emissions (Fenn et al., 2018; Kuttippurath et al., 2020; Wu et al., 2020). Based on results from the Laboratoire de Météorologie Dynamique general circulation model (LMDz) coupled with the Interactions with Chemistry and Aerosols (INCA) model, the annual mean surface concentrations of inorganic NH_4^+ are 1 to 2 μg m^{-3} across the eastern and central US, 2 to 3 μg m^{-3} in northern Europe, and 4 to 5 μg m^{-3} in northern China (Hauglustaine et al., 2014). The aforementioned regions have not only high concentrations of SO_4^{2-} and HNO_3 but also high emissions of NH_3 from agricultural activities.

Another substantial fraction of N-containing compounds in PM is in the form of NO_3^-. Inorganic NO_3^- is an important chemical component of fine PM (Zhang et al., 2007). It is mainly formed in the atmosphere via the chemical oxidation of NO_x (= nitrogen oxide (NO) + nitrogen dioxide (NO_2)), involving homogeneous gas-phase oxidation and heterogeneous hydrolysis. Although NO_x emissions can be from natural

sources (e.g., lightning, soil, wildfires), a substantial fraction of NO_x emissions come from anthropogenic activities, particularly combustion-related processes (Butler et al., 2020; Hu, 2021; Song et al., 2019). Urban areas with intensive anthropogenic activities are hotspots for NO_x emissions compared to rural areas. About 90 to 95 % of the NO_x is usually emitted as NO. During the day, NO_x in the atmosphere rapidly cycles between NO and NO_2 via different photochemical reactions (Seinfeld and Pandis, 2016). This cycling between NO and NO_2 is several orders of magnitude higher than the oxidation rate of NO_x to form NO_3^- (Xin et al., 2023). NO_2 formed during the daytime is oxidized by hydroxyl radicals (•OH) to produce HNO_3, which then reacts with NH_3 to form particulate inorganic NO_3^- (Seinfeld and Pandis, 2016). At night, nitrogen pentoxide (N_2O_5) formed through the reversible reaction between NO_2 and nitrate radicals (NO_3•) reacts with the wet surfaces of PM to yield particulate inorganic NO_3^- (Brown and Stutz, 2012; Ravishankara, 1997). Inorganic NO_3^- is an increasingly important PM component in regions with significant reductions in SO_2 emissions, slight reductions in NO_x, and stable NH_3 concentrations (Bauer et al., 2007; Heald et al., 2012). Such asynchronous reduction of air pollutants has increased the contributions of inorganic NO_3^- to PM, especially in urban areas (Wang et al., 2018; Zou et al., 2018). This is clearly demonstrated in urbanized regions in China, where the increasing NO_3^- concentration was found to be primarily due to decreased SO_2 emissions, enhanced atmospheric oxidation capacity, and reduced NO_3^- deposition (Xie et al., 2022). Xie et al. (2022) found that reducing NH_3 emissions was the most effective strategy for reducing NO_3^- pollution in China. There have been some studies on the future total N deposition in China. They suggested that future emission controls such as reductions in the NO_x, SO_2, and VOC emissions could effectively reduce oxidized N (e.g., NO_3^-, NO_2^-) deposition while slightly decreasing reduced N deposition by 2030 (Liu et al., 2022; Zhu et al., 2022). However, in domestic regions of China with higher agricultural NH_3 emissions, the decrease in NO_x and SO_2 emissions could enhance reduced N dry deposition, thereby diminishing the effectiveness of NH_3 emission control (Zhu et al., 2022).

Using the Goddard Institute for Space Studies (GISS) general circulation model, Bauer et al. (2007) determined that the mean surface concentrations of inorganic NO_3^- are 1.5 μg m^{-3} in the most polluted regions, such as East China and Europe. Their model showed that the inorganic NO_3^- concentrations would climb to as high as 3 μg m^{-3} by 2030. The predictions for NO_3^- concentrations in 2030 were based on anticipated future changes. The authors predicted that the increasing emissions of NH_3 could potentially have a more significant impact on increasing NO_3^- concentration compared to changes in the emissions of NO_x and SO_2. However, there are several uncertainties associated with these projections, including the implementation of new clean air policies, climate change, and future changes in land use and population densities. These uncertainties will also complicate projections of N deposition trends.

Organic NO_3^- can be classified as primary or secondary. Biomass burning and fossil fuel combustion are mostly responsible for the direct emissions of organic NO_3^- (Lin et al., 2021). Organic NO_3^- can also be formed in the atmosphere through oxidation reactions between VOCs and •OH in the presence of NO_x during the daytime and through nighttime oxidation reactions between VOCs and NO_3• (Brown and Stutz, 2012; Li et al., 2022). If the organic NO_3^- compounds formed from these gas-phase reactions have sufficiently low vapor pressure, they will partition into the particulate phase to form particulate organic NO_3^- (Ng et al., 2017). Many studies have found larger contributions of organic NO_3^- to secondary organic PM at night compared to the daytime (Fry et al., 2013; Huang et al., 2019; Rollins et al., 2012). Organic NO_3^- is an effective sink and reservoir of NO_x, thus facilitating its long-range and vertical transport through the troposphere. The mass yields of organic NO_3^- from NO_3•-mediated oxidation are typically substantially higher than from •OH-mediated oxidation of VOCs (Ng et al., 2017). Model simulations using the Goddard Earth Observing System-Chemistry (GEOS-Chem) revealed that the global mean surface concentration of organic NO_3^- is 0.47 μg m^{-3}. Regions affected by anthropogenic sources and biomass burning had the highest organic NO_3^- concentrations, whereas remote oceanic areas had the lowest concentrations of organic NO_3^- (Li et al., 2023).

2.3. S-containing compounds

Most S-containing compounds in PM are in the form of SO_4^{2-}. Inorganic SO_4^{2-} constitutes a major mass fraction of atmospheric fine PM (Zhang et al., 2007). Inorganic SO_4^{2-} is mainly formed in the atmosphere via gas-phase and aqueous-phase oxidation reactions of SO_2, the main S-containing gas-phase compound emitted into the atmosphere. Anthropogenic sources contribute 98 % of global SO_2 emissions. Over 65 % of global SO_2 emissions come from industrial and power generation sources (Zhong et al., 2020). Volcanic eruptions are a major natural source of SO_2 (Heaviside et al., 2021). Besides direct emission, SO_2 is also formed in the atmosphere by •OH-mediated and NO_3•-mediated oxidation of dimethyl sulfide ($(CH_3)_2S$) (Veres et al., 2020). The formation of inorganic SO_4^{2-} from gas-phase oxidation involves the reaction of SO_2 with •OH, whereas the aqueous-phase oxidation of SO_2 involves oxidation reactions with dissolved O_3, hydrogen peroxide, and NO_2 with transition metal ions as catalysts (Gao et al., 2022; Liu et al., 2020b). SO_2 dissolves into cloud droplets, which serve as a reaction medium to convert dissolved SO_2 to SO_4^{2-} (Ye et al., 2023). In addition to its formation in the atmosphere, particulate inorganic SO_4^{2-} can be emitted directly into the atmosphere from sources such as residential coal combustion, sea spray, soil, and shipping activities (Dai et al., 2019; Dominguez et al., 2008; Li et al., 2020; Moon et al., 2023). Based on the LMDz-INCA model, the surface inorganic SO_4^{2-} concentrations are 4 to 5 μg m^{-3} over the eastern US, eastern and southern Europe, and China (Hauglustaine et al., 2014). The contribution of inorganic SO_4^{2-} to fine PM has decreased in many countries (e.g., China, USA) due to air quality regulations implemented to reduce SO_2 emissions. For instance, since the implementation of China's Air Pollution Prevention and Control Action Plan in 2013, the SO_2 concentration has decreased from 14.1 ± 8.2 ppbv in 2013 to 5.5 ppbv in 2017, and the corresponding SO_4^{2-} concentration in urban Beijing showed a decline from 10.1 ± 14.6 μg m^{-3} in 2013 to 4.2 ± 6.2 μg m^{-3} in 2017 (Wang et al., 2020).

Organic S-containing compounds are typically present in PM as organosulfates, sulfoxides, sulfonates, and sulfones (Jiang et al., 2022). Organosulfates are the most abundant class of organic S compounds in atmospheric PM. As previously reviewed by Brüggemann et al. (2020) and Fan et al. (2022), a variety of multiphase reaction pathways can lead to organosulfate formation, including photochemical reactions of different VOCs in the presence of particulate SO_4^{2-}, SO_4^{2-} esterification reactions, reactions driven by sulfoxy radical anions, and heterogeneous reactions of SO_2 with unsaturated organic compounds. Most organosulfates have low volatilities; thus, they are mostly present in PM. Organosulfates have been detected in a variety of locations, including polar, urban, rural, and marine environments, due to interactions between anthropogenic and biogenic emissions during long-range transport (Glasius et al., 2022; Hawkins et al., 2010; Lukács et al., 2009; Meng et al., 2018). However, the concentrations of organosulfates are location-dependent. The total concentrations of organosulfates in the Antarctic and Arctic have been reported to be 47 to 260 ng m^{-3} and 46 to 670 ng m^{-3}, respectively (Ye et al., 2021). In contrast, areas with large isoprene emissions (e.g., southeastern USA) can have total mean organosulfate concentrations reaching 1000 ng m^{-3} (Brüggemann et al., 2020).

2.4. P-containing compounds

P-containing compounds are predominantly found in the particulate form due to their low volatilities. Both natural (e.g., desert dust, sea spray, bioaerosols, and volcanic ash) and anthropogenic (e.g., fossil fuel combustion, biomass burning, agricultural activities) sources contribute

to atmospheric P. Several modeling studies have attempted to identify the major sources of atmospheric P. According to Mahowald et al. (2008), desert dust is a major emission source, accounting for 1.15 Tg yr^{-1} (>82 %) of the global P emissions. However, Wang et al. (2015b) reported that previous calculations of the global budget of atmospheric P were unbalanced, with global deposition exceeding the emissions of 1.39 Tg yr^{-1} estimated by Mahowald et al. (2008). The model calculations performed by Wang et al. (2015b) showed that combustion-related emissions represented >50 % (1.8 Tg yr^{-1}) of the global P emissions. They also estimated that the total global P emission was 3.5 Tg yr^{-1}, thus resulting in a depositional sink of 0.8 Tg yr^{-1} to oceans and 2.7 Tg yr^{-1} to land. These two studies highlight some of the uncertainties underlying the estimates of P emissions since they can differ drastically depending on the model assumptions. Regarding surface concentrations, mineral dust in the major dust regions contributes 0.1 to 1 μg m^{-3} of atmospheric P, while biomass burning emissions in Asian and central African countries contribute concentrations ranging from 10 to 100 ng m^{-3} (Myriokefalitakis et al., 2016).

Historically, organic P has not been studied as well as inorganic P. The contributions of organic P to global emissions are estimated to be 0.13 Tg yr^{-1} (Kanakidou et al., 2012). Anthropogenic and natural sources, including bioaerosols, biomass burning, dust, sea salt, and agricultural activities, contribute to atmospheric organic P (Myriokefalitakis et al., 2016; Violaki et al., 2018). According to Violaki et al. (2018), bioaerosols are the dominant source of atmospheric organic P. Bioaerosols are composed of cellular materials of microorganisms (e.g., algae, bacteria, fungi, moss) and plants (e.g., pollen). Some of the organic P-containing compounds in bioaerosols include inositol PO_4^{3-}, sugar PO_4^{3-}, phosphoamides, phospholipids, and phosphoproteins (Karl and Björkman, 2015; Myriokefalitakis et al., 2016). Anthropogenic sources release organic P-containing compounds, especially in the form of organophosphate esters. Organophosphate esters are synthetic organic compounds that are used as plasticizers, flame retardants, combustion engine fuel additives, antifoam agents, and pesticides in the construction, electronics, textiles, transportation, and manufacturing industries (Fabiańska et al., 2019). They are released into the atmosphere via volatilization, leaching, and abrasion. Urban areas are a hotspot for organophosphate ester emissions. The highest ambient air concentrations of organophosphate esters are found in New York, USA (15,100 pg m^{-3}), and London, UK (14,100 pg m^{-3}), with the lowest concentrations observed in Kolkata, India (464 pg m^{-3}) (Saini et al., 2020). The organic P concentrations in PM in coastal areas range from 0.01 to 30 ng m^{-3} (Kanakidou et al., 2012).

3. Atmospheric deposition processes

Atmospheric deposition is the process whereby atmospheric PM (and gases) move from the atmosphere to the earth's surface. Fig. 1 shows a schematic of the two types of atmospheric deposition processes: wet deposition and dry deposition. Wet deposition is a natural process by which atmospheric PM (and gases) are scavenged by atmospheric water droplets (e.g., clouds, rain, and snow) and deposited onto the earth's surface. Wet deposition involves two scavenging processes for precipitation: rainout (in-cloud scavenging) and washout (below-cloud scavenging) (Seinfeld and Pandis, 2016). The effectiveness of wet deposition depends foremost on the availability of precipitation locally. The wet deposition of atmospheric chemical species mainly depends on their water solubility, as characterized by their Henry's Law constants. The chemical composition of PM is diverse, with the number of chemical species in PM likely in the thousands (Zhang et al., 2007). Each chemical species within PM exhibit different water solubilities, thus they will be scavenged by atmospheric water droplets at different efficiencies. Additionally, some of these chemical species (e.g., trace metals, as discussed above) exhibit PM-size dependent solubility (Yang et al., 2023). Dry deposition is a slower and more incessant process that removes PM (and gases) from the atmosphere by a variety of mechanisms that include gravitational sedimentation, turbulent diffusion, Brownian motion, interception, inertial forces, electrical migration, diffusiophoresis, and thermophoresis (Seinfeld and Pandis, 2016). PM with aerodynamic diameters >5 μm are mostly deposited by gravitational sedimentation and inertial impaction. However, both processes are less effective for the deposition of PM with smaller aerodynamic diameters due to their lower fall speeds and momentum. PM with sizes ranging from 0.2 to 2 μm can travel long distances in the atmosphere before being deposited (Lovett, 1994). Gases, on the other hand, are deposited mostly through turbulent diffusion and Brownian motion (Pacyna,

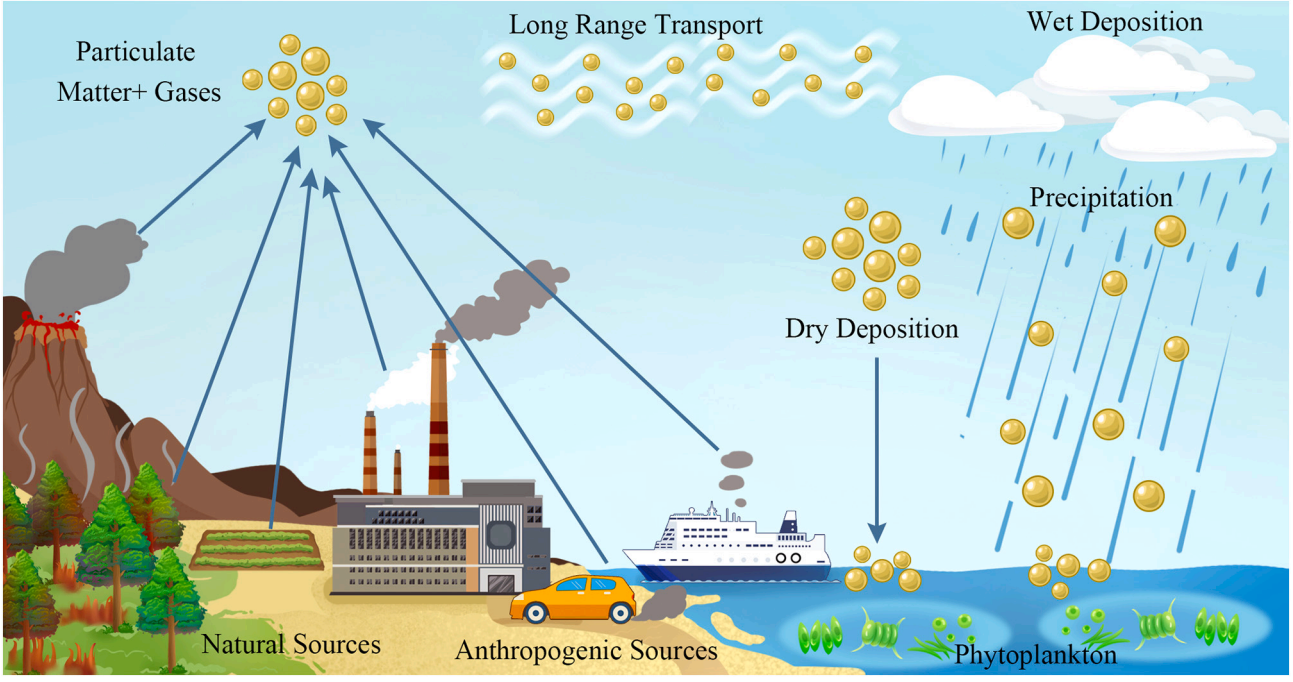

Fig. 1. Schematic illustration of atmospheric emission sources and deposition processes.

2008).

The deposition rates/fluxes to oceans vary for different atmospheric chemical species. Trace metal depositions to oceans show spatiotemporal variations, especially in marginal seas, which are more affected by the long-range transport of contaminants from continental areas than open oceans. By extrapolating measurement data, Duce et al. (1991) estimated the global atmospheric PM trace metal fluxes to oceans to be in the range of 0.01 Tg yr^{-1}, 0.0004 to 0.0007 Tg yr^{-1}, 0.002 to 0.007 Tg yr^{-1}, 0.014 to 0.017 Tg yr^{-1}, 0.011 to 0.06 Tg yr^{-1}, and 0.0013 to 0.0029 Tg yr^{-1} for Pb, Cd, Cu, Ni, Zn, and As, respectively. Zhang et al. (2015) used the Community Earth System model and computed the deposition fluxes of total Mg, Mn, and Fe associated with mineral dust to oceans to be 2.83 Tg yr^{-1}, 109.89 Gg yr^{-1}, and 6.10 Tg yr^{-1}, respectively.

Observational and modeling predictions have primarily focused on the atmospheric deposition of Fe, with less emphasis on other trace metals. Table 1 summarizes the reported atmospheric deposition fluxes of Fe to oceans along with their associated uncertainties. Duce et al. (1991) reported the first estimate of Fe deposition flux from mineral dust to oceans, 32 Tg yr^{-1}, with 29 Tg yr^{-1} in the particulate form and 3 Tg yr^{-1} in the soluble form. Since then, Fung et al. (2000) compiled previous dust deposition data and estimated the total Fe deposition to oceans to be 6.6 Tg yr^{-1}. Gao et al. (2001) compiled particulate Fe or dust concentrations from in situ measurements at 73 marine locations and derived a Fe deposition flux of 14 Tg yr^{-1}. Similarly, Okin et al. (2011) used estimates of desert dust and Fe deposition from previous measurements to arrive at a soluble Fe deposition flux of 0.36 Tg yr^{-1} to oceans.

Besides the forementioned observational and data compilation-based estimates, chemical transport models have been used to estimate atmospheric deposition fluxes of Fe to oceans. Modeling studies have reported a range of total Fe deposition fluxes to oceans, varying between 6 and 30 Tg yr^{-1} (Ito, 2015; Ito and Shi, 2016; Myriokefalitakis et al., 2018; Wang et al., 2015a; Zhang et al., 2015). Similarly, the soluble Fe deposition fluxes from various modeling studies ranged from 0.11 to 0.76 Tg yr^{-1} (Hamilton et al., 2020; Ito, 2015; Ito and Shi, 2016; Johnson and Meskhidze, 2013; Myriokefalitakis et al., 2018, 2015). The ranges of total and soluble Fe deposition fluxes to oceans obtained from model estimations could be attributed to the model-specific emission sources and their estimates. For instance, Myriokefalitakis et al. (2015) computed the global soluble Fe deposition flux to oceans to be 0.191 Tg yr^{-1}, which was lower than the previous estimated deposition flux of 0.26 Tg yr^{-1} (Johnson and Meskhidze, 2013). This was because the former study used a dust emission of 1091 Tg yr^{-1}, which was lower than the dust emission value (1900 Tg yr^{-1}) used in the latter study. Similarly, Wang et al. (2015a) reported larger Fe deposition resulting from coal combustion (0.455 Tg yr^{-1}) compared to the deposition value (0.14 Tg yr^{-1}) reported by Ito (2015) due to differences in the emission source estimations. Most studies have reported large uncertainties associated with emission sources. Nevertheless, mineral dust contributes the most to the deposition of total and soluble Fe to oceans (Ito, 2015; Ito and Shi, 2016; Wang et al., 2015a), with minor contributions from biomass burning and fossil fuel combustion. Myriokefalitakis et al. (2018) conducted the first model intercomparison study using four state-of-the-art global PM models (Community Atmosphere Model version 4 (CAM4), Integrated Massively Parallel Atmospheric Chemical Transport (IMPACT), GEOS-Chem, and Tracer Model 4 of the Environmental Chemical Processes Laboratory (TM4-ECPL)) and reported multi-model ensemble average Fe deposition flux values of 15 and 0.3 Tg yr^{-1} for total Fe and soluble Fe, respectively. Recently, Ito and Miyakawa (2023) used the IMPACT model and reported deposition fluxes of soluble Fe from anthropogenic, lithogenic, and pyrogenic sources to oceans to be 0.216 Tg yr^{-1}. Considering the numerous observational and modeling studies on Fe deposition to oceans, we recommend further research into the deposition fluxes of other trace metals.

Table 2 summarizes the reported atmospheric deposition fluxes of N to oceans along with their associated uncertainties. Globally, both inorganic and organic N contribute to the total N deposition to oceans. From the extrapolations of available observational data, Okin et al. (2011) estimated a total N deposition flux of 63 Tg yr^{-1} to oceans. Based on the previously available data, Duce et al. (2008) estimated the deposition flux of total N to oceans for the year 2000 to be 67 Tg yr^{-1}, which was higher than the net deposition of 39 Tg yr^{-1} reported by Jickells et al. (2017) for the year 2005. Using a global biogeochemical elemental cycling model, Krishnamurthy et al. (2007) found that the inorganic N deposition flux to oceans increased from 22 Tg yr^{-1} in the

Table 1
Summary of atmospheric deposition flux of Fe with uncertainties.

Fe form	Model/observation	Deposition flux (Tg yr^{-1})	Uncertainty	Reference
Total Fe	Extrapolation of measured Fe concentrations to areas over the ocean where measurements were not available, and the application of appropriate exchange coefficients for dry and wet deposition	32	Uncertain by a factor of 2 to 3	Duce et al. (1991)
Total Fe	Compilation of existing data	6.6	Uncertain by a factor of 10 and 100 at 10 % and 1 % solubility, respectively	Fung et al. (2000)
Total Fe	Analysis of in situ measurement data	14	Not reported	Gao et al. (2001)
Soluble Fe	Compilation of previous estimates of Fe deposition	0.36	Not reported	Okin et al. (2011)
Soluble Fe	GEOS-Chem model	0.26	Uncertainty by a factor of 5	Johnson and Meskhidze (2013)
Total Fe	Community Earth System model	6.10	Not reported	Zhang et al. (2015)
Total Fe	LMDz-INCA	8.4	Not reported	Wang et al. (2015a)
Soluble Fe	TM4-ECPL	0.191	Uncertainty of 50 %	Myriokefalitakis et al. (2015)
Total and soluble Fe	IMPACT	Total Fe: 13 Soluble Fe: 0.34	Not reported	Ito (2015)
Total and soluble Fe	IMPACT	Total Fe: 10 Soluble Fe: 0.11 to 0.12	Not reported	Ito and Shi (2016)
Total and soluble Fe	CAM4, GEOS-Chem, IMPACT, and TM4-ECPL	Total Fe: 10 to 30 Soluble Fe: 0.2 to 0.4	Not reported	Myriokefalitakis et al. (2018)
Soluble Fe	Global Earth system model	0.70–0.76	Not reported	Hamilton et al. (2020)
Soluble Fe	IMPACT	0.216	Factor of 15	Ito and Miyakawa (2023)

Table 2
Summary of atmospheric deposition flux of N with uncertainties.

N form	Model/observation	Deposition flux (Tg yr^{-1})	Uncertainty	Reference
Total organic N	Data compilation	1860: 6.1 (3.0–9.1) 2000: 20 (10−30) 2030: 23	Uncertainty of ±50 %	Duce et al. (2008)
Soluble organic N	TM4-ECPL	12.8	Uncertain by a factor of 5	Kanakidou et al. (2012)
Soluble organic N	IMPACT	10	Uncertain by a factor of 5	Ito et al. (2014)
Total soluble organic N	IMPACT	With biomass burning: 14 Without biomass burning: 12	Not reported	Ito et al. (2015)
Total and soluble organic particulate N	GEOS-Chem model	Total N: 10 Soluble N: 7.5	Simulated deposition fluxes were lower than the observed deposition fluxes by a factor of three	Li et al. (2023)
Inorganic N	Biogeochemical Elemental Cycling model	Pre-industrial: 22 1990: 39 2100: 69	Not reported	Krishnamurthy et al. (2007)
Total N	Observational based estimates	63	Uncertainty of ±25 to 50 %	Okin et al. (2011)
Total N	TM4-ECPL	39	Not reported	Jickells et al. (2017)
Inorganic N	TM4-ECPL	Pre-industrial: 20 Present: 40 Future: 35	Not reported	Myriokefalitakis et al. (2020)

pre-industrial era to 39 Tg yr^{-1} in the 1990s, with projections reaching 69 Tg yr^{-1} by 2100. Myriokefalitakis et al. (2020) reported that the present-day (2001 to 2020) atmospheric deposition flux of inorganic N to oceans was 40 Tg yr^{-1}, doubling from 19.74 Tg yr^{-1} in the pre-industrial era (1851 to 1870) due to increased NH_3 and NO_x emissions. However, future (2081 to 2100) predictions revealed a decrease in inorganic N deposition flux (35 Tg yr^{-1}) to oceans due to reductions in NO_x emissions being offset by increased NH_3 emissions.

Global estimates of total organic N deposition are highly uncertain due to the uncertainties surrounding their sources, transformation, and deposition processes. Duce et al. (2008) estimated the deposition flux of organic N to oceans for the pre-industrial era (1860), the years 2000 and 2030 to be 6.1, 20, and 23 Tg yr^{-1}, respectively. Anthropogenic emissions were reported to have a greater impact on the organic N deposition compared to biogenic emissions. The estimated range of organic N deposition flux to oceans from various models was 10 to 14 Tg yr^{-1}.

Table 3
Summary of atmospheric deposition flux of P with uncertainties.

P form	Model/observation	Deposition rate/flux	Uncertainty	Reference
Total and soluble P	Field observation	Total P: 1.4 Tg yr^{-1} Soluble P: 0.22 Tg yr^{-1}	Uncertain by a factor of 2 to 3	Graham and Duce (1979)
Total P and phosphate	MATCH	Total P: 0.558 Tg yr^{-1} Phosphate: 0.0965 Tg yr^{-1}	Large uncertainty in the emission sources	Mahowald et al. (2008)
Total and soluble organic P	TM4-ECPL	Total P: 0.43 Tg yr^{-1} Soluble P: 0.35 Tg yr^{-1}	An order of magnitude uncertainty, sources of uncertainty in emission estimates and deposition velocities	Kanakidou et al. (2012)
Total P	LMDz-INCA	0.8 Tg yr^{-1}	A 90 % confidence interval of 0.2 to 1.6 Tg yr^{-1}, uncertainties associated with atmospheric emissions and transport of P, and sample contamination	Wang et al. (2015b)
Total, dissolved, and bioavailable P	TM4-ECPL	Total P: 0.270 Tg yr^{-1} (Past), 0.281 Tg yr^{-1} (Present), 0.272 Tg yr^{-1} (Future) Dissolved P: 0.133 Tg yr^{-1} (Past), 0.169 Tg yr^{-1} (Present), 0.142 Tg yr^{-1} (Future) Bioavailable P: 0.135 Tg yr^{-1} (Past), 0.172 Tg yr^{-1} (Present), 0.144 Tg yr^{-1} (Future)	Uncertainty of about 70 % associated with present-day estimates, scarcity of observational data, and the gaps in knowledge of P emissions and fate in the atmosphere	Myriokefalitakis et al. (2016)
Total, total dissolved P and dissolved inorganic P	Critical analysis of previously published deposition rates	Bulk deposition (Total P) Geometric mean-28.6 mg m^{-2} yr^{-1} Bulk deposition (Total dissolved P) Geometric mean-9.4 mg m^{-2} yr^{-1} Bulk deposition (Dissolved inorganic P) Geometric mean-4.3 mg m^{-2} yr^{-1} Dry deposition (Total P) Geometric mean-13.7 mg m^{-2} yr^{-1} NA Dry deposition (Dissolved inorganic P) Geometric mean-2.9 mg m^{-2} yr^{-1} Wet deposition (Total P) Geometric mean-9.5 mg m^{-2} yr^{-1} Wet deposition (Total dissolved P) Geometric mean-1.1 mg m^{-2} yr^{-1} Wet deposition (Dissolved inorganic P) Geometric mean-2.9 mg m^{-2} yr^{-1}	Uncertainties are still unclear as studies are scarce	Diao et al. (2023)

Using the TM4-ECPL model, Kanakidou et al. (2012) estimated that 12.8 Tg yr^{-1} of soluble organic N in PM form was deposited into oceans. However, these estimates were reported to be underestimated when compared to available observational data, suggesting contributions from other emission sources or transformation mechanisms for soluble organic N. Ito et al. (2014) subsequently used the IMPACT model to investigate the potential anthropogenic sources of soluble organic N and their deposition to oceans. They reported that the deposition flux of soluble organic N to oceans increased from 6.7 Tg yr^{-1} in the pre-industrial era to 10 Tg yr^{-1} in the present day. Of the total deposition, 1.1 Tg yr^{-1} was from secondary oxidized organic N, 3.4 Tg yr^{-1} was from primary organic N, and 5.7 Tg yr^{-1} was from secondary reduced organic N. Recent studies have reported that biomass burning contribute the most to the deposition flux of organic N to oceans. Ito et al. (2015) found that the deposition flux of soluble organic N to oceans was higher when open biomass burning was considered (14 Tg yr^{-1}) compared to when open biomass burning was ignored (12 Tg yr^{-1}). Additionally, the estimated deposition of soluble organic N from secondary formation (1.0 Tg yr^{-1}) was nearly equal to that from primary sources (1.2 Tg yr^{-1}), which suggested that the atmospheric processing of biomass burning emissions has a significant impact on the soluble organic N deposited to oceans. Recently, using the GEOS-Chem model, Li et al. (2023) estimated the total organic N deposited to oceans to be 10 Tg yr^{-1}, with 7.5 Tg yr^{-1} in the soluble form. Biomass burning emissions contributed around 24 % of the total deposition to the ocean.

Table 3 summarizes the reported atmospheric deposition fluxes of P to oceans along with their associated uncertainties. Graham and Duce (1979) conducted the first global estimate of total P deposition flux based on observational extrapolations and reported a value of 1.4 Tg yr^{-1}, with 0.22 Tg yr^{-1} in the soluble form. Beyond observational extrapolations, three-dimensional chemistry transport models such as TM4-ECPL, LMDz-INCA, and the Model of Atmospheric Transport and Chemistry (MATCH) have been used to estimate the atmospheric deposition fluxes of P. Mahowald et al. (2008) estimated that oceans receive a global average of 0.558 Tg yr^{-1} of total P and 0.0965 Tg yr^{-1} of PO_4^{3-}. Wang et al. (2015b) estimated an oceanic depositional flux of 0.8 Tg yr^{-1} for total P. Both studies reported uncertainties related to P emissions, transport, and sample contamination. Using TM4-ECPL, Myriokefalitakis et al. (2016) refined previous models by incorporating different forms of P (total, dissolved, and bioavailable P) for their past (1850), present (2008), and future (2100) simulations. Their results showed that the oceanic deposition fluxes of total, dissolved, and bioavailable P were 0.27, 0.133, and 0.135 Tg yr^{-1}, respectively, in the past; 0.281, 0.169, and 0.172 Tg yr^{-1}, respectively, in the present; and 0.272, 0.142, and 0.144 Tg yr^{-1}, respectively, in the future. The present-day total P deposition flux reported by Myriokefalitakis et al. (2016) was about half of that estimated by Mahowald et al. (2008) and at the lower end of the range reported by Wang et al. (2015b). For dissolved P, the deposition flux reported by Myriokefalitakis et al. (2016) (0.169 Tg yr^{-1}) was 75 % higher than the estimate reported by Mahowald et al. (2008) (0.096 Tg yr^{-1}). This difference was attributed to the inclusion of P-solubilization processes and different aerosol size representations in model simulations by Myriokefalitakis et al. (2016), which affected the lifetime of airborne P-containing PM. More recently, Diao et al. (2023) compiled atmospheric P deposition rates from 2000 to 2022 (228 sites) and reported geometric mean bulk deposition rates of 28.6, 9.4, and 4.3 mg m^{-2} yr^{-1} for total P, total dissolved P, and dissolved inorganic P, respectively, in the oceanic and coastal zones. These rates were lower compared to the urban, farmland, and forest zones because of the lower levels of anthropogenic activities in the oceanic and coastal zones. Measurements of atmospheric organic P are scarce, and little has been reported about the deposition fluxes of organic P to oceans. Using TM4-ECPL simulations, Kanakidou et al. (2012) estimated the total organic P deposited to oceans to be 0.43 Tg yr^{-1}, with 0.35 Tg yr^{-1} in the soluble form.

The above-discussed deviations in the results obtained from different models and observation datasets highlight the need for a better understanding of the mechanisms controlling the emissions and transformations of atmospheric chemical species that can affect aquatic ecosystems upon their deposition. Therefore, systematic comparisons between models, as well as between observations and models, are necessary.

4. Impact of atmospheric deposition of PM on phytoplankton

Several factors determine whether the atmospheric deposition of PM will positively or negatively impact phytoplankton. These include the nature of the chemical species deposited, the deposition rate, species sensitivity, the interaction between nutrients and pollutants, and the response time (Weathers and Ponette-González, 2011). In addition to field observations, the impacts of atmospheric deposition on phytoplankton can be evaluated by bio-incubation studies conducted under controlled laboratory or field conditions (e.g., bottle incubation experiments conducted during a cruise). Fig. 2 shows the general experimental setup for bottle incubation experiments conducted under field conditions. Surface seawater is collected using acid-washed Teflon-coated bottles and filtered. The filtered seawater, along with PM and external nutrients, is transferred to acid-washed incubation bottles. Seawater samples are collected throughout the incubation periods to analyze various parameters, including nutrient levels, chlorophyll-a (chl-a) concentration, and phytoplankton identification. In bottle incubation experiments mimicking field conditions, natural phytoplankton assemblages from collected seawater are utilized, whereas laboratory incubation experiments typically use commercially available phytoplankton species. The dominant phytoplankton groups in aquatic ecosystems include diatoms, dinoflagellates, haptophytes, chlorophytes, and cyanobacteria (Simon et al., 2009). Fig. 3 shows the scanning

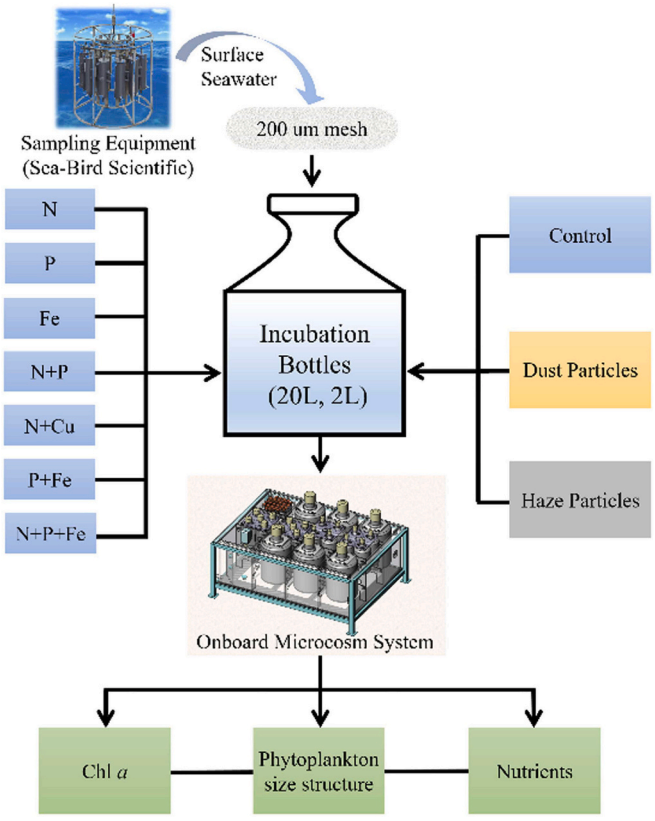

Fig. 2. Experimental setup of bottle incubation experiments (Reprinted with permission from Zhang et al. (2022)). These experiments are used to examine the response of phytoplankton under field conditions.

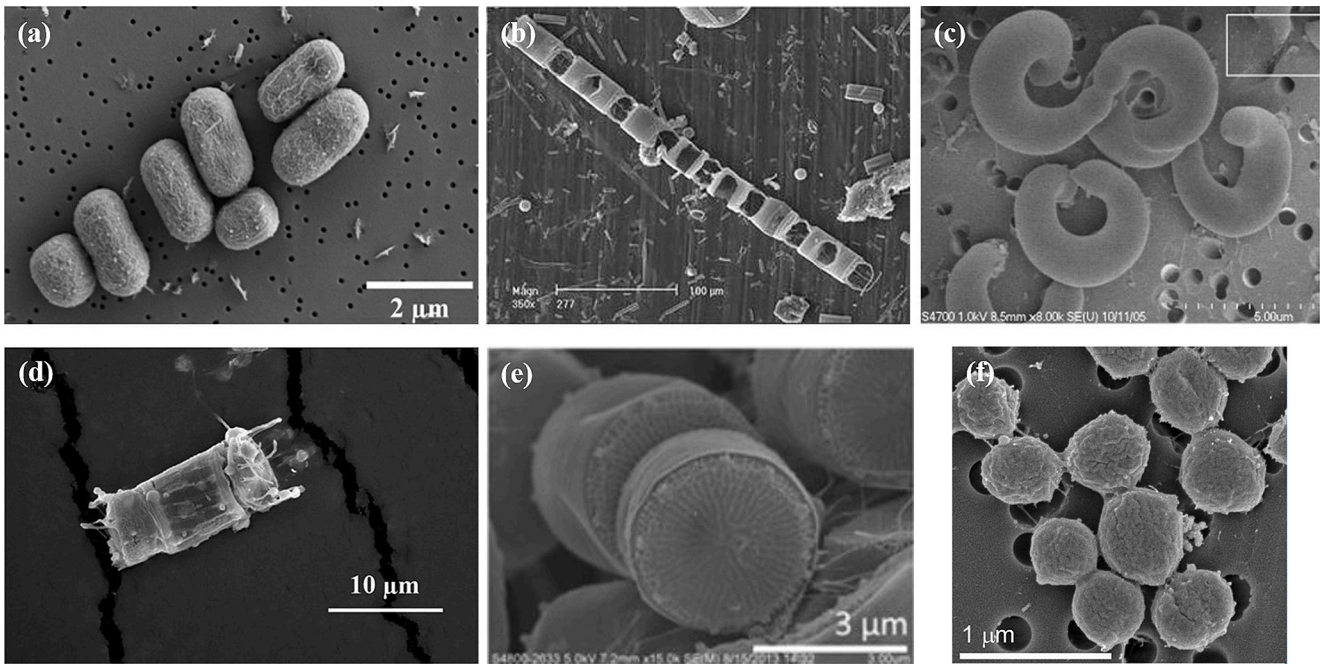

Fig. 3. Scanning electron microscopic image of (a) *Synechococcus* sp. PCC7002 (Reprinted with permission from De Oliveira et al. (2020). Copyright 2020 American Chemical Society), (b) Antarctic *Chaetoceros dichaeta* (Reprinted from Ligowski et al. (2012)), (c) *Raphidocelis subcapitata* (Reprinted with permission from Metzler et al. (2011)), (d) *Skeletonema costatum* (Reprinted with permission from Zhu et al. (2019)), (e) *Thalassiosira pseudonana* (Reprinted with permission from Yung et al. (2015)), and (f) *Prochlorococcus* strain MIT9312 (Reprinted from Johnson and Lin (2009)).

electron microscopic images of representative phytoplankton species that are typically used in incubation experiments.

Most bottle incubation studies did not jointly report the deposition fluxes of individual PM species. However, the PM concentrations used in most bottle incubation studies were largely realistic since they were based on previously reported PM deposition fluxes in the studied region. For instance, in bottle incubation studies conducted by Ridame et al. (2014) and Lagaria et al. (2017) in the northwestern oligotrophic Mediterranean Sea and the east Mediterranean Sea, respectively, the amounts of mineral dust added were based on previously reported atmospheric dust deposition. Only a few studies that investigated the impacts of individual PM species on phytoplankton jointly measured the deposition fluxes of the individual PM species in their study areas. For instance, Jordi et al. (2012) measured the dry deposition flux of Cu (11.80 µg m^{-2} d^{-1}) during their investigation of the effects of atmospheric deposition events characterized by high Cu concentrations on phytoplankton biomass in the western Mediterranean Sea. Meanwhile, laboratory incubation studies using anthropogenic PM (e.g., tire wear PM, welding fume PM) typically used a range of exposure concentrations that were not based on deposition flux. Details of the reported PM concentrations and deposition fluxes, if available, are provided in the discussions presented in the upcoming sections.

4.1. Impact of trace metals

The impacts of atmospherically deposited trace metals on phytoplankton are summarized in Table 4. Different phytoplankton taxa have different metal requirements. Fe is a crucial trace metal in biogeochemical cycles that acts as a growth-limiting nutrient for phytoplankton, making it the most extensively studied trace metal in this context. Cu, the second-most studied trace metal, exerts positive and negative effects on phytoplankton at low and high concentrations, respectively. The impacts of trace metals on phytoplankton are also influenced by their bioavailability, which depends on their chemical form (i.e., soluble) rather than their overall concentration. However, the soluble forms of metals can potentially undergo complexation reactions with organic ligands produced by phytoplankton in water, thus reducing their concentrations and minimizing their impacts.

4.2. Iron

Fe is an essential micronutrient for phytoplankton and various metabolic processes, including chl-a biosynthesis, photosynthetic reactions, and electron transport. It is also a co-factor in enzymes such as catalase, chelatase, nitrogenase, nitrate/nitrite reductase, and peroxidase (Wang et al., 2017). Fe exists in two oxidation states: Fe^{2+} and Fe^{3+}, with Fe^{2+} being more bioavailable and more easily uptaked by phytoplankton (Schoffman et al., 2016). Under oxic and near-neutral pH conditions in aquatic waters, Fe is predominantly in the Fe^{3+} form and has low dissolved Fe concentrations. Open oceans and a few freshwater lakes have low dissolved Fe concentrations, often in the nanomolar or sub-nanomolar range (Lis et al., 2015).

Fe deficiency is the limiting factor for phytoplankton growth in high-nutrient, low chlorophyll (HNLC) oceans, where significant amounts of N and P at the water surface remain unused by phytoplankton. Fe deposited into these HNLC regions serves as a nutrient by stimulating the assimilation of unused nutrients by phytoplankton and increasing primary productivity. Due to the challenges associated with directly measuring phytoplankton biomass over large oceanic areas, chl-a, a key component in photosynthesis, is typically used as the primary indicator of productivity and trophic status in marine and oceanic waters (Boyer et al., 2009). Numerous bio-incubation experiments conducted under both controlled laboratory conditions and field conditions have demonstrated that atmospheric Fe can alleviate the growth limitations of phytoplankton in marine and oceanic waters. Duggen et al. (2007) provided the first concrete evidence via bottle incubation studies, showing that the marine diatom *Chaetoceros dichaeta* utilized Fe from subduction zone volcanic ash, which resulted in enhanced levels of photosynthetic efficiency (F_v/F_m) and chl-a. External Fe addition experiments corroborated these findings, showing that *Chaetoceros dichaeta* experienced a decrease in F_v/F_m under Fe limiting conditions, which rapidly recovered within 24 h upon adding excess Fe. These

Table 4
Effects of atmospherically deposited trace metals on phytoplankton.

Source	Type of incubation	Composition	Phytoplankton species/community	Measured Indicator	Major Findings	Reference
Arenal, Costa Rica, Sakura-jima, Japan, and Mt. Spurr, Alaska	Bottle incubation	Fe	*Chaetoceros dichaeta*	F_v/F_m, and chl-a	Fe increased the marine primary productivity in Fe-limited or low-Fe oceanic areas	Duggen et al. (2007)
Eyjafjallajökull volcano	Bottle incubation	Fe	Natural phytoplankton assemblages	F_v/F_m, and chl-a	Ash containing Fe stimulated phytoplankton growth and nutrient drawdown	Achterberg et al. (2013)
Kasatochi volcano, Alaska, and Chaiten volcano, Chile	Bottle incubation	Fe	Natural phytoplankton assemblages	Chl-a, primary production, and phytoplankton pigments	Fe-laden Kasatochi shifted the dominant taxa from haptophytes to diatoms and was responsible for triggering the 2008 northeast Pacific bloom	Mélançon et al. (2014)
Namibian and Mauritanian dust	Laboratory incubation	Fe	*Actinocyclus* sp. *Thalassiosira* sp.	Growth rate	The impact of dust addition has differed between the two diatom species	Visser et al. (2003)
East Antarctica Plateau	Laboratory incubation	Fe	*Eucampia antarctica*	Cell number, chl-a, F_v/F_m, and POC production	Fe has altered nutrient assimilation differently across diatom species	Conway et al. (2016)
			Proboscia inermis	Chl-a, F_v/F_m, and POC production		
Kalahari Desert, Africa, and Orange NSW, Australia	Laboratory incubation	Fe	*Cyclotella meneghiniana*	Total chlorophyll concentrations	A possibility of solid particle-mediated Fe-acquiring mechanisms by diatoms in addition to reductive uptake mechanism	Hettiarachchi et al. (2021)
Tengger desert, China	Bottle incubation	Fe	Natural phytoplankton assemblages	Chl-a	pH changes interfered with Fe speciation, organic ligands, and transporters, reducing Fe bioavailability to phytoplankton	Mélançon et al. (2016)
Western tropical North Atlantic	Bottle incubation	Fe	*Trichodesmium*	Fe uptake	*Trichodesmium* has assimilated more Fe than needed for its maximum growth demonstrating a large luxury uptake of Fe	Chen et al. (2011)
Tudor Hill observatory, southwestern tip of Bermuda	Bottle incubation	Cu	*Synechococcus*	Chl-a, and cell abundance	*Synechococcus* has exhibited resistance to Cu toxicity when Cu^{2+} concentrations were below toxicity thresholds	Mackey et al. (2012a)
		Co, Mn, and Ni		Growth	*Synechococcus* utilized Co, Mn, and Ni for their growth	
African (Sahara Desert) PM and European PM was collected locally at the Gulf of Aqaba	Bottle incubation	Cu	Natural phytoplankton assemblages	Chl-a, and cell number	High concentrations of Cu were toxic to Picoeukaryotes and *Synechococcus* as supported by laboratory toxicity tests	Paytan et al. (2009)
			Picoeukaryotes and *Synechococcus*	Growth, and F_v/F_m		
Montseny station, Catalonia, Spain	Satellite observation (western Mediterranean Sea)	Cu	Natural phytoplankton assemblages	Chl-a, and phytoplankton biomass	High concentrations of Cu were to natural phytoplankton assemblages over a vast area of the Mediterranean Sea	Jordi et al. (2012)
Huaniao Island in the Zhoushan Archipelago	Bottle incubation	Cu	Natural phytoplankton assemblages	Chl-a	High concentrations of Cu were toxic to natural phytoplankton assemblages	Wang et al. (2017)
		Cu and Fe			High concentration of Fe alleviated the toxicity of Cu	
PM from Guangzhou and rainwater near Shanwei	Bottle incubation	Cu	Subsurface phytoplankton	Chl-a, and growth rate	Elevated Cu levels in PM in the Qiongdong upwelling zone significantly inhibited subsurface phytoplankton due to their lack of adaptations to metal deposition	Zhou et al. (2021a)
Laboratory tire wear particles	Laboratory incubation	Zn	*Raphidocelis subcapitata*	Growth inhibition	Toxicity was related to the tire exposed surface with lower pH influencing the release and toxicity of Zn	Gualtieri et al. (2005)
Unused car tire	Laboratory incubation	Zn	*Raphidocelis subcapitata*	Growth rate	Zn and lipophilic organic compounds inhibited the growth	Wik et al. (2009)
Unused winter car tire	Laboratory incubation	Zn	*Rhodomonas salina*, *Thalassiosira weissflogii* and *Heterocapsa steinii*	Cell density, and growth rate	Higher Zn concentrations leached from tire wear particle leachates was responsible for growth inhibition	Page et al. (2022)
Saharan dust	Bottle incubation	Al	Natural phytoplankton assemblages	Chl-a, and primary productivity	Dissolved Al that has formed toxic Al nanoparticles inhibited phytoplankton growth	Krom et al. (2016)

(*continued on next page*)

Table 4 (*continued*)

Source	Type of incubation	Composition	Phytoplankton species/community	Measured Indicator	Major Findings	Reference
Electrodes	Laboratory incubation	Cr, Mn, Ni, Si, Ti, and Vn	*Heterosigma akashiwo*	Growth inhibition, and morphological changes	Toxicity was dependent on Ti and Cr content in welding emission, summarizing that the toxicity of particulate emissions was linked to their chemical composition	Kirichenko et al. (2019)
Diesel-fueled heavy-duty vehicle	Laboratory incubation	Cd, Cu, Cr, Pb, and Zn	*Scenedesmus subspicatus*	Growth inhibition	Aqueous leachate at pH 2.0 inhibited the growth in comparison to aqueous leachate at pH 5.0 and solvent extract	Corrêa et al. (2017)
Motorcycle, light-duty, and heavy-duty vehicle	Laboratory incubation	As, Ba, Cd, Co, Cu, Cr, Mn, Mo, Ni, Pb, Sb, Sn, and Zn	*Heterosigma akashiwo* and *Porphyridium purpureum*	Cell size, membrane potential, and esterase activity	Trace metals emitted from vehicles powered by diesel engines posed a significant risk to phytoplankton when compared to particles emitted from gasoline-powered vehicles	Pikula et al. (2019)
Brake disc and pads	Laboratory incubation	Iron oxide, Al, Cu, Cr, Si, Sn, and Zn	*Raphidocelis subcapitata*	Growth inhibition	Particulate form of trace metals has induced greater toxicity compared to the water-soluble fraction of PM	Volta et al. (2020)
Electroplating processes (Aluminum cleaning, aluminum etching, chemical degreasing, nonferrous metals etching, and nickel plating)	Laboratory incubation	Salts of Fe, Mg, Al, and Zn, as well as particulate Zn Cu, Zn, Pb, Ni, Fe, and Al	*Heterosigma akashiwo*, and *Porphyridium purpureum*	Growth inhibition, cell size, and membrane potential	Trace metal emission from the aluminum cleaning process induced a dose and time-dependent toxicity, while trace metal emission from the non-ferrous metal etching processes induced a hormetic dose-response toxicity	Pikula et al. (2021)
Arenal, Costa Rica, Popocatepetl, Mexico, Rabaul-Tavurvur, Papua New Guinea, Sakura-jima, Japan, and Apoyeque, Nicaragua	Laboratory incubation	Cu, Co, Fe, and Mn	*Thalassiosira pseudonana*, and *Emiliania huxleyi*	Growth rate, and cell number	Highest concentration of Mn, Co, and Fe and the lowest concentration of Cu promoted the growth rate of *T. pseudonana*, while high concentrations of Fe and Mn suppressed the growth rate of *E. huxleyi*	Hoffmann et al. (2012)
Etna (Sicily), and Chaitén (Chile)	Bottle incubation	Fe and Mn	Natural phytoplankton assemblages	Chlorophyll, and F_v/F_m	Enhanced response to ash was a result of the relief of Fe and Mn (co)limitation	Browning et al. (2014)
Hong Kong University of Science and Technology, Hong Kong	Bottle incubation	Fe, Mn, and Zn	*Crocosphaera*, *Prochlorococcus*, *Synechococcus*, and *Trichodesmium*	Phytoplankton abundance, and gene transcripts	Inhibitory effect of PM due to Fe scavenging and trace metal toxicity	Tan et al. (2019)
Huaniao Island, China	Bottle incubation	Cu and Fe	*Skeletonema costatum*	Chl-a	Fe and Cu together increased the proportion of *S. costatum*	Li et al. (2021)

results suggested that Fe is a governing nutrient for the growth of *Chaetoceros dichaeta* (Timmermans et al., 2001). The introduction of Eyjafjallajökull volcanic ash (9 mg L^{-1}) into North Atlantic waters in bottle incubation experiments revealed the rapid accumulation of chl-a and increased F_v/F_m within natural phytoplankton populations. However, the observed effects were less than half the stimulatory influence caused by 2 nM dissolved $FeCl_3$ addition. This is because the ash contained a small fraction (0.02 %) of bioavailable Fe as a result of excess dissolved Fe released from the ash being lost through rapid precipitation caused by ineffective stabilization by free ligands in seawater (Achterberg et al., 2013). Mélançon et al. (2014) reported that the introduction of Kasatochi volcanic ash (1.2 mg L^{-1}) into Fe-deficient seawater increased chl-a concentrations, increased C fixation rates, and shifted the dominant taxa from haptophytes to diatoms. In addition, the ash stimulated the biomasses of cyanobacteria, cryptophytes, pelagophytes, and haptophytes. These observations led the authors to conclude that the 2008 northeast Pacific bloom was triggered by ash deposition. A study mimicking a large Saharan dust deposition event reported that even though the solubility of dust added (1.34 mg L^{-1}) into incubation bottles was very low, the dust released sufficient dissolved Fe to relieve Fe limitation of the phytoplankton community in the northeast Atlantic Ocean (Blain et al., 2004).

Different phytoplankton groups have different requirements for Fe in Fe-limited waters because they are influenced by cell size, physiology, uptake, etc. Visser et al. (2003) conducted the first laboratory incubation study using 1 and 5 mg of dust (from Namibia and Mauritania) focusing on individual species of Antarctic diatoms, *Actinocyclus* sp. and *Thalassiosira* sp. The 1 mg of dust used in these incubation experiments represented a high dust input condition based on the amount of dust that phytoplankton receives per month in the North Atlantic and per year in the South Pacific and South Atlantic. *Thalassiosira* sp., a small diatom (70 μm) with low Fe requirements, showed rapid growth under Fe-limited conditions but limited response to Fe-dust additions. In contrast, *Actinocyclus* sp., a larger diatom (140 μm), exhibited slow growth in Fe-limited conditions but experienced an increase in growth rate following the addition of Fe-laden dust. Similarly, laboratory incubation experiments using the Antarctic diatom species *Eucampia antarctica* and *Proboscia inermis* revealed species-dependent responses to Fe-dust (0.22 mg L^{-1}) from the Last Glacial Maximum portion of the Antarctic ice core (Conway et al., 2016). *Eucampia antarctica* exhibited a strong growth response, characterized by increased cell number, chl-a, and particulate organic carbon (POC) production due to its high Fe requirement. In contrast, *Proboscia inermis*, which has a low Fe requirement, exhibited a more subtle response with increased chl-a and POC production but not cell number. In addition, *Eucampia antarctica* decreased silicate uptake for the same NO_3^- and C uptake, whereas *Proboscia inermis* increased C and NO_3^- uptake for the same silicate uptake. These findings suggested that Fe altered nutrient assimilation differently across the diatom species. Diatoms acquire Fe through a reductive uptake mechanism by reducing dissolved Fe^{3+} to Fe^{2+} (Sutak

et al., 2012). However, in incubation experiments conducted by Hettiarachchi et al. (2021), mineral dust (20 mg) significantly enhanced the growth of *Cyclotella meneghiniana*, a marine-centric diatom, in terms of total chlorophyll (chl) concentrations. This growth enhancement was more pronounced than when the mineral dust was physically separated. This indicated the potential involvement of solid PM-mediated Fe-acquiring mechanisms by the diatoms.

Ocean acidification has been proposed to have significant implications for the bioavailability and speciation of Fe, thus influencing its effects on phytoplankton. To investigate this hypothesis, Mélançon et al. (2016) conducted short-term bottle incubation experiments using HNLC northeast subarctic Pacific waters treated with either 2 mg L^{-1} of Asian dust or 0.6 nmol L^{-1} of iron (II) sulfate ($FeSO_4$). Their findings indicated that at pH 8.0, both dust and $FeSO_4$ treatment doubled chl-a levels, thus relieving the Fe-limitation of the phytoplankton assemblage belonging to non-calcifying taxa (diatoms and cyanobacteria). However, under more acidified conditions (pH 7.8), there was a significant reduction in chl-a and POC concentrations, as evidenced by the decrease in the abundance of phytoplankton belonging to calcifying taxa (haptophytes) and, to some extent, pelagophytes and cyanobacteria. Consequently, the observed changes in the growth response of non-calcifying taxa led to the proposition that pH changes might interfere with Fe speciation, organic ligands, and transporters, thus reducing Fe bioavailability to phytoplankton.

Several investigations into the atmospheric deposition of Fe have focused on diazotrophs, especially *Trichodesmium*, since they are known to form blooms and enhance nitrogen fixation rates in response to Fe deposition. The high demand for Fe in *Trichodesmium* can be attributed to the increased requirement for the Fe-rich nitrogenase enzyme, which catalyzes nitrogen fixation. In the western tropical North Atlantic, *Trichodesmium* assimilated more Fe from PM than necessary for optimal growth (Chen et al., 2011). In addition, Fe is hypothesized to limit nitrogen fixation in oligotrophic oceans. The additions of Saharan dust (0.5 and 2 mg L^{-1}) to simulate a strong dust deposition event in the eastern tropical North Atlantic in bottle incubation experiments resulted in stimulated nitrogen fixation caused by the provision of Fe and P from the added Saharan dust, thus relieving the Fe and P co-limitation of diazotrophs (Mills et al., 2004). Natural populations of *Trichodesmium* can also employ colony-forming strategies as an adaptive mechanism to utilize Fe from deposited dust as a nutrient source. Rubin et al. (2011) suggested that the puff-shaped colonies formed by natural *Trichodesmium* collected from the Red Sea effectively dissolved dust by trapping and concentrating the dust within the colony core, thus facilitating the assimilation of dissolved Fe through unspecified cell-surface processes (Rubin et al., 2011). In addition, the natural colonies of *Trichodesmium* reportedly can sense Fe and selectively choose Fe-rich dust over Fe-free dust (Kessler et al., 2019). In contrast to natural populations, laboratory strains such as *Trichodesmium erythraeum* IMS101 typically exist as single filaments (trichomes). These laboratory culture strains do not interact with dust-containing Fe when growing as single filaments. However, colony formation prompted interactions with Fe-rich dust induced by Fe limitation and high trichome density (Kessler et al., 2019). A bio-incubation study on single *Trichodesmium* colonies conducted by Eichner et al. (2020) using 2 mg L^{-1} of dust reported that dust accumulation in the colony core had negligible effects on the oxygen and pH microenvironments. *Trichodesmium* colonies also exhibit a symbiotic relationship with bacteria capable of synthesizing siderophores, thus facilitating Fe acquisition from dust. This was demonstrated in a short-term incubation study involving natural *Trichodesmium*, whereby dust additions significantly enhanced the production of ferrioxamine siderophores by bacteria residing within the *Trichodesmium* colonies. These siderophores interacted with the dust in the colony core and promoted Fe-dissolution by forming Fe-siderophores complexes. Subsequently, both *Trichodesmium* and its associated bacteria acquired Fe, thus establishing a mutual relationship benefiting the consortium partners (Basu et al., 2019).

4.3. Copper

Cu is an essential micronutrient for phytoplankton, serving as a co-factor in redox proteins integral to respiration and photosynthesis (Barber-Lluch et al., 2023). However, since Cu is also a potential toxin to phytoplankton, its dual functionality underlines its complex interplay in aquatic ecosystems. The chemical form of Cu is crucial for phytoplankton, with only some specific forms being bioavailable. The bioavailability of dissolved Cu depends on free cupric ion (Cu^{2+}) concentrations and Cu complexes with organic ligands (Ruacho et al., 2022). In oligotrophic oceanic regions, typical Cu^{2+} concentrations range from 10^{-15} to $10^{-13.5}$ M, which induces growth limitation due to Cu starvation (Barber-Lluch et al., 2023). However, Cu^{2+} concentrations beyond their threshold levels ($\sim 10^{-11}$ M) are toxic to phytoplankton (Brand et al., 1986). The aquatic lifetime of bioavailable Cu is short due to fast Cu-organic ligand complexation processes, which regulate the concentration of Cu^{2+} and protect phytoplankton from Cu toxicity (Moffett and Brand, 1996).

Several bio-incubation studies have demonstrated the role of Cu as a nutrient essential for marine phytoplankton. For instance, Mackey et al. (2012a) observed that *Synechococcus* in the Sargasso Sea exhibited resistance to Cu toxicity when free Cu^{2+} concentrations in deposited PM were below toxicity thresholds of $\sim 10^{-11}$ M. Phytoplankton also employ adaptive strategies such as the internal sequestration of Cu by organic chelation, the release of organic complexing ligands, and the upregulation of Cu efflux mechanisms to mitigate the adverse effects of Cu exposure (Echeveste et al., 2018). Interestingly, *Synechococcus* produced high concentrations of Cu-binding ligands without Cu toxicity. Similarly, a study by Hoffmann et al. (2012) found that *Thalassiosira pseudonana* produced greater Cu-binding ligands when incubated with volcanic ash having low Cu concentrations. Although the production of organic ligands was hypothesized not to function exclusively as a Cu detoxification mechanism, considering the non-specificity of many organic ligands to metals, other factors could have contributed to their production.

The toxicity of atmospheric Cu to phytoplankton is typically associated with its high concentrations. Satellite observations covering an extensive region of the western Mediterranean Sea found that atmospheric deposition events characterized by high Cu concentrations and a dry deposition flux of 11.80 μg m^{-2} d^{-1} significantly decreased phytoplankton biomass (Jordi et al., 2012). Bottle incubation experiments conducted in the East China Sea found that high Cu concentrations significantly decreased chl-a concentrations in natural phytoplankton assemblages (Wang et al., 2017). However, it should be noted that the high Cu concentrations reported in bottle incubation experiments conducted in the East China Sea were due to the addition of 0.45 mg L^{-1} of PM, which was ~50 % higher than the estimated dry deposition (17 to 276 mg m^{-3}) for that region. In both the forementioned studies, Cu did not cause complete mortality but significantly reduced phytoplankton growth rate by inhibiting photosynthesis, altering electron transport, and inactivating photosystem II (PSII) reaction centers. High concentrations of Cu can also lead to the formation of strong Cu complexes with biomolecules, thus causing toxicity through interactions with thiol sites on proteins and the production of reactive oxygen species, promoting lipid peroxidation chain reactions (Biswas and Bandyopadhyay, 2017).

Bottle incubation experiments in the Red Sea using 0.75 mg L^{-1} of PM (equivalent to 14 days of deposition during dust storms) contained high Cu concentrations that significantly reduced chl-a levels in natural phytoplankton assemblages, thus affecting the cell numbers of specific phytoplankton taxa such as picoeukaryote and *Synechococcus* (Paytan et al., 2009). Moreover, a direct assessment of metal toxicity revealed that adding Cu impaired *Synechococcus* growth and reduced F_v/F_m levels, thus indicating Cu as the leading cause of toxicity in bio-incubation experiments. Cu toxicity in *Synechococcus* was mainly caused by membrane damage and loss of membrane permeability that promoted Cu^{2+} uptake, damage to PSII, or inhibition of electron

transport (inhibition of photosynthesis). The damage to the photosynthetic apparatus induced oxidative stress, ultimately inhibiting growth (Stuart et al., 2009). Although surface phytoplankton can adapt to Cu toxicity, subsurface phytoplankton are susceptible to toxicity during upwelling events. For instance, bottle incubation experiments conducted in the Qiongdong upwelling zone using 3.3 mg L^{-1} of PM (representing summer dry deposition based on the annual dust deposition flux of 10 to 120 g m^{-2} to the coastal sea) and 10 % rainwater (representing summer wet deposition based on ~300 mm precipitation between June and August) contained elevated Cu levels, which significantly inhibited subsurface phytoplankton due to their lack of adaptations to Cu deposition (Zhou et al., 2021a).

4.4. Zinc

Total dissolved Zn (Zn^{2+}) concentrations in open ocean waters are typically in the nanomolar range and display nutrient-like behavior (Sinoir et al., 2016). While Zn is essential for the growth and development of phytoplankton, concentrations exceeding their growth requirements can reduce growth, affect photosynthesis, and generate oxidative stress (Gebara et al., 2023). Page et al. (2022) conducted laboratory incubation experiments using different leachate concentrations (1, 10, 25, and 50 %) from 1 g L^{-1} tire wear particles and reported that Zn is a key factor in the growth inhibition of three phytoplankton: *Rhodomonas salina*, *Thalassiosira weissflogii*, and *Heterocapsa steinii*. High Zn concentrations from tire wear PM leachates (1053.26 ± 74.04 μg L^{-1}) were responsible for this growth inhibition. Similarly, Gualtieri et al. (2005) studied the effects of eluates from tire PM (1, 10, 50, and 100 %) in a laboratory setting, mimicking the normal wear of a tire. They found that the aqueous leachate from 50 g L^{-1} tire PM at pH 3 (EC_{50}: 0.93 %) contained higher Zn concentrations than those from 100 g L^{-1} tire wear PM (EC_{50}: 1.64 %), inhibiting the growth of *Raphidocelis subcapitata*. The toxicity was associated with the tire-exposed surface at a lower pH, which influenced the release and toxicity of Zn. Likewise, Wik et al. (2009) reported that the sequential aqueous leachates from three different used tires contained Zn and lipophilic organic compounds, inhibiting the growth of *Raphidocelis subcapitata*. Zn affected the F_v/F_m of *Raphidocelis subcapitata*, potentially replacing Mg in chl, thus affecting oxygen evolution and generating unstable chl-a. Additionally, Zn can affect the water splitting of PSII, thus affecting photosynthesis processes (Gebara et al., 2020).

4.5. Other trace metals

In addition to Fe, Cu, and Zn, there have been investigations into the effects of other trace metals on phytoplankton. Numerous laboratory investigations have delved into the aquatic toxicity associated with anthropogenically emitted trace metals. The chemical composition of PM emissions determines their toxicity in aquatic environments. For example, the presence of Ti and Cr in welding fume PM (1, 10, and 100 mg L^{-1}) from rutile-coated electrodes inhibited growth and induced morphological changes such as irregular shape, softness, multiple protrusions, and folds of algae cell membranes in marine phytoplankton *Heterosigma akashiwo*. In contrast, the absence of Cr and lower concentrations of Ti from the emissions of rutile-cellulose-coated electrodes reduced toxicity (Kirichenko et al., 2019). Even though the chemical composition potentially modulates the toxicological response, aqueous extracts of PM have greater significance since the ecotoxicological effects in aquatic environments depend on the bioavailability of soluble metals. For example, the aqueous leachate of diesel exhaust PM (0.39, 0.78, 1.56, 3.12, 6.25, and 12.5 % v/v) at pH 2 revealed that the concentrations of soluble metals such as Cd, Cr, Cu, Pb, and Zn significantly inhibited the growth of *Scenedesmus subspicatus*, in contrast to the aqueous leachate at pH 5 and the solvent extract (Corrêa et al., 2017). This could be attributed to acidic environments enhancing the dissolution of trace metals in PM. Acid processing of PM during transportation is an important mechanism for converting water-insoluble trace metals to water-soluble forms. Krom et al. (2016) simulated the atmospheric acid processing of Saharan dust and introduced the simulated acid-processed Saharan dust to samples from the Eastern Mediterranean during bio-incubation experiments. Although simulated-acid-processed Saharan dust supplied greater bioavailable P (18.4 nM mg $dust^{-1}$) than fresh dust (0.45 nM mg $dust^{-1}$), the large amount of dissolved Al released during the simulated acid processing partially decreased both chl-a and primary productivity (Krom et al., 2016). This is because Al, a non-essential metal with no biological function, caused toxic effects on phytoplankton by affecting photosynthesis, ROS generation, lipid peroxidation, and ultrastructural damage (Gebara et al., 2023). Pikula et al. (2021) reported that PM samples (10, 25, and 50 % v/v) collected during Al cleaning in electroplating operations contained Fe, Mg, Al, and Zn salts, which induced dose- and time-dependent growth inhibition and increased cell size of *Porphyridium purpureum* and *Heterosigma akashiwo*. The increase in cell size of both species was attributed to increased extracellular and intracellular ROS production and metabolic disorders in toxic cells. Trace metals (Cu, Zn, Pb, Ni, Fe, and Al) from non-ferrous metal etching processes significantly inhibited the growth of *Heterosigma akashiwo* at high concentrations and stimulated it at low concentrations, indicating a hormetic dose-response relationship. The toxic effects observed at high concentrations were attributed to cell membrane hyperpolarization, indicative of membrane dysfunction and disruption of metabolic processes.

Although toxicity is related to the chemical composition and solubility of trace metals in water, some studies have shown that some trace metals in PM are intrinsically toxic regardless of their composition and solubility. For example, trace metals such as As, Ba, Cd, Co, Cu, Cr, Mn, Mo, Ni, Pb, Sb, Sn, and Zn in vehicular PM inhibited growth, altered membrane potential, and esterase activity in marine phytoplankton *Porphyridium purpureum* and *Heterosigma akashiwo* (Pikula et al., 2019). Likewise, the trace metals in PM from vehicular brake emissions exhibited greater toxicity to *Raphidocelis subcapitata* than the soluble fraction of PM (Volta et al., 2020). In both studies, physical damage from metal agglomeration with phytoplankton caused toxic effects.

4.6. Combined effects of co-existing trace metals

The impacts of trace metals on phytoplankton extend beyond simple nutrient or toxic effects since the complex interactions between co-existing trace metals must also be considered. Mn plays an important role in regulating the antagonistic and synergistic effects of different trace metals. Mn is also one of the most critical trace metals in photosynthesis since it is an integral component of the metalloenzyme cluster of the oxygen-evolving complex. Hoffmann et al. (2012) found that volcanic ash characterized by high concentrations of Mn, Co, and Fe and low Cu concentrations promoted and suppressed the growth rates of *Thalassiosira pseudonana* and *Emiliania huxleyi*, respectively. The observed differences in toxicity could be attributed to the high Mn concentrations and species-specific uptake mechanisms. In the case of *Thalassiosira pseudonoma*, the high concentrations of Mn competed with Cd, Cu, and Zn for the uptake systems, thereby preventing the uptake of co-existing metals and alleviating their toxic effects. However, Mn did not prevent the uptake of co-existing toxic metals by *Emiliania huxleyi* since its metal uptake mechanisms for Cd, Co, and Zn differed from those observed in *Thalassiosira pseudonoma*. Significant increases in the F_v/F_m and chl-a concentrations of the natural phytoplankton population were observed after basaltic or rhyolitic volcanic ash was added to samples from the Southern Ocean during bottle incubation experiments. This was attributed to the greater bioavailability of Fe^{2+} and the release of co-limiting Mn upon adding volcanic ash (Browning et al., 2014). Tan et al. (2019) demonstrated the combined effects of Fe limitation and trace metal toxicity on the phytoplankton community in the Western North Pacific Ocean through bottle incubation experiments and metatranscriptomic analyses. The addition of East Asian PM (0.2 mg L^{-1}

representing a high-flux dust event of 0.1 to 0.5 mg L^{-1} deposition) rich in macronutrients and trace metals (Fe, Mn, and Zn) induced Fe limitation and decreased the cellular abundances of *Crocosphaera, Prochlorococcus*, *Synechococcus*, and *Trichodesmium*. The elevated levels of transcripts involved in Fe metabolism, such as tonB, feoB, irr, and exbB, supported Fe limitation. The expression of resistance genes, such as czcD, czcB, and czcA (a probable Co/Zn/Cd efflux protein), and a range of genes functioning against oxidative stress indicated trace metal toxicity. Results from the dust incubation experiments (1.1 mg L^{-1} of Saharan dust representing a realistic dust deposition of 8 g m^{-2}) carried out in the oligotrophic Mediterranean Sea led Ridame et al. (2011) to hypothesize that trace elements such as Cd, Co, Mn, Mo, Ni, and Zn in Saharan dust alleviated nutrient limitations on diazotrophic activity by stimulating nitrogen fixation.

Interestingly, some co-existing trace metals have shown the ability to alleviate the toxicity of Cu in phytoplankton. For example, in bottle incubation experiments conducted in the East China Sea, Wang et al. (2017) added 0.45 mg L^{-1} of PM to simulate PM concentrations observed during extreme or frequent dust events in the region (17 to 276 mg m^{-3}), and found that increased concentrations of soluble Fe and Cu led to the increased concentrations of chl-a. Similarly, the results of bioassay experiments carried out in the East China Sea by the same research group revealed that soluble Fe and Cu in PM (1.5 mg L^{-1} based on a stronger atmospheric deposition estimated by Mackey et al. (2017)) increased the relative abundance of *Skeletonema costatum* (Li et al., 2021). Some mechanisms have been proposed for the observed increased chl-a levels. Firstly, the complex formation between Cu and organic compounds that were deposited along with elevated fluxes of soluble Fe could have reduced the toxicity of Cu by lowering the concentration of free Cu^{2+}. Secondly, the combined effect of Fe and Cu on chl-a concentration could be influenced by phytoplankton community uptake and metabolism mechanisms, which could vary in other oceanic regions with different phytoplankton community structures. One way of determining the utilization of metals by phytoplankton is by calculating the drawdown of metals in the open ocean. In bottle incubation experiments conducted by Mackey et al. (2012a) in the Sargasso Sea, the addition of high concentrations of PM simulating levels after a moderately strong deposition event typical of the central North Atlantic (20 g m^{-2} yr^{-1}) led to the release of trace metals such as Co, Mn, and Ni. Based on the subsequent depletion of these trace metals in the system, the authors concluded that these trace metals were collectively utilized by *Synechococcus* for their growth.

Some studies have investigated the impacts that atmospherically deposited metals have on phytoplankton in lakes. Since high-elevation lakes are often oligotrophic, a slight variation in nutrient availability can greatly impact their productivity. Moser et al. (2010) discovered a shift in diatom assemblages at Marshall Lakes in the Uinta Mountains, USA caused by atmospheric metal pollution (Cu, Pb, Cd, and Zn). Diatom alterations in the early 1900s were defined by the near extinction of *Cyclotella pseudostelligera* and *Cyclotella stelligera*, as well as an increase in benthic, metal-tolerant diatoms, *Achnanthes* species. Littoral organisms with superior plasticity, tolerance to metals, and the ability to form biofilms were responsible for the shift in abundance from planktonic to benthic species in contaminated areas. Moreover, diatom species have adapted quickly to environmental changes due to their unique ecological tolerances and short life spans (Cotiyane-Pondo and Bornman, 2021).

4.7. Impact of N-containing compounds

N is the most essential nutrient for phytoplankton. Phytoplankton use a wide range of N-containing compounds, including NO_3^-, NO_2^-, NH_4^+, N_2, and organic N. Phytoplankton have developed efficient ways of acquiring these compounds through diffusion and active transport processes. Dissolved N bioavailable to phytoplankton in aquatic waters comprises of both inorganic and organic N. Biogeochemical processes (e.g., mineralization, nitrification, and denitrification) transform these N-containing compounds from one form to another (Jani and Toor, 2018). For example, NO_3^- is the oxidized N species that is reduced to NO_2^- by the enzyme nitrate reductase. NO_2^- is reduced to NH_4^+ by the enzyme nitrite reductase. The concentrations of NO_3^-, NO_2^-, and NH_4^+ in marine ecosystems typically range from 1 to 500 μM, 0.1 to 50 μM, and 1 to 50 μM, respectively (Tovar et al., 2002).

Studies on the impacts of atmospherically deposited N-containing compounds on phytoplankton are summarized in Table 5. Microphytoplankton (e.g., diatoms) prefer NO_3^-, while picophytoplankton (e.g., cyanobacteria, dinoflagellate) prefer NH_4^+ instead (Glibert et al., 2016). Picophytoplankton, characterized by its small size (<2 μm), high surface area to volume ratio, high metabolic rate, and efficient nutrient internalization, is typically competitive in adapting to N-limiting environments. The form of the N deposited into N-limited waters can disrupt the stability of phytoplankton communities by shifting the size-fractionation proportion towards large cells. Such alterations in the phytoplankton size structures affect the physiology and competitiveness of phytoplankton for nutrient acquisition and biomass expansion (Guieu et al., 2014). Diatoms are the species that benefit the most from N deposition in oceans. Bottle incubation experiments conducted in the oligotrophic western Pacific Ocean showed that the addition of PM containing high NO_3^- concentrations enhanced diatom growth, as evident from the increase in chl-a levels and the relatively higher abundances of chloroplast sequences of diatoms (Maki et al., 2016). Among the diatom species, *Chaetoceros* showed the most significant growth when 0.25 mg L^{-1} of PM was added to simulate a heavy dust event, while *Pseudo-nitzschia* sp. thrived when 0.05 mg L^{-1} of PM was added to simulate a light dust event. In the oligotrophic Northwestern Pacific Ocean, N-laden dust promoted the growth of microphytoplankton and nanophytoplankton rather than picophytoplankton due to the presence of NO_3^- in the dust (Wang et al., 2019). The effects on the growth of phytoplankton differed among the dominant genera. Enhanced growths were observed in *Pseudo-nitzschia* and *Chaetoceros* because of their larger cell sizes. In contrast, *Prorocentrum* growth was inhibited, and the growths of *Thalassiosira*, *Heterocapsa,* and *Scrippsiella* were not significantly impacted. Zhou et al. (2021b) reported that N deposition fluxes from rainwater in the Eastern Indian Ocean (0.75 to 1.43 mg m^{-2} mon^{-1}) were significantly higher than the pre-2000 levels (0.25 mg m^{-2} mon^{-1}) reported by Okin et al. (2011). This rainwater contained substantial concentrations of NO_3^- and negligible NH_4^+, which enhanced chl-a biomass and accelerated the transition in phytoplankton dominance from picophytoplankton (cyanobacteria) to microphytoplankton (diatom). The faster growth and dominance of microphytoplankton resulted from their higher F_v/F_m and ability to uptake excess nutrients.

Some phytoplankton taxa prefer NH_4^+ uptake as it involves less energetic investment compared to NO_3^- uptake. However, NH_4^+ uptake may inhibit NO_3^- uptake for some phytoplankton taxa such as diatoms. Sedwick et al. (2018) reported that the addition of 100 mL rainwater to incubation bottles containing oligotrophic waters from the Mid-Atlantic Bight to simulate an intense rain event did not result in any significant drawdown in NO_3^- and NO_2^-. However, there was a significant drawdown in NH_4^+ that accompanied the chl-a increase and biomass accumulation. In the South China Sea, rainwater (at 5 and 10 % v/v) containing NH_4^+ and NO_3^- altered the dominance of the phytoplankton community, shifting from picophytoplankton (cyanobacteria) to microphytoplankton (diatoms) (Cui et al., 2016). Notably, diatoms such as *Asterionellopsis* sp., *Chaetoceros* sp., *Navicula* sp., *Pseudo-nitzschia* sp., and *Skeletonema* sp. became the dominant species. Despite the rainwater having a high NH_4^+ concentration, which is favorable for cyanobacteria growth, a larger proportion of diatoms that prefer NO_3^- increased instead. The increase in diatom proportion was attributed to nutrient competition among the phytoplankton for other compounds present in the rainwater, thus inhibiting cyanobacteria growth. In bottle incubation experiments conducted in the N-limited Bay of Bengal (N:P = 2.21

Table 5
Effects of atmospherically deposited N-containing compounds on phytoplankton.

Source	Type of experiment	Phytoplankton species/community	Measured Indicator	Major Findings	Reference
Snow cover at Murododaira on Mt. Tateyama	Bottle incubation	Natural phytoplankton assemblages	Chl-a, microscopic identification, and gene sequencing	Higher NO_3^- concentrations promoted diatom growth, especially *Chaetoceros* and *Pseudo-nitzschia* species	Maki et al. (2016)
Laboratory building. Visakhapatnam, India	Bottle incubation	Natural phytoplankton assemblages	Chl-a, diadinoxanthin, fucoxanthin, and zeaxanthin	High concentrations of NO_3^- and NH_4^+ enhanced diatom growth and biomass	Yadav et al. (2016)
Mu Us Sandland, China	Bottle incubation	Natural phytoplankton assemblages	Chl-a, F_v/F_m, species composition, and microscopic identification	Growth was promoted in *Pseudo-nitzschia* and *Chaetoceros*, inhibited in *Prorocentrum*, and no influence on *Thalassiosira*, *Heterocapsa* and *Scrippsiella*	Wang et al. (2019)
Qingdao, China	Bottle incubation	Natural phytoplankton assemblages	Chl-a	Low and medium doses (0.03–0.6 mg L^{-1}) stimulated growth and altered phytoplankton size structure towards nano- and micro-sized cells	Zhang et al. (2019a)
Eastern Indian Ocean	Bottle incubation	Natural phytoplankton assemblages	Chl-a, microscopic identification, and cell density	NO_3^- shifted the regime from picophytoplankton cyanobacteria to microphytoplankton diatom	Zhou et al. (2021b)
Old Dominion University, Norfolk, Virginia, USA	Bottle incubation	Natural phytoplankton assemblages	Chl-a, and primary prodcutivity	No significant drawdown in NO_3^-, and NO_2^- but a significant drawdown of NH_4^+ that supported chl-a increase and biomass accumulation	Sedwick et al. (2018)
South China Sea	Bottle incubation	Natural phytoplankton assemblages	Chl-a, and microscopic identification	Shift from picophytoplankton to microphytoplankton and diatoms was the predominant species	Cui et al. (2016)
Qingdao, China	Bottle incubation	Natural phytoplankton assemblages	Chl-a	Large amount of dust promoted phytoplankton biomass, in contrast to lower amount of dust	Liu et al. (2013)
Saharan soil, southern Tunisia	Bottle incubation	Natural phytoplankton assemblages	Chl-a, and primary production	Dry and wet deposition events induced contrasting phytoplankton community response due to the difference in bioavailable nutrients	Ridame et al. (2014)
Dust	Bottle incubation	Natural phytoplankton assemblages	Chl-a, other phytoplankton pigments, primary production, and microscopic observation	Effects of single addition and repetitive addition of N-containing dust were similar	Lagaria et al. (2017)
Mu Us Desert, China	Bottle incubation	Natural phytoplankton assemblages	Chl-a, relative abundance, and specific growth rate	Excess supply of N relative to P altered N:P ratio of varying trophic seawaters	Zhang et al. (2019b)
Mt. Tateyama, Japan	Bottle incubation	Natural phytoplankton assemblages	Chl-a, and growth rate	NO_3^- containing dust promoted phytoplankton growth in oligotrophic waters in contrast to nutrient-rich seawater	Maki et al. (2021)
CSIR-National Institute of Oceanography, Goa, India	Bottle incubation	Natural phytoplankton assemblages	Growth rate, chl-a, and other phytoplankton pigments	Co-enrichment of N and Fe promoted phytoplankton growth	Sharma et al. (2022)
Gobi Desert, Mu Us Desert, and Tengger Desert	Bottle incubation	Natural phytoplankton assemblages	Chl-a	Both N and P rather than N alone was responsible for promoting the growth and shifting phytoplankton size structure towards larger cells	Zhang et al. (2022)
Lake shore at the Tahoe City Field Station, Tahoe City, California, USA	Bottle incubation	Natural phytoplankton assemblages	Chl-a, and cell count	High NH_4^+ and low P content promoted the growth of picophytoplankton and filamentous cyanobacteria that increased primary productivity of Lake Tahoe during the Wheeler and Angora Fires	Mackey et al. (2013)

to 9.13), Yadav et al. (2016) demonstrated a linear relationship between the concentrations of inorganic N added and increased phytoplankton biomass. The addition of PM with high concentrations of NO_3^- and NH_4^+ increased the N:P ratio of surface seawater and enhanced diatom growth and biomass, as evidenced by an increase in the diatom marker pigment, fucoxanthin. These high concentrations of NO_3^- and NH_4^+ in the PM were attributed to the elevated dry depositional flux of inorganic N, ranging from 106 ± 31 to 1049 ± 302 μmol m^{-2} d^{-1} during the sampling period. This flux was an order of magnitude higher than the computed value of 2 to 83 μmol m^{-2} d^{-1} for offshore waters previously reported by Srinivas et al. (2011) for the same study region.

Under co-limitation conditions, N enrichment with P or a trace metal can relieve nutrient limitation conditions. For example, the co-enrichment of N and Fe from atmospheric dust promoted phytoplankton growth in the N-limiting Arabian Sea. The higher concentration of NH_4^+ compared to NO_3^- in the dust induced the growth of mixotrophic dinoflagellate *Gymnodinium* (Sharma et al., 2022). Ridame et al. (2014) examined the response of phytoplankton to different Saharan dust events (wet and dry deposition) in the northwestern oligotrophic Mediterranean Sea. The amount of dust added (41.5 g) in the incubation experiments represented a high and environmentally realistic atmospheric dust deposition of 10 g m^{-2} (Guieu et al., 2010). Dry deposition did not significantly impact primary production and chl-a levels, as it was deemed a minor source of NO_3^-. In contrast, wet deposition containing a significant source of dissolved inorganic P and NO_3^- induced rapid, strong, and long increases in primary production and chl-a levels. However, the higher NO_3^- levels relative to dissolved inorganic phosphate (DIP) in dust led to a substantial increase in the NO_3^-/DIP ratio, suggesting a switch from an initial N-limited or NP co-limited condition to a severe P-limited condition. In the Northwest Pacific Ocean, Zhang et al. (2022) found that both N and P, rather than N alone, were responsible for promoting the growth of phytoplankton and shifting their size structure towards larger cells. The substantial supply of N relative to P promoted the initiation of dissolved organic phosphate (DOP) utilization in seawater, thereby strengthening the consumption of bioavailable P. In this study, the concentrations of dissolved inorganic N used (577 to 1007 μmol g^{-1}) were comparable to the levels (90 to 1264 μmol g^{-1}) found in PM deposited during a strong dust event in the Yellow Sea (Shi et al., 2012). The same authors found that in the subtropical gyre of the Northwest Pacific Ocean, a combination of N—P or N + P + Fe from the dust was responsible for phytoplankton growth, with large-sized phytoplankton dominating the phytoplankton community (Zhang et al., 2018). The authors added 2 mg L^{-1} of dust to simulate deposition due to a strong dust event (20 g m^{-2}) based on the

annual deposition flux of Asian dust (10 to 80 g m^{-2} yr^{-1}) in the Northwest Pacific Ocean regions (Liu et al., 2013). The enhanced solubility of P from dust or the mineralization of DOP in the seawater contributed to the source of P. During a ten-day study, Lagaria et al. (2017) found similar effects for a single addition of 4 g of Saharan dust compared to repetitive additions (1, 2, and 1 g on days 0, 1, and 2, respectively) to the ultra-oligotrophic waters of the Eastern Mediterranean Sea. The total amount of 4 g of dust represented a realistic atmospheric dust deposition event in the east Mediterranean Sea. The release of dissolved inorganic N and P was responsible for increased chl-a and primary production in both cases. The response of phytoplankton to both dust events evolved through two distinct phases. The initial phase (i.e., 1 to 2 days) after dust addition was marked by an elevated orthophosphate concentration that increased picophytoplankton chl-normalized production rates, whereas the second phase (i.e., 3 to 4 days after dust addition) was marked by elevated N concentrations that increased chl-normalized production rates associated with larger cells (>5 μm).

The Redfield ratio of 106C:16N:1P is the basis for the N:P ratio, which is widely used to determine whether phytoplankton growth in surface waters is N-limited or P-limited. However, the varying trophic states of oceans have made the shift patterns of phytoplankton community structure complex. To illustrate this, Zhang et al. (2019b) conducted bottle incubation experiments with varying concentrations of dust (0.2, 1, and 2 mg L^{-1}) using seawater sampled from the East China Sea (eutrophic region), the subtropical gyre (low-nutrient and low-chlorophyll (LNLC) region), and the Kuroshio-Oyashio transition region (HNLC region) of the Northwest Pacific Ocean. The deposition of N-containing dust to the LNLC (N:P = 3), HNLC (N:P = 14:1), and eutrophic (N:P = 52:1) regions were able to relieve, supplement, and enhance the N demand of phytoplankton, respectively. Despite the differences in the trophic states among these three regions, N from the dust was assimilated by phytoplankton and stimulated their growth. The amount of dust added (0.2, 1, and 2 mg L^{-1}) was based on dust deposition fluxes of 2 g m^{-2} (mild dust events), 10 g m^{-2} (medium dust events), and 20 g m^{-2} (strong dust events) for the Northwest Pacific Ocean (Iwamoto et al., 2011). The addition of 1 and 2 mg L^{-1} of N-containing dust enhanced the chl-a levels and shifted the phytoplankton size structures from picophytoplankton to microphytoplankton (diatoms) in both the HNLC and LNLC regions. These regions exhibited N:P ratios close to the Redfield ratio, allowing diatoms to dominate due to their higher nutrient demands and uptake thresholds compared to smaller cells. The dominance of diatoms can have positive ecological effects as they are relatively efficient in exporting carbon from surface waters to deep oceans. In contrast, in the eutrophic region, increasing concentrations of N-containing dust (1 and 2 mg L^{-1}) shifted the phytoplankton size structures from picophytoplankton to nanophytoplankton (dinoflagellates). The eutrophic region, characterized by high N:P ratios (52:1), was not conducive to diatom growth. Instead, dinoflagellates thrived due to their adaptations to nutrient-limiting environments as a result of their mixotrophic and vertical migration characteristics and higher P uptake efficiency (Zhang et al., 2019b). In the long term, a shift towards a dinoflagellate-dominated community raises serious concerns about the potential for an increase in toxic dinoflagellate species. Similarly, the nutrient status of the western Pacific Ocean is known to switch frequently between oligotrophic and nutrient-rich conditions. Maki et al. (2021) conducted bottle incubation experiments in the oligotrophic and nutrient-rich waters of the western Pacific Ocean during which dust concentrations of 0.05 and 0.25 mg L^{-1} were added to simulate a light and heavy dust event in that region, respectively (Uematsu et al., 1985). In oligotrophic waters, NO_3^- released from the dust increased the chl-a levels and the abundance of diatoms, especially for the *Pseudo-nitzschia* and *Chaetoceros* species. In contrast, nutrient-rich seawater incubations with the added dust showed little increase in the chl-a concentrations, with similar levels to the control/untreated samples.

Depending on the loads of PM deposited, N deposition has the potential to relieve, alter, or intensify N limitation in oceans. For example, bottle incubation experiments conducted in the southern Yellow Sea showed that the addition of 20 mg L^{-1} of dust (N: 0.22 μM, P: 5.0 nM Fe: 245.3 nM) significantly increased the chl-a levels and phytoplankton biomass, which were not apparent at a low dust loading of 2 mg L^{-1} (N: 0.022 μM, P: 0.5 nM Fe: 24.5 nM). The amount of dust added was based on the observational results of the Yellow Sea in 2007 by Shi et al. (2012). The addition of large amounts of dust contributed to the increase in growth through the synergistic effects of N and Fe or the interactions of macronutrients and trace metals (Liu et al., 2013). Zhang et al. (2019a) conducted bottle incubation experiments in the N-limited Northwest Pacific Ocean using haze PM containing dissolved inorganic N (NO_3^-, NO_2^-, and NH_4^+) at low and medium doses (0.03 to 0.6 mg L^{-1}). Low doses (<0.1 mg L^{-1}) simulated a typical PM deposition of ≤1 g m^{-2} into the upper 10 m layer of the water column, while medium doses (0.1 to 0.6 mg L^{-1}) simulated a strong deposition of 1 to 6 g m^{-2} into the upper 10 m layer of the water column. Both low and medium doses of haze PM promoted the growth of phytoplankton and shifted phytoplankton size structure towards nano- and micro-sized cells. Bottle incubation experiments conducted in the East China Sea revealed that PM containing affluent N slightly increased chl-a concentrations under initial N-replete conditions (N:P ~ 50) and a high N:P ratio in PM (>300), thus suggesting the limited impacts of atmospherically deposited N on phytoplankton growth when P was in short supply (Ma et al., 2021). PM with a lower NH_4^+:NO_3^- ratio increased the cell number of two diatom species (*Nitzschia closterium* and *Nitzschia longissima*), while a higher NH_4^+:NO_3^- ratio favored the growth of dinoflagellates, with *Prorocentrum* becoming the most abundant taxa. However, parallel bio-incubation experiments with high concentrations of external N and P revealed increased chl-a concentration, thus suggesting alleviation of P-limitation on phytoplankton growth (Ma et al., 2021). Similar bio-incubation experiments conducted in the East China Sea showed that the addition of 1.5 mg L^{-1} of PM (based on atmospheric deposition values estimated by Mackey et al. (2017)) with 0.375 μM PO_4^{3-} increased the chl-a concentrations by 2 times compared to the addition of PM alone (1.5 mg L^{-1}), thus indicating that affluent N could have been consumed if affluent P was provided from another source (Li et al., 2021).

The effects of atmospheric N deposition on phytoplankton in lakes have received considerably less attention. Even though N-limitation is the natural state of most unproductive lakes, their states can be altered by the levels of atmospheric N deposition. Increased growth of phytoplankton in N-limited lakes has been attributed to elevated inputs of N. Bergström and Jansson (2006) reported that N deposition (100 to 1450 kg km^{-2} yr^{-1}) to various lakes in the northern hemisphere (Europe and North America) resulted in eutrophication and increased phytoplankton biomass (chl-a). An important implication of elevated N-deposition is that it increases N concentrations in surface waters and may shift lakes from N-limited to P-limited or aggravate P-limitation. This was observed in unproductive Swedish lakes where elevated inputs of atmospheric N (100 to 1800 kg km^{-2} yr^{-1}) switched them from N-limited regimes to P-deficient regimes (Bergström et al., 2005). Similarly, atmospheric deposition of N to lakes in Norway, Sweden, and Colorado, USA altered the N:P stoichiometry and shifted nutrient limitation patterns, wherein phytoplankton growth was N-limited under low N deposition conditions and P-limited under high N deposition conditions (Elser et al., 2009a). In some regions, the levels of deposited N that the lakes receive are related to the regional patterns of phytoplankton nutrient restriction. It was found that phytoplankton in unproductive Swedish lakes in the boreal region were N-limited due to the low levels of atmospheric N deposition. This was in contrast to the unproductive lakes in southern Sweden, which were N-rich due to the high levels of atmospheric N deposition (Bergström et al., 2008). In northern Lake Taihu, China, high atmospheric N deposition (157 to 333 kg km^{-2} mon^{-1}) during the seasons of favorable algal growth (summer and autumn) has been hypothesized to foster cyanobacterial blooms (Zhai et al., 2009). From 1969 to 1975,

inorganic N enrichment (0.90 kg ha^{-1} yr^{-1}) in the ultra-oligotrophic Hoh Lake, USA enhanced the relative abundances of sediment diatom assemblages, specifically *Fragilaria tenera* and *Asterionella formosa* (Sheibley et al., 2014). These diatom species indicated N enrichment and were used to determine the threshold level of N deposition.

Bottle incubation studies conducted in Lake Tahoe, USA using PM with high NH_4^+ and low P content and natural phytoplankton assemblages showed that the growths of picophytoplankton and filamentous cyanobacteria were favored, whereas the growths of larger nanophytoplankton only became more competitive when more P was available (Mackey et al., 2013). Nevertheless, picophytoplankton contributed to primary productivity without largely increasing chl-a or biomass. The results of these incubation experiments suggested that picophytoplankton and possibly other phytoplankton were responsible for the increased primary productivity of Lake Tahoe during the Wheeler and Angora Fires. A deposition rate of ~140 mg m^{-2} d^{-1} was used to calculate the amount of PM to be added to the water. Short-term bio incubation experiments conducted by Elser et al. (2009b) showed that elevated inputs of atmospheric N (>6 kg ha^{-1} yr^{-1} based on levels of 6 to 8 kg ha^{-1} annual deposition of inorganic N) to N-limited alpine lakes in the Rocky Mountains of Colorado, USA increased the concentrations of NO_3^- and N:P ratios, which in turn increased phytoplankton biomass, as evident from the increased chl-a and seston C concentrations (Elser et al., 2009b). The high deposition of N in lakes has several ecological implications. First, high N deposition reduces phytoplankton diversity by favoring phytoplankton taxa with a strong competitive ability to uptake and sequestrate P and sustain growth with low cellular P quotas. Second, it affects the food chain, as P-limited phytoplankton are a poor source of food for primary consumers, such as zooplankton.

4.8. Impact of P-containing compounds

P-containing compounds undergo transformations during long-range transport. These transformation processes, which are influenced by PM acidity, aging, cloud processing, and chemical speciation, will ultimately lead to the supply of bioavailable P upon deposition (Diao et al., 2023). Acid processing of mineral dust is the primary mechanism for converting insoluble P to soluble P (Baker et al., 2021; Nenes et al., 2011). Not all forms of P deposited from the atmosphere are solubilized and/or can be assimilated by phytoplankton. DIP, which includes orthophosphates (e.g., $H_2PO_4^-$, HPO_4^{2-}, PO_4^{3-}) and condensed-phase inorganic P (meta-, pyro-, and polyphosphates), is the most bioavailable form of P preferred by phytoplankton for their growth (Myriokefalitakis et al., 2016). The concentrations of DIP are typically low in aquatic environments, and they limit phytoplankton growth. In DIP-limited waters, phytoplankton such as *Emiliania huxleyi*, *Synechococcus* sp., *Thalassiosira* sp., and *Trichodesmium* sp. can use more replete DOP (e.g., phosphate esters) by synthesizing the enzyme alkaline phosphatase, which catalyzes the hydrolysis of DOP into DIP (Ivančić et al., 2010; Liang et al., 2022). In various marine environments, some studies have reported that alkaline phosphatase activity is induced at varying concentration thresholds of DIP. These included <10 nM in the Sargasso Sea (Lomas et al., 2010), 20 nM in the subtropical Pacific (Suzumura et al., 2012), ~30 nM in the eastern subtropical Atlantic (Mahaffey et al., 2014), and 0.1 μM in the northwest African upwelling region (Sebastián et al., 2004).

Studies on the impacts of atmospherically deposited P-containing compounds on phytoplankton are summarized in Table 6. We focused mainly on the impacts of P-containing compounds in PM. P is a limiting nutrient for biological production in oligotrophic waters with low nutrient levels (N:P < 16). Some studies reported that P supplied through atmospheric depositions is negligible compared to N inputs, thus aggravating P-limitation (Chu et al., 2018; Farahat and Abuelgasim, 2019; Zhang et al., 2019b). Chien et al. (2016) conducted incubation experiments in the western tropical Atlantic Ocean, adding P-laden dust at concentrations of 0.06 mg L^{-1} (based on a dust deposition flux of 10 g m^{-2} yr^{-1}) and 1 mg L^{-1} (based on a dust deposition flux of 150 g m^{-2} yr^{-1}) to P-deficient waters. Their results showed that the addition of 0.06 mg L^{-1} dust did not significantly stimulate the growth of *Synechococcus*, picoeukaryotes, or *Prochlorococcus*. Meanwhile, the addition of 1 mg L^{-1} dust increased chl-a slightly, thus indicating that high levels of atmospheric deposition would not alleviate P limitation and promote

Table 6
Effects of atmospherically deposited P-containing compounds on phytoplankton.

Source	Type of experiment	Phytoplankton species/community	Measured Indicator	Major Findings	Reference
Saharan soil	Bottle incubation	Diazotrophs	Nitrogen fixation, and chl-a	DIP from Saharan dust relieved P-limitation of nitrogen fixation	Ridame et al. (2011)
Red Sea (Eilat, Israel), the Sargasso Sea (Tudor Hill, Bermuda), and Monterey Bay (Elkhorn Slough, California)	Bottle incubation	Natural phytoplankton community	Chl-a	Accumulation of DIP in the surface ocean depends on the nutritional needs of phytoplankton	Mackey et al. (2012b)
Ragged Point on the easternmost coast of Barbados	Bottle incubation	*Synechococcus*, and picoeukaryotes *Prochlorococcus*	Chl-a, and cell concentration Cell abundance	*Prochlorococcus* thrived in environment with high N and Fe deposition relative to P as it required low P for its growth	Chien et al. (2016)
Dust from Laoshan campus of Ocean University of China, Qingdao, and rainwater during the cruise in the South China Sea	Bottle incubation	Natural phytoplankton community	Chl-a, and phytoplankton community identification	Trace metals in the dust accelerated the transformation and assimilation of DOP, which increased phytoplankton growth	Chu et al. (2018)
Hunshandake Sandy Land, China	Bottle incubation	Natural phytoplankton community	Phytoplankton abundance	P containing dust induced variable effects on different sizes of phytoplankton	Chen et al. (2019)
Western United States (Arizona, California, Idaho, New Mexico, and Texas)	Laboratory incubation	*Scenedesmus obliquus*	Growth rate, and P cell quota	Phytoplankton acclimatized to higher temperatures and low pH conditions by P-supplied by dust	González-Olalla et al. (2024)
Laoshan campus of Ocean University of China	Bottle incubation	Dinoflagellates	Chl-a, and alkaline phosphatase activity	PM addition alleviated P limitation by promoting the utilization of DOP	Wang et al. (2022)
Sierra Nevada, Spain	Field study	Natural phytoplankton community	Chl-a	A direct correlation between P deposition and chl-a suggested P fertilization in the two alpine lakes	Morales-Baquero et al. (2006)
Sierra Nevada Mountains, Spain	Field study	Natural phytoplankton community	Growth, and species diversity	Pulsed inputs of P and bacterial abundance altered phytoplankton community structure, reducing species diversity	Pulido-Villena et al. (2008)
Southwest, West-Central, and Northwestern regions of Wind River Range, Wyoming, USA	Field study	Natural phytoplankton community	Diatom abundance	Regional variation in P deposition altered the diatom composition	Brahney et al. (2014)

phytoplankton growth in the western tropical Atlantic Ocean. Martino et al. (2014) reported that phytoplankton in the highly P-deficient Western Pacific compensated for P deficiency in PM by consuming some of the residual excess P (i.e., excess P with respect to N compared to the N:P ratio), thereby increasing primary productivity along with N and Fe. Phytoplankton have developed various adaptation mechanisms to cope with P-limited conditions. In the P-limited waters of the Yellow Sea and East China Sea, PM characterized by a high N:P ratio enhanced the growth of dinoflagellates due to their high tolerance to low P concentrations as well as their potential to utilize DOP as a P source by upregulating the synthesis and activity of alkaline phosphatase (Wang et al., 2022). Furthermore, the increased P bioavailability resulting from DOP conversion supported the growth of nanophytoplankton and picophytoplankton. In bottle incubation experiments conducted in the N/P co-limited South China Sea, dust addition (1.09 mg L^{-1} representing the middle of the annual dust deposition range) increased phytoplankton growth, as indicated by the elevated chl-a levels. This growth was likely due to the release of trace metals from the dust, which could have enhanced the transformation and assimilation of DOP by phytoplankton (Chu et al., 2018). Trace metals, particularly Fe and Zn, play vital roles in the P cycle as the enzyme alkaline phosphatase uses either Fe or Zn as a co-factor to increase its activity and facilitate the conversion of DOP to DIP in P-limited waters (Mahaffey et al., 2014). In oligotrophic oceans where Zn, Fe, and P are co-limited, DOP production by alkaline phosphatase can be restricted by Zn and Fe availability. Higher alkaline phosphatase activity has been associated with higher Zn and Fe demands (Shaked et al., 2006; Yong et al., 2014). However, the exact mechanism by which Zn and Fe modulate the enzymatic activity of alkaline phosphatase in P-limited waters remains unknown. Nevertheless, the external deposition of these trace metals can promote alkaline phosphate activity and increase the bioavailability of DOP to phytoplankton.

The biological demand of phytoplankton regulates the accumulation of dissolved P in the surface ocean. Mackey et al. (2012b) conducted bottle incubation experiments using P-containing dust at concentrations of 5, 25, and 50 μg total suspended particulate L^{-1} in the Red Sea and 167 μg total suspended particulate L^{-1} in the Sargasso Sea. These concentrations were based on the annual average deposition rate for the Sargasso Sea, the equatorial North Atlantic, or a high deposition event equivalent to 10 times the annual average deposition rate for the Sargasso Sea. The concentrations in the Red Sea incubation studies were based on a high deposition event 10 times higher than the annual average deposition rate. The addition of dust to the P-limited Red Sea increased DIP concentrations, which were assimilated by phytoplankton, as indicated by a significant increase in the chl-a levels. In contrast, in the Sargasso Sea where phytoplankton are not P-limited, DIP concentrations exceeded the growth requirements of phytoplankton, resulting in DIP accumulation due to the biological mineralization of DOP to DIP (Mackey et al., 2012b). Similarly, in bottle incubation experiments conducted in the P-limited Yellow Sea, Chen et al. (2019) reported that the addition of sand-dust (2 and 20 mg L^{-1}, based on observational data from Shi et al. (2012)) or inorganic P-containing compounds (sodium dihydrogen phosphate) led to an increased abundance of large-sized (10 to 20 μm) phytoplankton during the early stages of incubation due to the abundance of P. This increase was more pronounced with the addition of 20 mg L^{-1} dust because of the continuous P supply. However, this growth tapered off in the later stages as the nutritional needs of phytoplankton were met. Ridame et al. (2011) reported that the addition of 1.1 mg L^{-1} of Saharan dust, representing a realistic dust deposition of 8 g m^{-2}, was a significant source of DIP in the Mediterranean Sea, relieving the P-limitation of nitrogen fixation. In laboratory experiments conducted by González-Olalla et al. (2024), increasing concentrations of P-laden dust (0, 10, 25, and 75 mg L^{-1}) corresponding to an extreme dust deposition event were incubated with freshwater phytoplankton *Scenedesmus obliquus* at different pHs (6.3, 6.8, and 7.3) and temperatures (19, 23, and 27 °C). A higher growth rate was observed at a dust concentration of 75 mg L^{-1}, 27 °C, and pH 6.3 due to the increased P cell content. In the same study, the authors corroborated the role of P-containing dust in altering the pH and thermal tolerance range of *Scenedesmus obliquus*. They found that P-containing dust enhanced pH and thermal tolerance in *Scenedesmus obliquus*. The optimal temperature for *Scenedesmus obliquus* growth increased from 22.94 °C without dust addition to 24.66 °C after 75 mg dust L^{-1} was added at pH 6.3. This indicated that the dust supplied the necessary nutrients for phytoplankton to cope with thermal stress. Likewise, the negative effect of low pH (6.3) on phytoplankton growth under no dust addition became positive under 75 mg L^{-1} dust addition and high temperature due to the positive effect of warming and nutrient availability on phytoplankton growth. Interactions between nutrients, temperature, and pH influence the competitive ability of different phytoplankton species.

Excess atmospheric N deposition is widely assumed to cause P-limitation of phytoplankton growth in lakes (Elser et al., 2009a; Goldman, 1988). However, in the Pyrenean lakes in Spain and the Sierra Nevada lakes in the USA, atmospheric P deposition is outpacing the N deposition, leading to scenarios of N-limiting phytoplankton growth (Camarero and Catalan, 2012; Vicars et al., 2010). Vicars et al. (2010) estimated a dry depositional flux of total P ranging between 7 and 118 μg m^{-2} d^{-1} to the Sierra Nevada lakes. Due to their extreme oligotrophic conditions, alpine lakes are susceptible to atmospheric deposition, with P deposition being the primary nutrient driving phytoplankton growth. Morales-Baquero et al. (2006) reported significant correlations between P deposition (dry and wet deposition ranging from 0.1 to 3.1 μmol m^{-2} d^{-1} and 0 to 2.4 μmol m^{-2} d^{-1}, respectively) by Saharan dust and chl-a levels in two alpine lakes (La Caldera and Río Seco) in Sierra Nevada, Spain, thus confirming the fertilizing efficiency of Saharan dust. Pulsed inputs of dust containing soluble P (dry and wet deposition ranging from <0.06 to 1.9 and 0 to 1 μmol m^{-2} d^{-1}, respectively) to a La Caldera alpine lake in the Sierra Nevada, USA increased the biomass of the chrysophyte *Chromulina nevadensis*, causing a decline in the phytoplankton species diversity (Pulido-Villena et al., 2008). This response of *Chromulina nevadensis* to P inputs was attributed to the coupled dynamic between bacteria abundance and P inputs. *Chromulina nevadensis* could have benefited from the co-existing bacterioplankton, which successfully competed for pulsed P inputs and increased their abundance. Mixotrophic phytoplankton benefited from increased bacteria abundance to access P directly from the bacteria through phagotrophic ingestion, thus increasing the *Chromulina nevadensis* biomass. Brahney et al. (2014) observed distinct phytoplankton species (diatom) composition patterns influenced by regional variations in P deposition in the alpine and subalpine lakes within the Wind River Range, Wyoming, USA. The southwestern region, when experiencing higher atmospheric dust P deposition fluxes (276 μg m^{-2} d^{-1}), exhibited a unique diatom species assemblage with higher concentrations of *Asterionella formosa*, *Pseudostaurosira pseudoconstruens*, and *Pseudostaurosira brevistriata.* Notably, *Asterionella formosa* had the highest cell number. In contrast, lakes in the other regions were dominated by other diatom species, namely, *Discostella stelligera* and *Stauroseira construens venter*.

4.9. Impact of S-containing compounds

The effects of S-containing compounds on phytoplankton have been less explored than the fore-discussed atmospheric species. Among the various S-containing compounds, SO_4^{2-} has been given the most attention. Satellite imaging showed an increase in chl-a following the eruption of the Miyake-Jima Volcano in Japan, which indicated that SO_4^{2-} deposition increased phytoplankton abundance in the nutrient-deficient zone south of the Kuroshio (Uematsu et al., 2004). In the study conducted by Kumari et al. (2022), the addition of PM containing SO_4^{2-} and NO_3^- to surface seawater collected from the Bay of Bengal led to a decrease in pH, which increased primary production, thus indicating that acidification of seawater promoted phytoplankton production. However, additional experiments conducted to understand the

individual impacts of pH and nutrients revealed that a decrease in pH accounted for a 22 % increase in primary production, whereas NO_3^- contributed to a 78 % increase in primary production. The increased primary production significantly increased photosynthetic pigments such as fucoxanthin and chl-b. Even though some field studies reported high concentrations of SO_4^{2-} in the deposited PM, the individual effects of SO_4^{2-} on phytoplankton were not discussed (Li et al., 2021; Tan et al., 2019).

There is some evidence that reductions in SO_4^{2-} deposition due to decreased SO_2 emissions could alter the abundance of phytoplankton species. For example, Sutherland et al. (2015) hypothesized that a decrease in SO_4^{2-} deposition in Brooktrout Lake, USA between 1980 and 2000 caused the water column pH to increase above 5.5 and enrich acid-sensitive phytoplankton species. In addition, atmospheric SO_4^{2-} deposition in Pockwock Lake, Canada decreased by 68 % from 1999 to 2015, thus increasing pH by 0.1 to 0.4 units. This chemical recovery of the lake from acidification favored the growth of geosmin-producing cyanobacterial species (*Anabaena*) that thrive in pH conditions between 6 and 9 (Anderson et al., 2017).

5. Conclusion and future directions

This review highlights the impacts of different compounds commonly found in atmospheric PM on phytoplankton. There have been several studies on the effects of the deposition of N-containing compounds, P-containing compounds, Fe, and Cu, but comparatively fewer studies on the impacts of other trace metals (e.g., Al, Zn) and S-containing compounds. Based on our observations, bottle incubation studies using natural phytoplankton assemblages were the preferred choice for assessing the impacts of N-containing and P-containing compounds. Both bottle and laboratory incubations were used to assess the impacts of trace metals. Marine ecosystems (oceans and seas) received greater attention than freshwater ecosystems (lakes). Bio-incubation experiments suggested that the deposition of atmospheric PM to surface waters would exert different effects on phytoplankton, which include positive effects by N, P, and Fe and negative (or toxic) effects by other trace metals (Cu, Al, and Zn). The relative composition of deposited atmospheric chemical species enhanced the growth of some phytoplankton species over others. Multiple endpoints, such as morphological changes, membrane potential, and enzymatic responses beyond growth responses (chl-a determination), were typically considered when assessing the impacts of trace metals on phytoplankton.

There are several knowledge gaps on the impacts of atmospheric PM deposition on phytoplankton that should be considered and addressed in future studies.

1. More studies should be done to assess the impacts of other trace metals and S-containing compounds.
2. Most nutrient release studies from dust and PM have mainly focused on soluble inorganic nutrients and typically do not consider their organic forms. Studies assessing the impacts of organic forms of N, P, and S on phytoplankton are limited. Future studies should compare the impacts of soluble inorganic versus soluble organic forms of N-containing compounds, P-containing compounds, and S-containing compounds on phytoplankton growth and community structure across aquatic ecosystems. Additionally, while there have been some studies on how polyaromatic hydrocarbons impact phytoplankton (Campos et al., 2012; Sheesley et al., 2005; Silva et al., 2015), research on other organic species in PM is scarce. Understanding the effects of organic compounds on phytoplankton is crucial, as phytoplankton searches for alternative sources of nutrients (mostly organic) when inorganic nutrients are depleted. Given that organic compounds comprise a large mass fraction of PM in many parts of the world (Zhang et al., 2007), future investigations must prioritize assessing the effects of atmospherically deposited ubiquitous organic compounds in PM on phytoplankton.
3. Organic species in PM can also transform via different aging mechanisms during atmospheric transport before deposition into aquatic systems. Moreover, after their deposition, these organic compounds can transform during their reactions with photochemically produced oxidants such as singlet oxygen ($^1O_2$) and excited states of chromophoric organic matter (^{3}CDOM*) present at the water surface. More research is required on the transformations and fates of atmospheric organic species before and after their deposition into aquatic ecosystems to better assess the actual exposure of phytoplankton to these organic species and their transformation products.
4. Marine ecosystems have been given more attention than freshwater ecosystems. Since phytoplankton species differ between marine and freshwater ecosystems, bottle incubation studies are needed to assess the impact of atmospheric chemical species on the freshwater natural phytoplankton community.
5. Climate change will likely alter environmental conditions (e.g., ocean acidification, warming, deoxygenation), affecting phytoplankton differently (Xin et al., 2022, 2019). However, only a few studies have considered these abiotic factors during their impact assessments. Future studies should consider these abiotic stressors when evaluating the impacts of atmospheric chemical species on phytoplankton.
6. In addition to implementing emission control strategies to reduce atmospheric deposition, modern innovative technologies such as the nitrifying-enriched activated sludge approach could be utilized for nutrient removal in eutrophic environments (Sepehri et al., 2020; Sepehri and Sarrafzadeh, 2019, 2018). Additionally, future research should aim to develop similar types of technologies to remove other contaminants deposited from the atmosphere.
7. Microplastics in the air and the leachates or contaminants that come off their surfaces could set off pathways that could endanger phytoplankton. While studies related to atmospheric microplastics are still emerging, direct toxicological investigations into the impacts of microplastics on phytoplankton suggest potential negative effects. Although there has been some evidence of the deposition of airborne microplastics in countries such as China (Cai et al., 2017; Liu et al., 2019), Germany (Klein and Fischer, 2019), France (Dris et al., 2016), and nonurban remote regions (mountain catchments in the French Pyrenees) (Allen et al., 2019), investigations into their ecological risk are currently lacking. Thus, more research is required to determine the effects of the atmospheric deposition of microplastics on phytoplankton.
8. Extensive in-depth bio-incubation assays with multiple endpoints beyond growth assessment (chl-a measurements) are needed to assess the acute and chronic effects of atmospherically deposited species.
9. Much of our current knowledge of the mechanisms by which atmospheric PM induces toxic effects comes from conventional, hypothesis-driven methods concentrating on well-established endpoint assays. However, it is challenging to identify molecular targets and novel pathways that underlie the toxicological response to intricate environmental exposures utilizing this approach. Thus, in addition to these conventional, hypothesis-driven methods, "omics technologies" such as proteomics and genomics could help strengthen the basis for the toxicological findings.

CRediT authorship contribution statement

Vignesh Thiagarajan: Writing – original draft, Investigation, Conceptualization. **Theodora Nah:** Writing – review & editing, Supervision, Resources, Funding acquisition, Conceptualization. **Xiaying Xin:** Writing – review & editing, Conceptualization.

Declaration of competing interest

The authors declare the following financial interests/personal

relationships which may be considered as potential competing interests: Theodora Nah reports financial support was provided by State Key Laboratory of Marine Pollution (SKLMP). Theodora Nah reports financial support was provided by Guangdong Basic and Applied Basic Research Fund Committee. If there are other authors, they declare that they have no known competing financial interests or personal relationships that could have appeared to influence the work reported in this paper.

Data availability

No data was used for the research described in the article.

Acknowledgements

This work was supported by the Guangdong Basic and Applied Basic Research Fund Committee (project number 2020B1515130003) and the State Key Laboratory of Marine Pollution (SKLMP) Director Discretionary Fund. The authors are particularly grateful to the editors and the anonymous reviewers for their insightful comments and suggestions.

References

Achterberg, E.P., Moore, C.M., Henson, S.A., Steigenberger, S., Stohl, A., Eckhardt, S., Avendano, L.C., Cassidy, M., Hembury, D., Klar, J.K., Lucas, M.I., MacEy, A.I., Marsay, C.M., Ryan-Keogh, T.J., 2013. Natural iron fertilization by the Eyjafjallajökull volcanic eruption. Geophys. Res. Lett. 40, 921–926. https://doi.org/10.1002/grl.50221.

Aguilar-Islas, A.M., Wu, J., Rember, R., Johansen, A.M., Shank, L.M., 2010. Dissolution of aerosol-derived iron in seawater: leach solution chemistry, aerosol type, and colloidal iron fraction. Mar. Chem. 120, 25–33. https://doi.org/10.1016/j.marchem.2009.01.011.

Al-Abadleh, H.A., Kubicki, J.D., Meskhidze, N., 2022. A Perspective on iron (Fe) in the Atmosphere: Air Quality, Climate, and the Ocean. Sci. Process. Impacts, Environ. https://doi.org/10.1039/d2em00176d.

Allen, S., Allen, D., Phoenix, V.R., Le Roux, G., Durántez Jiménez, P., Simonneau, A., Binet, S., Galop, D., 2019. Atmospheric transport and deposition of microplastics in a remote mountain catchment. Nat. Geosci. 12, 339–344. https://doi.org/10.1038/s41561-019-0335-5.

Anderson, L.E., Krkošek, W.H., Stoddart, A.K., Trueman, B.F., Gagnon, G.A., 2017. Lake recovery through reduced sulfate deposition: a new paradigm for drinking water treatment. Environ. Sci. Technol. 51, 1414–1422. https://doi.org/10.1021/acs.est.6b04889.

Baker, A.R., Kanakidou, M., Nenes, A., Myriokefalitakis, S., Croot, P.L., Duce, R.A., Gao, Y., Guieu, C., Ito, A., Jickells, T.D., Mahowald, N.M., Middag, R., Perron, M.M.G., Sarin, M.M., Shelley, R., Turner, D.R., 2021. Changing Atmospheric Acidity as a Modulator of Nutrient Deposition and Ocean Biogeochemistry. Adv, Sci. https://doi.org/10.1126/sciadv.abd8800.

Barber-Lluch, E., Nieto-Cid, M., Santos-Echeandía, J., Sánchez-Marín, P., 2023. Effect of dissolved organic matter on copper bioavailability to a coastal dinoflagellate at environmentally relevant concentrations. Sci. Total Environ. 901, 165989 https://doi.org/10.1016/j.scitotenv.2023.165989.

Basu, S., Gledhill, M., de Beer, D., Prabhu Matondkar, S.G., Shaked, Y., 2019. Colonies of marine cyanobacteria Trichodesmium interact with associated bacteria to acquire iron from dust. Commun. Biol. 2, 1–8. https://doi.org/10.1038/s42003-019-0534-z.

Bauer, S.E., Koch, D., Unger, N., Metzger, S.M., Shindell, D.T., Streets, D.G., 2007. Nitrate aerosols today and in 2030: a global simulation including aerosols and tropospheric ozone. Atmos. Chem. Phys. 7, 5043–5059. https://doi.org/10.5194/acp-7-5043-2007.

Bergström, A.K., Jansson, M., 2006. Atmospheric nitrogen deposition has caused nitrogen enrichment and eutrophication of lakes in the northern hemisphere. Glob. Chang. Biol. 12, 635–643. https://doi.org/10.1111/j.1365-2486.2006.01129.x.

Bergström, A.K., Blomqvist, P., Jansson, M., 2005. Effects of atmospheric nitrogen deposition on nutrient limitation and phytoplankton biomass in unproductive Swedish lakes. Limnol. Oceanogr. 50, 987–994. https://doi.org/10.4319/lo.2005.50.3.0987.

Bergström, A.K., Jonsson, A., Jansson, M., 2008. Phytoplankton responses to nitrogen and phosphorus enrichment in unproductive Swedish lakes along a gradient of atmospheric nitrogen deposition. Aquat. Biol. 4, 55–64. https://doi.org/10.3354/ab00099.

Bhattarai, H., Saikawa, E., Wan, X., Zhu, H., Ram, K., Gao, S., Kang, S., Zhang, Q., Zhang, Y., Wu, G., Wang, X., Kawamura, K., Fu, P., Cong, Z., 2019. Levoglucosan as a tracer of biomass burning: recent progress and perspectives. Atmos. Res. 220, 20–33. https://doi.org/10.1016/J.ATMOSRES.2019.01.004.

Bianco, A., Vaïtilingom, M., Bridoux, M., Chaumerliac, N., Pichon, J.M., Piro, J.L., Deguillaume, L., 2017. Trace metals in cloud water sampled at the puy de Dôme Station. Atmosphere (Basel). 8, 225. https://doi.org/10.3390/atmos8110225.

Biswas, H., Bandyopadhyay, D., 2017. Physiological responses of coastal phytoplankton (Visakhapatnam, SW Bay of Bengal, India) to experimental copper addition. Mar. Environ. Res. 131, 19–31. https://doi.org/10.1016/j.marenvres.2017.09.008.

Blain, S., Guieu, C., Claustre, H., Leblanc, K., Moutin, T., Quéguiner, B., Ras, J., Sarthou, G., 2004. Availability of iron and major nutrients for phytoplankton in the Northeast Atlantic Ocean. Limnol. Oceanogr. 49, 2095–2104. https://doi.org/10.4319/lo.2004.49.6.2095.

Boyer, J.N., Kelble, C.R., Ortner, P.B., Rudnick, D.T., 2009. Phytoplankton bloom status: chlorophyll a biomass as an indicator of water quality condition in the southern estuaries of Florida. USA. Ecol. Indic. 9, S56–S67. https://doi.org/10.1016/j.ecolind.2008.11.013.

Brahney, J., Ballantyne, A.P., Kociolek, P., Spaulding, S., Otu, M., Porwoll, T., Neff, J.C., 2014. Dust mediated transfer of phosphorus to alpine lake ecosystems of the Wind River range, Wyoming, USA. Biogeochemistry 120, 259–278. https://doi.org/10.1007/s10533-014-9994-x.

Brand, L.E., Sunda, W.G., Guillard, R.R.L., 1986. Reduction of marine phytoplankton reproduction rates by copper and cadmium. J. Exp. Mar. Bio. Ecol. 96, 225–250. https://doi.org/10.1016/0022-0981(86)90205-4.

Brown, S.S., Stutz, J., 2012. Nighttime radical observations and chemistry. Chem. Soc. Rev. 41, 6405–6447. https://doi.org/10.1039/c2cs35181a.

Browning, T.J., Bouman, H.A., Henderson, G.M., Mather, T.A., Pyle, D.M., Schlosser, C., Woodward, E.M.S., Moore, C.M., 2014. Strong responses of Southern Ocean phytoplankton communities to volcanic ash. Geophys. Res. Lett. 41, 2851–2857. https://doi.org/10.1002/2014GL059364.

Brüggemann, M., Xu, R., Tilgner, A., Kwong, K.C., Mutzel, A., Poon, H.Y., Otto, T., Schaefer, T., Poulain, L., Chan, M.N., Herrmann, H., 2020. Organosulfates in ambient aerosol: state of knowledge and future research directions on formation, abundance, fate, and importance. Environ. Sci. Technol. 54, 3767–3782. https://doi.org/10.1021/acs.est.9b06751.

Buck, C.S., Landing, W.M., Resing, J.A., Measures, C.I., 2010. The solubility and deposition of aerosol Fe and other trace elements in the North Atlantic Ocean: observations from the A16N CLIVAR/CO2 repeat hydrography section. Mar. Chem. 120, 57–70. https://doi.org/10.1016/j.marchem.2008.08.003.

Butler, T., Lupascu, A., Nalam, A., 2020. Attribution of ground-level ozone to anthropogenic and natural sources of nitrogen oxides and reactive carbon in a global chemical transport model. Atmos. Chem. Phys. 20, 10707–10731. https://doi.org/10.5194/acp-20-10707-2020.

Cai, L., Wang, J., Peng, J., Tan, Z., Zhan, Z., Tan, X., Chen, Q., 2017. Characteristic of microplastics in the atmospheric fallout from Dongguan city, China: preliminary research and first evidence. Environ. Sci. Pollut. Res. 24, 24928–24935. https://doi.org/10.1007/s11356-017-0116-x.

Camarero, L., Catalan, J., 2012. Atmospheric phosphorus deposition may cause lakes to revert from phosphorus limitation back to nitrogen limitation. Nat. Commun. 2012 31 3, 1–5. doi:https://doi.org/10.1038/ncomms2125.

Campos, I., Abrantes, N., Vidal, T., Bastos, A.C., Gonçalves, F., Keizer, J.J., 2012. Assessment of the toxicity of ash-loaded runoff from a recently burnt eucalypt plantation. Eur. J. For. Res. 131, 1889–1903. https://doi.org/10.1007/s10342-012-0640-7.

Carstensen, J., Heiskanen, A.S., 2007. Phytoplankton responses to nutrient status: application of a screening method to the northern Baltic Sea. Mar. Ecol. Prog. Ser. 336, 29–42. https://doi.org/10.3354/meps336029.

Chen, H., Grassian, V.H., 2013. Iron dissolution of dust source materials during simulated acidic processing: the effect of sulfuric, acetic, and oxalic acids. Environ. Sci. Technol. 47, 10312–10321. https://doi.org/10.1021/es401285s.

Chen, Y., Tovar-Sanchez, A., Siefert, R.L., Sañudo-Wilhelmy, S.A., Zhuang, G., 2011. Luxury uptake of aerosol iron by Trichodesmium in the western tropical North Atlantic. Geophys. Res. Lett. 38 https://doi.org/10.1029/2011GL048972.

Chen, X., Liu, G.X., Huang, X., Chen, H.J., Zhang, C., Zhao, Y.G., 2019. Effects of asian dust and phosphorus input on abundance and trophic structure of protists in the southern Yellow Sea. Water (Switzerland) 11, 1188. https://doi.org/10.3390/w11061188.

Chester, R., Nimmo, M., Preston, M.R., 1999. The trace metal chemistry of atmospheric dry deposition samples collected at cap Ferrat: a coastal site in the Western Mediterranean. Mar. Chem. 68, 15–30. https://doi.org/10.1016/S0304-4203(99)00062-6.

Chu, Q., Liu, Y., Shi, J., Zhang, C., Gong, X., Yao, X., Guo, X., Gao, H., 2018. Promotion effect of Asian dust on phytoplankton growth and potential dissolved organic phosphorus utilization in the South China Sea. J. Geophys. Res. Biogeo. 123, 1101–1116. https://doi.org/10.1002/2017JG004088.

Conway, T.M., Hoffmann, L.J., Breitbarth, E., Strzepek, R.F., Wolff, E.W., 2016. The growth response of two diatom species to atmospheric dust from the last glacial maximum. PloS One 11, e0158553. https://doi.org/10.1371/journal.pone.0158553.

Corrêa, A.X.R., Testolin, R.C., Torres, M.M., Cotelle, S., Schwartz, J.J., Millet, M., Radetski, C.M., 2017. Ecotoxicity assessment of particulate matter emitted from heavy-duty diesel-powered vehicles: influence of leaching conditions. Environ. Sci. Pollut. Res. 24, 9399–9406. https://doi.org/10.1007/S11356-017-8521-8/TABLES/4.

Cotiyane-Pondo, P., Bornman, T.G., 2021. Environmental heterogeneity determines diatom colonisation on artificial substrata: implications for biomonitoring in coastal marine waters. Front. Ecol. Evol. 9, 877. https://doi.org/10.3389/fevo.2021.767960.

Cui, D.Y., Wang, J.T., Tan, L.J., Dong, Z.Y., 2016. Impact of atmospheric wet deposition on phytoplankton community structure in the South China Sea. Estuar. Coast. Shelf Sci. 173, 1–8. https://doi.org/10.1016/j.ecss.2016.02.011.

Da Silva Souza, T., Christofoletti, C.A., Bozzatto, V., Fontanetti, C.S., 2014. The use of diplopods in soil ecotoxicology - a review. Ecotoxicol. Environ. Saf. https://doi.org/10.1016/j.ecoenv.2013.10.025.

Dai, Q., Bi, X., Song, W., Li, T., Liu, B., Ding, J., Xu, J., Song, C., Yang, N., Schulze, B.C., Zhang, Y., Feng, Y., Hopke, P.K., 2019. Residential coal combustion as a source of primary sulfate in Xi'an. China. Atmos. Environ. 196, 66–76. https://doi.org/10.1016/J.ATMOSENV.2018.10.002.

De Oliveira, T.T.S., Andreu, I., Machado, M.C., Vimbela, G., Tripathi, A., Bose, A., 2020. Interaction of Cyanobacteria with Nanometer and Micron Sized Polystyrene Particles in Marine and Fresh Water. Langmuir 36, 3963–3969. https://doi.org/10.1021/acs.langmuir.9b03644.

Diao, X., Widory, D., Ram, K., Tripathee, L., Bikkina, S., Kawamura, K., Gao, S., Wan, X., Wu, G., Pei, Q., Wang, X., Cong, Z., 2023. Atmospheric phosphorus and its geochemical cycling: fundamentals, progress, and perspectives. Earth-Science Rev. https://doi.org/10.1016/j.earscirev.2023.104492.

Dominguez, G., Jackson, T., Brothers, L., Barnett, B., Nguyen, B., Thiemens, M.H., 2008. Discovery and measurement of an isotopically distinct source of sulfate in Earth's atmosphere. Proc. Natl. Acad. Sci. U. S. A. 105, 12769–12773. https://doi.org/10.1073/pnas.0805255105.

Dris, R., Gasperi, J., Saad, M., Mirande, C., Tassin, B., 2016. Synthetic fibers in atmospheric fallout: a source of microplastics in the environment? Mar. Pollut. Bull. 104, 290–293. https://doi.org/10.1016/j.marpolbul.2016.01.006.

Duce, R.A., Liss, P.S., Merrill, J.T., Atlas, E.L., Buat-Menard, P., Hicks, B.B., Miller, J.M., Prospero, J.M., Arimoto, R., Church, T.M., Ellis, W., Galloway, J.N., Hansen, L., Jickells, T.D., Knap, A.H., Reinhardt, K.H., Schneider, B., Soudine, A., Tokos, J.J., Tsunogai, S., Wollast, R., Zhou, M., 1991. The atmospheric input of trace species to the world ocean. Global Biogeochem. Cycles 5, 193–259. https://doi.org/10.1029/91GB01778.

Duce, R.A., LaRoche, J., Altieri, K., Arrigo, K.R., Baker, A.R., Capone, D.G., Cornell, S., Dentener, F., Galloway, J., Ganeshram, R.S., Geider, R.J., Jickells, T., Kuypers, M.M., Langlois, R., Liss, P.S., Liu, S.M., Middelburg, J.J., Moore, C.M., Nickovic, S., Oschlies, A., Pedersen, T., Prospero, J., Schlitzer, R., Seitzinger, S., Sorensen, L.L., Uematsu, M., Ulloa, O., Voss, M., Ward, B., Zamora, L., 2008. Impacts of atmospheric anthropogenic nitrogen on the open ocean. Science 80-.). 320, 893–897. https://doi.org/10.1126/science.1150369.

Duggen, S., Croot, P., Schacht, U., Hoffmann, L., 2007. Subduction zone volcanic ash can fertilize the surface ocean and stimulate phytoplankton growth: evidence from biogeochemical experiments and satellite data. Geophys. Res. Lett. 34, 1612. https://doi.org/10.1029/2006GL027522.

Echeveste, P., Croot, P., von Dassow, P., 2018. Differences in the sensitivity to cu and ligand production of coastal vs offshore strains of Emiliania huxleyi. Sci. Total Environ. 625, 1673–1680. https://doi.org/10.1016/j.scitotenv.2017.10.050.

Eichner, M., Basu, S., Wang, S., de Beer, D., Shaked, Y., 2020. Mineral iron dissolution in Trichodesmium colonies: the role of O2 and pH microenvironments. Limnol. Oceanogr. 65, 1149–1160. https://doi.org/10.1002/lno.11377.

Elser, J.J., Andersen, T., Baron, J.S., Bergström, A.K., Jansson, M., Kyle, M., Nydick, K.R., Steger, L., Hessen, D.O., 2009a. Shifts in lake N: P stoichiometry and nutrient limitation driven by atmospheric nitrogen deposition. Science 80-.). 326, 835–837. https://doi.org/10.1126/science.1176199.

Elser, J.J., Kyle, M., Steuer, L., Nydick, K.R., Baron, J.S., 2009b. Nutrient availability and phytoplankton nutrient limitation across a gradient of atmospheric nitrogen deposition. Ecology 90, 3062–3073. https://doi.org/10.1890/08-1742.1.

Fabiańska, M.J., Kozielska, B., Konieczyński, J., Bielaczyc, P., 2019. Occurrence of organic phosphates in particulate matter of the vehicle exhausts and outdoor environment – a case study. Environ. Pollut. 244, 351–360. https://doi.org/10.1016/j.envpol.2018.10.060.

Fan, W., Chen, T., Zhu, Z., Zhang, H., Qiu, Y., Yin, D., 2022. A review of secondary organic aerosols formation focusing on organosulfates and organic nitrates. J. Hazard. Mater. 430, 128406 https://doi.org/10.1016/j.jhazmat.2022.128406.

Fang, T., Guo, H., Zeng, L., Verma, V., Nenes, A., Weber, R.J., 2017. Highly acidic ambient particles, soluble metals, and oxidative potential: a link between sulfate and aerosol toxicity. Environ. Sci. Technol. 51, 2611–2620. https://doi.org/10.1021/acs.est.6b06151.

Farahat, A., Abuelgasim, A., 2019. Role of atmospheric nutrient pollution in stimulating phytoplankton growth in small area and shallow depth water bodies: Arabian gulf and the sea of Oman. Atmos. Environ. 219, 117045 https://doi.org/10.1016/j.atmosenv.2019.117045.

Fenn, M.E., Bytnerowicz, A., Schilling, S.L., Vallano, D.M., Zavaleta, E.S., Weiss, S.B., Morozumi, C., Geiser, L.H., Hanks, K., 2018. On-road emissions of ammonia: An underappreciated source of atmospheric nitrogen deposition. Sci. Total Environ. 625, 909–919. https://doi.org/10.1016/j.scitotenv.2017.12.313.

Fry, J.L., Draper, D.C., Zarzana, K.J., Campuzano-Jost, P., Day, D.A., Jimenez, J.L., Brown, S.S., Cohen, R.C., Kaser, L., Hansel, A., Cappellin, L., Karl, T., Hodzic Roux, A., Turnipseed, A., Cantrell, C., Lefer, B.L., Grossberg, N., 2013. Observations of gas- and aerosol-phase organic nitrates at BEACHON-RoMBAS 2011. Atmos. Chem. Phys. 13, 8585–8605. https://doi.org/10.5194/acp-13-8585-2013.

Fung, I.Y., Meyn, S.K., Tegen, I., Doney, S.C., John, J.G., Bishop, J.K.B., 2000. Iron supply and demand in the upper ocean. Global Biogeochem. Cycles 14, 281–295. https://doi.org/10.1029/1999gb900059.

Fuzzi, S., Baltensperger, U., Carslaw, K., Decesari, S., Denier Van Der Gon, H., Facchini, M.C., Fowler, D., Koren, I., Langford, B., Lohmann, U., Nemitz, E., Pandis, S., Riipinen, I., Rudich, Y., Schaap, M., Slowik, J.G., Spracklen, D.V., Vignati, E., Wild, M., Williams, M., Gilardoni, S., 2015. Particulate matter, air quality and climate: lessons learned and future needs. Atmos. Chem. Phys. https://doi.org/10.5194/acp-15-8217-2015.

Gao, Y., Kaufman, Y.J., Tanré, D., Kolber, D., Falkowski, P.G., 2001. Seasonal distributions of Aeolian iron fluxes to the global ocean. Geophys. Res. Lett. 28, 29–32. https://doi.org/10.1029/2000GL011926.

Gao, J., Shi, G., Zhang, Z., Wei, Y., Tian, X., Feng, Y., Russell, A.G., Nenes, A., 2022. Targeting atmospheric oxidants can better reduce sulfate aerosol in China: H2O2Aqueous oxidation pathway dominates sulfate formation in haze. Environ. Sci. Technol. 56, 10608–10618. https://doi.org/10.1021/acs.est.2c01739.

Gebara, R.C., Alho, L. de O.G., Rocha, G.S., Mansano, A. da S., Melão, M. da G.G., 2020. Zinc and aluminum mixtures have synergic effects to the algae Raphidocelis subcapitata at environmental concentrations. Chemosphere 242, 125231. doi: https://doi.org/10.1016/j.chemosphere.2019.125231.

Gebara, R.C., Alho, L. de O.G., Mansano, A. da S., Rocha, G.S., Melão, M. da G.G., 2023. Single and combined effects of Zn and Al on photosystem II of the green microalgae Raphidocelis subcapitata assessed by pulse-amplitude modulated (PAM) fluorometry. Aquat. Toxicol. 254, 106369. doi:https://doi.org/10.1016/j.aquatox.2022.106369.

Glasius, M., Thomsen, D., Wang, K., Iversen, L.S., Duan, J., Huang, R.J., 2022. Chemical characteristics and sources of organosulfates, organosulfonates, and carboxylic acids in aerosols in urban Xi'an. Northwest China. Sci. Total Environ. 810, 151187 https://doi.org/10.1016/j.scitotenv.2021.151187.

Glibert, P.M., Wilkerson, F.P., Dugdale, R.C., Raven, J.A., Dupont, C.L., Leavitt, P.R., Parker, A.E., Burkholder, J.M., Kana, T.M., 2016. Pluses and minuses of ammonium and nitrate uptake and assimilation by phytoplankton and implications for productivity and community composition, with emphasis on nitrogen-enriched conditions. Limnol. Oceanogr. 61, 165–197. https://doi.org/10.1002/lno.10203.

Goldman, C.R., 1988. Primary productivity, nutrients, and transparency during the early onset of eutrophication in ultra-oligotrophic Lake Tahoe. Califomia-Nevada. Limnol. Oceanogr. 33, 1321–1333. https://doi.org/10.4319/lo.1988.33.6.1321.

González-Olalla, J.M., Powell, J.A., Brahney, J., 2024. Dust storms increase the tolerance of phytoplankton to thermal and pH changes. Glob. Chang. Biol. 30, e17055 https://doi.org/10.1111/gcb.17055.

Graham, W.F., Duce, R.A., 1979. Atmospheric pathways of the phosphorus cycle. Geochim. Cosmochim. Acta 43, 1195–1208. https://doi.org/10.1016/0016-7037(79)90112-1.

Greaver, T.L., Sullivan, T.J., Herrick, J.D., Barber, M.C., Baron, J.S., Cosby, B.J., Deerhake, M.E., Dennis, R.L., Dubois, J.J.B., Goodale, C.L., Herlihy, A.T., Lawrence, G.B., Liu, L., Lynch, J.A., Novak, K.J., 2012. Ecological effects of nitrogen and sulfur air pollution in the US: what do we know? Front. Ecol. Environ. https://doi.org/10.1890/110049.

Grennfelt, P., Hultberg, H., 1986. Effects of nitrogen deposition on the acidification of terrestrial and aquatic ecosystems. Water Air Soil Pollut. 30, 945–963. https://doi.org/10.1007/BF00303359/METRICS.

Gualtieri, M., Andrioletti, M., Vismara, C., Milani, M., Camatini, M., 2005. Toxicity of tire debris leachates. Environ. Int. 31, 723–730. https://doi.org/10.1016/j.envint.2005.02.001.

Guieu, C., Dulac, F., Desboeufs, K., Wagener, T., Pulido-Villena, E., Grisoni, J.M., Louis, F., Ridame, C., Blain, S., Brunet, C., Bon Nguyen, E., Tran, S., Labiadh, M., Dominici, J.M., 2010. Large clean mesocosms and simulated dust deposition: a new methodology to investigate responses of marine oligotrophic ecosystems to atmospheric inputs. Biogeosciences 7, 2765–2784. https://doi.org/10.5194/bg-7-2765-2010.

Guieu, C., Dulac, F., Ridame, C., Pondaven, P., 2014. Introduction to project DUNE, a DUst experiment in a low nutrient, low chlorophyll ecosystem. Biogeosciences 11, 425–442. https://doi.org/10.5194/bg-11-425-2014.

Hamilton, D.S., Moore, J.K., Arneth, A., Bond, T.C., Carslaw, K.S., Hantson, S., Ito, A., Kaplan, J.O., Lindsay, K., Nieradzik, L., Rathod, S.D., Scanza, R.A., Mahowald, N.M., 2020. Impact of changes to the atmospheric soluble Iron deposition flux on ocean biogeochemical cycles in the Anthropocene. Global Biogeochem. Cycles 34, e2019GB006448. https://doi.org/10.1029/2019GB006448.

Harrison, R.M., Jones, A.M., Gietl, J., Yin, J., Green, D.C., 2012. Estimation of the contributions of brake dust, tire wear, and resuspension to nonexhaust traffic particles derived from atmospheric measurements. Environ. Sci. Technol. 46, 6523–6529. https://doi.org/10.1021/es300894r.

Hauglustaine, D.A., Balkanski, Y., Schulz, M., 2014. A global model simulation of present and future nitrate aerosols and their direct radiative forcing of climate. Atmos. Chem. Phys. 14, 11031–11063. https://doi.org/10.5194/acp-14-11031-2014.

Hawkins, L.N., Russell, L.M., Covert, D.S., Quinn, P.K., Bates, T.S., 2010. Carboxylic acids, sulfates, and organosulfates in processed continental organic aerosol over the Southeast Pacific Ocean during VOCALS-REx 2008. J. Geophys. Res. Atmos. 115, 13201. https://doi.org/10.1029/2009JD013276.

Heald, C.L., Collett, J.L., Lee, T., Benedict, K.B., Schwandner, F.M., Li, Y., Clarisse, L., Hurtmans, D.R., Van Damme, M., Clerbaux, C., Coheur, P.F., Philip, S., Martin, R.V., Pye, H.O.T., 2012. Atmospheric ammonia and particulate inorganic nitrogen over the United States. Atmos. Chem. Phys. 12, 10295–10312. https://doi.org/10.5194/acp-12-10295-2012.

Heaviside, C., Witham, C., Vardoulakis, S., 2021. Potential health impacts from Sulphur dioxide and sulphate exposure in the UK resulting from an Icelandic effusive volcanic eruption. Sci. Total Environ. 774, 145549 https://doi.org/10.1016/J.SCITOTENV.2021.145549.

Hessen, D.O., 2013. Inorganic nitrogen deposition and its impacts on N: P-ratios and lake productivity. Water (Switzerland). https://doi.org/10.3390/w5020327.

Hettiarachchi, E., Ivanov, S., Kieft, T., Goldstein, H.L., Moskowitz, B.M., Reynolds, R.L., Rubasinghege, G., 2021. Atmospheric processing of Iron-bearing mineral dust aerosol and its effect on growth of a marine diatom, Cyclotella meneghiniana. Environ. Sci. Technol. 55, 871–881. https://doi.org/10.1021/acs.est.0c06995.

Hien, T.T., Chi, N.D.T., Huy, D.H., Le, H.A., Oram, D.E., Forster, G.L., Mills, G.P., Baker, A.R., 2022. Soluble trace metals associated with atmospheric fine particulate matter in the two most populous cities in Vietnam. Atmos. Environ. X 15, 100178. https://doi.org/10.1016/j.aeaoa.2022.100178.

Hoffmann, L.J., Breitbarth, E., Ardelan, M.V., Duggen, S., Olgun, N., Hassellöv, M., Wängberg, S.Å., 2012. Influence of trace metal release from volcanic ash on growth of Thalassiosira pseudonana and Emiliania huxleyi. Mar. Chem. 132–133, 28–33. https://doi.org/10.1016/J.MARCHEM.2012.02.003.

Hu, S.M., 2021. Trace gas measurements using cavity ring-down spectroscopy, in: Advances in Spectroscopic Monitoring of the Atmosphere. Elsevier, pp. 413–441. doi:https://doi.org/10.1016/B978-0-12-815014-6.00002-6.

Huang, W., Saathoff, H., Shen, X., Ramisetty, R., Leisner, T., Mohr, C., 2019. Chemical characterization of highly functionalized Organonitrates contributing to night-time organic aerosol mass loadings and particle growth. Environ. Sci. Technol. 53, 1165–1174. https://doi.org/10.1021/acs.est.8b05826.

Isley, C.F., Taylor, M.P., 2020. Atmospheric remobilization of natural and anthropogenic contaminants during wildfires. Environ. Pollut. 267, 115400 https://doi.org/10.1016/j.envpol.2020.115400.

Ito, A., 2015. Atmospheric processing of combustion aerosols as a source of bioavailable iron. Environ. Sci. Technol. Lett. 2, 70–75. https://doi.org/10.1021/acs.estlett.5b00007.

Ito, A., Miyakawa, T., 2023. Aerosol Iron from metal production as a secondary source of bioaccessible Iron. Environ. Sci. Technol. 57, 4091–4100. https://doi.org/10.1021/acs.est.2c06472.

Ito, A., Shi, Z., 2016. Delivery of anthropogenic bioavailable iron from mineral dust and combustion aerosols to the ocean. Atmos. Chem. Phys. 16, 85–99. https://doi.org/10.5194/acp-16-85-2016.

Ito, A., Lin, G., Penner, J.E., 2014. Reconciling modeled and observed atmospheric deposition of soluble organic nitrogen at coastal locations. Global Biogeochem. Cycles 28, 617–630. https://doi.org/10.1002/2013GB004721.

Ito, A., Lin, G., Penner, J.E., 2015. Global modeling study of soluble organic nitrogen from open biomass burning. Atmos. Environ. 121, 103–112. https://doi.org/10.1016/j.atmosenv.2015.01.031.

Ivančić, I., Fuks, D., Radić, T., Lyons, D.M., Šilović, T., Kraus, R., Precali, R., 2010. Phytoplankton and bacterial alkaline phosphatase activity in the northern Adriatic Sea. Mar. Environ. Res. 69, 85–94. https://doi.org/10.1016/j.marenvres.2009.08.004.

Iwamoto, Y., Yumimoto, K., Toratani, M., Tsuda, A., Miura, K., Uno, I., Uematsu, M., 2011. Biogeochemical implications of increased mineral particle concentrations in surface waters of the northwestern North Pacific during an Asian dust event. Geophys. Res. Lett. 38 https://doi.org/10.1029/2010GL045906.

Jani, J., Toor, G.S., 2018. Composition, sources, and bioavailability of nitrogen in a longitudinal gradient from freshwater to estuarine waters. Water Res. 137, 344–354. https://doi.org/10.1016/j.watres.2018.02.042.

Jiang, S.Y.N., Yang, F., Chan, K.L., Ning, Z., 2014. Water solubility of metals in coarse PM and PM2.5 in typical urban environment in Hong Kong. Atmos. Pollut. Res. 5, 236–244. https://doi.org/10.5094/APR.2014.029.

Jiang, H., Li, J., Tang, J., Cui, M., Zhao, S., Mo, Y., Tian, C., Zhang, X., Jiang, B., Liao, Y., Chen, Y., Zhang, G., 2022. Molecular characteristics, sources, and formation pathways of organosulfur compounds in ambient aerosol in Guangzhou, South China. Atmos. Chem. Phys. 22, 6919–6935. https://doi.org/10.5194/acp-22-6919-2022.

Jickells, T., Moore, C.M., 2015. The importance of atmospheric deposition for ocean productivity. Annu. Rev. Ecol. Evol. Syst. 46, 481–501. https://doi.org/10.1146/annurev-ecolsys-112414-054118.

Jickells, T.D., Buitenhuis, E., Altieri, K., Baker, A.R., Capone, D., Duce, R.A., Dentener, F., Fennel, K., Kanakidou, M., LaRoche, J., Lee, K., Liss, P., Middelburg, J.J., Moore, J. K., Okin, G., Oschlies, A., Sarin, M., Seitzinger, S., Sharples, J., Singh, A., Suntharalingam, P., Uematsu, M., Zamora, L.M., 2017. A reevaluation of the magnitude and impacts of anthropogenic atmospheric nitrogen inputs on the ocean. Global Biogeochem. Cycles 31, 289–305. https://doi.org/10.1002/2016GB005586.

Johnson, Z.I., Lin, Y., 2009. Prochlorococcus: Approved for export. Proc. Natl. Acad. Sci. U. S. A. https://doi.org/10.1073/pnas.0905187106.

Johnson, M.S., Meskhidze, N., 2013. Atmospheric dissolved iron deposition to the global oceans: effects of oxalate-promoted Fe dissolution, photochemical redox cycling, and dust mineralogy. Geosci. Model Dev. 6, 1137–1155. https://doi.org/10.5194/gmd-6-1137-2013.

Jordi, A., Basterretxea, G., Tovar-Sánchez, A., Alastuey, A., Querol, X., 2012. Copper aerosols inhibit phytoplankton growth in the Mediterranean Sea. Proc. Natl. Acad. Sci. U. S. A. 109, 21246–21249. https://doi.org/10.1073/pnas.1207567110.

Journet, E., Desboeufs, K.V., Caquineau, S., Colin, J.L., 2008. Mineralogy as a critical factor of dust iron solubility. Geophys. Res. Lett. 35, 7805. https://doi.org/10.1029/2007GL031589.

Kanakidou, M., Duce, R.A., Prospero, J.M., Baker, A.R., Benitez-Nelson, C., Dentener, F. J., Hunter, K.A., Liss, P.S., Mahowald, N., Okin, G.S., Sarin, M., Tsigaridis, K., Uematsu, M., Zamora, L.M., Zhu, T., 2012. Atmospheric fluxes of organic N and P to the global ocean. Global Biogeochem. Cycles 26, 3026. https://doi.org/10.1029/2011GB004277.

Kanakidou, M., Myriokefalitakis, S., Tsigaridis, K., 2018. Aerosols in atmospheric chemistry and biogeochemical cycles of nutrients. Environ. Res. Lett. https://doi.org/10.1088/1748-9326/aabcdb.

Karagulian, F., Belis, C.A., Dora, C.F.C., Prüss-Ustün, A.M., Bonjour, S., Adair-Rohani, H., Amann, M., 2015. Contributions to cities' ambient particulate matter (PM): a systematic review of local source contributions at global level. Atmos. Environ. 120, 475–483. https://doi.org/10.1016/J.ATMOSENV.2015.08.087.

Karl, D.M., Björkman, K.M., 2015. Dynamics of dissolved organic phosphorus. In: Biogeochemistry of Marine Dissolved Organic Matter, Second edition. Academic Press, pp. 233–334. https://doi.org/10.1016/B978-0-12-405940-5.00005-4.

Kessler, N., Armoza-Zvuloni, R., Wang, S., Basu, S., Weber, P.K., Stuart, R.K., Shaked, Y., 2019. Selective collection of iron-rich dust particles by natural Trichodesmium colonies. ISME J. 2019 141 14, 91–103. doi:https://doi.org/10.1038/s41396-019-0505-x.

Kirichenko, K., Zakharenko, A., Pikula, K., Chaika, V., Markina, Z., Orlova, T., Medvedev, S., Waissi, G., Kholodov, A., Tsatsakis, A., Golokhvast, K., 2019. Dependence of welding fume particle toxicity on electrode type and current intensity assessed by microalgae growth inhibition test. Environ. Res. 179, 108818 https://doi.org/10.1016/j.envres.2019.108818.

Klein, M., Fischer, E.K., 2019. Microplastic abundance in atmospheric deposition within the metropolitan area of Hamburg. Germany. Sci. Total Environ. 685, 96–103. https://doi.org/10.1016/J.SCITOTENV.2019.05.405.

Krishnamurthy, A., Moore, J.K., Zender, C.S., Luo, C., 2007. Effects of atmospheric inorganic nitrogen depostion on ocean biogeochemistry. J. Geophys. Res. Biogeo. 112, 2019. https://doi.org/10.1029/2006JG000334.

Krom, M.D., Shi, Z., Stockdale, A., Berman-Frank, I., Giannakourou, A., Herut, B., Lagaria, A., Papageorgiou, N., Pitta, P., Psarra, S., Rahav, E., Scoullos, M., Stathopoulou, E., Tsiola, A., Tsagaraki, T.M., 2016. Response of the eastern mediterranean microbial ecosystem to dust and dust affected by acid processing in the atmosphere. Front. Mar. Sci. 3, 213314 https://doi.org/10.3389/fmars.2016.00133.

Kumari, V.R., Neeraja, B., Rao, D.N., Ghosh, V.R.D., Rajula, G.R., Sarma, V.V.S.S., 2022. Impact of atmospheric dry deposition of nutrients on phytoplankton pigment composition and primary production in the coastal bay of Bengal. Environ. Sci. Pollut. Res. 29, 82218–82231. https://doi.org/10.1007/s11356-022-21477-3.

Kuttippurath, J., Singh, A., Dash, S.P., Mallick, N., Clerbaux, C., Van Damme, M., Clarisse, L., Coheur, P.F., Raj, S., Abbhishek, K., Varikoden, H., 2020. Record high levels of atmospheric ammonia over India: spatial and temporal analyses. Sci. Total Environ. 740, 139986 https://doi.org/10.1016/J.SCITOTENV.2020.139986.

Lagaria, A., Mandalakis, M., Mara, P., Papageorgiou, N., Pitta, P., Tsiola, A., Kagiorgi, M., Psarra, S., 2017. Phytoplankton response to Saharan dust depositions in the eastern Mediterranean Sea: a mesocosm study. Front. Mar. Sci. 3, 287. https://doi.org/10.3389/FMARS.2016.00287.

Lazo, P., Stafilov, T., Qarri, F., Allajbeu, S., Bekteshi, L., Frontasyeva, M., Harmens, H., 2019. Spatial distribution and temporal trend of airborne trace metal deposition in Albania studied by moss biomonitoring. Ecol. Indic. 101, 1007–1017. https://doi.org/10.1016/j.ecolind.2018.11.053.

Li, J., Zhang, Y.L., Cao, F., Zhang, W., Fan, M., Lee, X., Michalski, G., 2020. Stable sulfur isotopes revealed a major role of transition-metal ion-catalyzed SO2 oxidation in haze episodes. Environ. Sci. Technol. 54, 2626–2634. https://doi.org/10.1021/acs.est.9b07150.

Li, H., Chen, Y., Zhou, S., Wang, F., Yang, T., Zhu, Y., Ma, Q., 2021. Change of dominant phytoplankton groups in the eutrophic coastal sea due to atmospheric deposition. Sci. Total Environ. 753, 141961 https://doi.org/10.1016/j.scitotenv.2020.141961.

Li, G.B., Cai, S.H., Long, B., 2022. New reactions for the formation of organic nitrate in the atmosphere. ACS Omega 7, 39671–39679. https://doi.org/10.1021/acsomega.2c03321.

Li, Y., Fu, T.M., Yu, J.Z., Yu, X., Chen, Q., Miao, R., Zhou, Y., Zhang, A., Ye, J., Yang, X., Tao, S., Liu, H., Yao, W., 2023. Dissecting the contributions of organic nitrogen aerosols to global atmospheric nitrogen deposition and implications for ecosystems. Natl. Sci. Rev. 10 https://doi.org/10.1093/nsr/nwad244.

Liang, Z., McCabe, K., Fawcett, S.E., Forrer, H.J., Hashihama, F., Jeandel, C., Marconi, D., Planquette, H., Saito, M.A., Sohm, J.A., Thomas, R.K., Letscher, R.T., Knapp, A.N., 2022. A global ocean dissolved organic phosphorus concentration database (DOPv2021). Sci. Data 9, 1–9. https://doi.org/10.1038/s41597-022-01873-7.

Lin, S., Litaker, R.W., Sunda, W.G., 2016. Phosphorus physiological ecology and molecular mechanisms in marine phytoplankton. J. Phycol. 52, 10–36. https://doi.org/10.1111/jpy.12365.

Ligowski, R., Jordan, R.W., Assmy, P., 2012. Morphological adaptation of a planktonic diatom to growth in Antarctic sea ice. Mar. Biol. 159, 817–827. https://doi.org/10.1007/s00227-011-1857-6.

Lin, C., Huang, R.J., Duan, J., Zhong, H., Xu, W., 2021. Primary and secondary organic nitrate in Northwest China: a case study. Environ. Sci. Technol. Lett. 8, 947–953. https://doi.org/10.1021/acs.estlett.1c00692.

Lis, H., Shaked, Y., Kranzler, C., Keren, N., Morel, F.M.M., 2015. Iron bioavailability to phytoplankton: An empirical approach. ISME J. 9, 1003–1013. https://doi.org/10.1038/ismej.2014.199.

Liu, Y., Zhang, T.R., Shi, J.H., Gao, H.W., Yao, X.H., 2013. Responses of chlorophyll a to added nutrients, Asian dust, and rainwater in an oligotrophic zone of the Yellow Sea: implications for promotion and inhibition effects in an incubation experiment. J. Geophys. Res. Biogeo. 118, 1763–1772. https://doi.org/10.1002/2013JG002329.

Liu, C., Li, J., Zhang, Y., Wang, L., Deng, J., Gao, Y., Yu, L., Zhang, J., Sun, H., 2019. Widespread distribution of PET and PC microplastics in dust in urban China and their estimated human exposure. Environ. Int. 128, 116–124. https://doi.org/10.1016/j.envint.2019.04.024.

Liu, L., Liu, Y., Wen, W., Liang, L., Ma, X., Jiao, J., Guo, K., 2020a. Source identification of trace elements in PM2.5 at a rural site in the North China plain. Atmosphere (Basel). 11, 179. https://doi.org/10.3390/atmos11020179.

Liu, P., Ye, C., Xue, C., Zhang, C., Mu, Y., Sun, X., 2020b. Formation mechanisms of atmospheric nitrate and sulfate during the winter haze pollution periods in Beijing: gas-phase, heterogeneous and aqueous-phase chemistry. Atmos. Chem. Phys. 20, 4153–4165. https://doi.org/10.5194/ACP-20-4153-2020.

Liu, M., Shang, F., Lu, X., Huang, X., Song, Y., Liu, B., Zhang, Q., Liu, X., Cao, J., Xu, T., Wang, T., Xu, Z., Xu, W., Liao, W., Kang, L., Cai, X., Zhang, H., Dai, Y., Zhu, T., 2022. Unexpected response of nitrogen deposition to nitrogen oxide controls and implications for land carbon sink. Nat. Commun. 13, 1–10. https://doi.org/10.1038/s41467-022-30854-y.

Lomas, M.W., Burke, A.L., Lomas, D.A., Bell, D.W., Shen, C., Dyhrman, S.T., Ammerman, J.W., 2010. Sargasso Sea phosphorus biogeochemistry: An important role for dissolved organic phosphorus (DOP). Biogeosciences 7, 695–710. https://doi.org/10.5194/bg-7-695-2010.

Lovett, G.M., 1994. Atmospheric deposition of nutrients and pollutants in North America: An ecological perspective. Ecol. Appl. 4, 629–650. https://doi.org/10.2307/1941997.

Luḱacs, H., Gelencśer, A., Hoffer, A., Kiss, G., Horv́ath, K., Hartýani, Z., 2009. Quantitative assessment of organosulfates in size-segregated rural fine aerosol. Atmos. Chem. Phys. 9, 231–238. doi:https://doi.org/10.5194/acp-9-231-2009.

Ma, Q., Chen, Y., Wang, F., Li, H., 2021. Responses of primary productivity and phytoplankton community to the atmospheric nutrient deposition in the East China Sea. Atmosphere (Basel). 12, 210. https://doi.org/10.3390/atmos12020210.

Maberly, S.C., Van de Waal, D.B., Raven, J.A., 2022. Phytoplankton Growth and Nutrients, in: Encyclopedia of Inland Waters. Elsevier, pp. 130–138. doi:https://doi.org/10.1016/B978-0-12-819166-8.00111-0.

Maciejczyk, P., Chen, L.C., Thurston, G., 2021. The role of fossil fuel combustion metals in PM2.5 air pollution health associations. Atmosphere (Basel). doi:https://doi.org/10.3390/atmos12091086.

Mackey, K.R.M., Buck, K.N., Casey, J.R., Cid, A., Lomas, M.W., Sohrin, Y., Paytan, A., 2012a. Phytoplankton responses to atmospheric metal deposition in the coastal and open-ocean Sargasso Sea. Front. Microbiol. 3, 359. https://doi.org/10.3389/fmicb.2012.00359.

Mackey, K.R.M., Roberts, K., Lomas, M.W., Saito, M.A., Post, A.F., Paytan, A., 2012b. Enhanced solubility and ecological impact of atmospheric phosphorus deposition upon extended seawater exposure. Environ. Sci. Technol. 46, 10438–10446. https://doi.org/10.1021/es3007996.

Mackey, K.R.M., Hunter, D., Fischer, E.V., Jiang, Y., Allen, B., Chen, Y., Liston, A., Reuter, J., Schladow, G., Paytan, A., 2013. Aerosol-nutrient-induced picoplankton growth in Lake Tahoe. J. Geophys. Res. Biogeo. 118, 1054–1067. https://doi.org/10.1002/jgrg.20084.

Mackey, K.R.M., Kavanaugh, M.T., Wang, F., Chen, Y., Liu, F., Glover, D.M., Te Chien, C., Paytan, A., 2017. Atmospheric and fluvial nutrients fuel algal blooms in the East China Sea. Front. Mar. Sci. 4, 225820 https://doi.org/10.3389/fmars.2017.00002.

Mahaffey, C., Reynolds, S., Davis, C.E., Lohan, M.C., 2014. Alkaline phosphatase activity in the subtropical ocean: insights from nutrient, dust and trace metal addition experiments. Front. Mar. Sci. 1, 122793 https://doi.org/10.3389/fmars.2014.00073.

Mahowald, N., Jickells, T.D., Baker, A.R., Artaxo, P., Benitez-Nelson, C.R., Bergametti, G., Bond, T.C., Chen, Y., Cohen, D.D., Herut, B., Kubilay, N., Losno, R., Luo, C., Maenhaut, W., McGee, K.A., Okin, G.S., Siefert, R.L., Tsukuda, S., 2008. Global distribution of atmospheric phosphorus sources, concentrations and deposition rates, and anthropogenic impacts. Global Biogeochem. Cycles 22. https://doi.org/10.1029/2008GB003240.

Mahowald, N.M., Hamilton, D.S., Mackey, K.R.M., Moore, J.K., Baker, A.R., Scanza, R.A., Zhang, Y., 2018. Aerosol trace metal leaching and impacts on marine microorganisms. Nat. Commun. 2018 91 9, 1–15. doi:https://doi.org/10.1038/s41467-018-04970-7.

Maki, T., Ishikawa, A., Mastunaga, T., Pointing, S.B., Saito, Y., Kasai, T., Watanabe, K., Aoki, K., Horiuchi, A., Lee, K.C., Hasegawa, H., Iwasaka, Y., 2016. Atmospheric aerosol deposition influences marine microbial communities in oligotrophic surface waters of the western Pacific Ocean. Deep. Res. Part I Oceanogr. Res. Pap. 118, 37–45. https://doi.org/10.1016/j.dsr.2016.10.002.

Maki, T., Lee, K.C., Pointing, S.B., Watanabe, K., Aoki, K., Archer, S.D.J., Lacap-Bugler, D.C., Ishikawa, A., 2021. Desert and anthropogenic mixing dust deposition influences microbial communities in surface waters of the western Pacific Ocean. Sci. Total Environ. 791, 148026 https://doi.org/10.1016/j.scitotenv.2021.148026.

Martino, M., Hamilton, D., Baker, A.R., Jickells, T.D., Bromley, T., Nojiri, Y., Quack, B., Boyd, P.W., 2014. Western Pacific atmospheric nutrient deposition fluxes, their impact on surface ocean productivity. Global Biogeochem. Cycles 28, 712–728. https://doi.org/10.1002/2013GB004794.

Mastin, J., Saini, A., Schuster, J.K., Harner, T., Dabek-Zlotorzynska, E., Celo, V., Gaga, E. O., 2023. Trace metals in global air: first results from the GAPS and GAPS megacities networks. Environ. Sci. Technol. 57, 14661–14673. https://doi.org/10.1021/acs.est.3c05733.

Mélançon, J., Levasseur, M., Lizotte, M., Delmelle, P., Cullen, J., Hamme, R.C., Peña, A., Simpson, K.G., Scarratt, M., Tremblay, J.É., Zhou, J., Johnson, K., Sutherland, N., Arychuk, M., Nemcek, N., Robert, M., 2014. Early response of the northeast subarctic Pacific plankton assemblage to volcanic ash fertilization. Limnol. Oceanogr. 59, 55–67. https://doi.org/10.4319/lo.2014.59.1.0055.

Mélançon, J., Levasseur, M., Lizotte, M., Scarratt, M., Tremblay, J.É., Tortell, P., Yang, G. P., Shi, G.Y., Gao, H., Semeniuk, D., Robert, M., Arychuk, M., Johnson, K., Sutherland, N., Davelaar, M., Nemcek, N., Peña, A., Richardson, W., 2016. Impact of ocean acidification on phytoplankton assemblage, growth, and DMS production following Fe-dust additions in the NE Pacific high-nutrient, low-chlorophyll waters. Biogeosciences 13, 1677–1692. https://doi.org/10.5194/bg-13-1677-2016.

Meng, Y., Wang, S., Wang, Z., Ye, N., Fang, H., 2018. Algal toxicity of binary mixtures of zinc oxide nanoparticles and tetrabromobisphenol a: roles of dissolved organic matters. Environ. Toxicol. Pharmacol. 64, 78–85. https://doi.org/10.1016/j.etap.2018.09.010.

Meskhidze, N., Völker, C., Al-Abadleh, H.A., Barbeau, K., Bressac, M., Buck, C., Bundy, R. M., Croot, P., Feng, Y., Ito, A., Johansen, A.M., Landing, W.M., Mao, J., Myriokefalitakis, S., Ohnemus, D., Pasquier, B., Ye, Y., 2019. Perspective on identifying and characterizing the processes controlling iron speciation and residence time at the atmosphere-ocean interface. Mar. Chem. 217, 103704 https://doi.org/10.1016/j.marchem.2019.103704.

Metzler, D.M., Li, M., Erdem, A., Huang, C.P., 2011. Responses of algae to photocatalytic nano-TiO2 particles with an emphasis on the effect of particle size. Chem. Eng. J. 170, 538–546. https://doi.org/10.1016/j.cej.2011.02.002.

Miller-Schulze, J.P., Shafer, M., Schauer, J.J., Heo, J., Solomon, P.A., Lantz, J., Artamonova, M., Chen, B., Imashev, S., Sverdlik, L., Carmichael, G., DeMinter, J., 2015. Seasonal contribution of mineral dust and other major components to particulate matter at two remote sites in Central Asia. Atmos. Environ. 119, 11–20. https://doi.org/10.1016/j.atmosenv.2015.07.011.

Mills, M.M., Ridame, C., Davey, M., La Roche, J., Geider, R.J., 2004. Iron and phosphorus co-limit nitrogen fixation in the eastern tropical North Atlantic. Nature 429, 292–294. https://doi.org/10.1038/nature02550.

Moffett, J.W., Brand, L.E., 1996. Production of strong, extracellular cu chelators by marine cyanobacteria in response to cu stress. Limnol. Oceanogr. 41, 388–395. https://doi.org/10.4319/lo.1996.41.3.0388.

Molina, L.T., 2021. Introductory lecture: air quality in megacities. Faraday Discuss. 226, 9–52. https://doi.org/10.1039/D0FD00123F.

Moon, A., Jongebloed, U., Dingilian, K.K., Schauer, A.J., Chan, Y.-C., Cesler-Maloney, M., Simpson, W.R., Weber, R.J., Tsiang, L., Yazbeck, F., Zhai, S., Wedum, A., Turner, A. J., Albertin, S., Bekki, S., Savarino, J., Gribanov, K., Pratt, K.A., Costa, E.J., Anastasio, C., Sunday, M.O., Heinlein, L.M.D., Mao, J., Alexander, B., 2023. Primary Sulfate Is the Dominant Source of Particulate Sulfate during Winter in Fairbanks. ACS ES&T Air, Alaska. https://doi.org/10.1021/acsestair.3c00023.

Morales-Baquero, R., Pulido-Villena, E., Reche, I., 2006. Atmospheric inputs of phosphorus and nitrogen to the Southwest Mediterranean region: biogeochemical responses of high mountain lakes. Limnol. Oceanogr. 51, 830–837. https://doi.org/10.4319/lo.2006.51.2.0830.

Moser, K.A., Mordecai, J.S., Reynolds, R.L., Rosenbaum, J.G., Ketterer, M.E., 2010. Diatom changes in two Uinta mountain lakes, Utah, USA: responses to anthropogenic and natural atmospheric inputs. Hydrobiologia 648, 91–108. https://doi.org/10.1007/s10750-010-0145-7.

Mukhtar, A., Limbeck, A., 2013. Recent developments in assessment of bio-accessible trace metal fractions in airborne particulate matter: a review. Anal. Chim. Acta. https://doi.org/10.1016/j.aca.2013.02.008.

Myriokefalitakis, S., Daskalakis, N., Mihalopoulos, N., Baker, A.R., Nenes, A., Kanakidou, M., 2015. Changes in dissolved iron deposition to the oceans driven by human activity: a 3-D global modelling study. Biogeosciences 12, 3973–3992. https://doi.org/10.5194/bg-12-3973-2015.

Myriokefalitakis, S., Nenes, A., Baker, A.R., Mihalopoulos, N., Kanakidou, M., 2016. Bioavailable atmospheric phosphorous supply to the global ocean: a 3-D global modeling study. Biogeosciences 13, 6519–6543. https://doi.org/10.5194/bg-13-6519-2016.

Myriokefalitakis, S., Ito, A., Kanakidou, M., Nenes, A., Krol, M.C., Mahowald, N.M., Scanza, R.A., Hamilton, D.S., Johnson, M.S., Meskhidze, N., Kok, J.F., Guieu, C., Baker, A.R., Jickells, T.D., Sarin, M.M., Bikkina, S., Shelley, R., Bowie, A., Perron, M. M.G., Duce, R.A., 2018. Reviews and syntheses: the GESAMP atmospheric iron deposition model intercomparison study. Biogeosciences. https://doi.org/10.5194/bg-15-6659-2018.

Myriokefalitakis, S., Gröger, M., Hieronymus, J., Döscher, R., 2020. An explicit estimate of the atmospheric nutrient impact on global oceanic productivity. Ocean Sci. 16, 1183–1205. https://doi.org/10.5194/os-16-1183-2020.

Nair, A.A., Yu, F., 2020. Quantification of atmospheric ammonia concentrations: a review of its measurement and modeling. Atmosphere (Basel). https://doi.org/10.3390/atmos11101092.

Nawrot, N., Wojciechowska, E., Rezania, S., Walkusz-Miotk, J., Pazdro, K., 2020. The effects of urban vehicle traffic on heavy metal contamination in road sweeping waste and bottom sediments of retention tanks. Sci. Total Environ. 749, 141511 https://doi.org/10.1016/j.scitotenv.2020.141511.

Nenes, A., Krom, M.D., Mihalopoulos, N., Van Cappellen, P., Shi, Z., Bougiatioti, A., Zarmpas, P., Herut, B., 2011. Atmospheric acidification of mineral aerosols: a source of bioavailable phosphorus for the oceans. Atmos. Chem. Phys. 11, 6265–6272. https://doi.org/10.5194/acp-11-6265-2011.

Ng, N.L., Brown, S.S., Archibald, A.T., Atlas, E., Cohen, R.C., Crowley, J.N., Day, D.A., Donahue, N.M., Fry, J.L., Fuchs, H., Griffin, R.J., Guzman, M.I., Herrmann, H., Hodzic, A., Iinuma, Y., Kiendler-Scharr, A., Lee, B.H., Luecken, D.J., Mao, J., McLaren, R., Mutzel, A., Osthoff, H.D., Ouyang, B., Picquet-Varrault, B., Platt, U., Pye, H.O.T., Rudich, Y., Schwantes, R.H., Shiraiwa, M., Stutz, J., Thornton, J.A., Tilgner, A., Williams, B.J., Zaveri, R.A., 2017. Nitrate radicals and biogenic volatile organic compounds: oxidation, mechanisms, and organic aerosol. Atmos. Chem. Phys. 17, 2103–2162. https://doi.org/10.5194/acp-17-2103-2017.

Okin, G.S., Baker, A.R., Tegen, I., Mahowald, N.M., Dentener, F.J., Duce, R.A., Galloway, J.N., Hunter, K., Kanakidou, M., Kubilay, N., Prospero, J.M., Sarin, M., Surapipith, V., Uematsu, M., Zhu, T., 2011. Impacts of atmospheric nutrient deposition on marine productivity: roles of nitrogen, phosphorus, and iron. Global Biogeochem. Cycles 25. https://doi.org/10.1029/2010GB003858.

Pacyna, J.M., 2008. Atmospheric deposition. Encycl. Ecol. Five-Volume Set 275–285. https://doi.org/10.1016/B978-008045405-4.00258-5.

Page, T.S., Almeda, R., Koski, M., Bournaka, E., Nielsen, T.G., 2022. Toxicity of Tyre wear particle leachates to marine phytoplankton. Aquat. Toxicol. 252, 106299 https://doi.org/10.1016/j.aquatox.2022.106299.

Pant, P., Harrison, R.M., 2013. Estimation of the contribution of road traffic emissions to particulate matter concentrations from field measurements: a review. Atmos. Environ. https://doi.org/10.1016/j.atmosenv.2013.04.028.
Paytan, A., Mackey, K.R.M., Chen, Y., Lima, I.D., Doney, S.C., Mahowald, N., Labiosa, R., Post, A.F., 2009. Toxicity of atmospheric aerosols on marine phytoplankton. Proc. Natl. Acad. Sci. U. S. A. 106, 4601–4605. https://doi.org/10.1073/pnas.0811486106.
Pikula, K.S., Chernyshev, V.V., Zakharenko, A.M., Chaika, V.V., Waissi, G., Hai, L.H., Hien, T.T., Tsatsakis, A.M., Golokhvast, K.S., 2019. Toxicity assessment of particulate matter emitted from different types of vehicles on marine microalgae. Environ. Res. 179, 108785 https://doi.org/10.1016/j.envres.2019.108785.
Pikula, K., Kirichenko, K., Vakhniuk, I., Kalantzi, O.I., Kholodov, A., Orlova, T., Markina, Z., Tsatsakis, A., Golokhvast, K., 2021. Aquatic toxicity of particulate matter emitted by five electroplating processes in two marine microalgae species. Toxicol. Reports 8, 880–887. https://doi.org/10.1016/j.toxrep.2021.04.004.
Piscitello, A., Bianco, C., Casasso, A., Sethi, R., 2021. Non-exhaust traffic emissions: sources, characterization, and mitigation measures. Sci. Total Environ. https://doi.org/10.1016/j.scitotenv.2020.144440.
Platt, S.M., El Haddad, I., Pieber, S.M., Zardini, A.A., Suarez-Bertoa, R., Clairotte, M., Daellenbach, K.R., Huang, R.J., Slowik, J.G., Hellebust, S., Temime-Roussel, B., Marchand, N., De Gouw, J., Jimenez, J.L., Hayes, P.L., Robinson, A.L., Baltensperger, U., Astorga, C., Prévôt, A.S.H., 2017. Gasoline cars produce more carbonaceous particulate matter than modern filter-equipped diesel cars. Sci. Rep. 7, 1–9. https://doi.org/10.1038/s41598-017-03714-9.
Pöschl, U., 2005. Atmospheric aerosols: composition, transformation, climate and health effects. Angew. Chemie - Int. Ed. https://doi.org/10.1002/anie.200501122.
Prospero, J.M., Ginoux, P., Torres, O., Nicholson, S.E., Gill, T.E., 2002. Environmental characterization of global sources of atmospheric soil dust identified with the Nimbus 7 Total ozone mapping spectrometer (TOMS) absorbing aerosol product. Rev. Geophys. 40 https://doi.org/10.1029/2000RG000095, 2-1-2–31.
Pulido-Villena, E., Reche, I., Morales-Baquero, R., 2008. Evidence of an atmospheric forcing on bacterioplankton and phytoplankton dynamics in a high mountain lake. Aquat. Sci. 70, 1–9. https://doi.org/10.1007/s00027-007-0944-8.
Rabalais, N.N., 2002. Nitrogen in aquatic ecosystems. Ambio 31, 102–112. https://doi.org/10.1579/0044-7447-31.2.102.
Ravishankara, A.R., 1997. Heterogeneous and multiphase chemistry in the troposphere. Science 80-.). 276, 1058–1065. https://doi.org/10.1126/science.276.5315.1058.
Ridame, C., Le Moal, M., Guieu, C., Ternon, E., Biegala, I.C., L'Helguen, S., Pujo-Pay, M., 2011. Nutrient control of N 2 fixation in the oligotrophic Mediterranean Sea and the impact of Saharan dust events. Biogeosciences 8, 2773–2783. https://doi.org/10.5194/bg-8-2773-2011.
Ridame, C., Dekaezemacker, J., Guieu, C., Bonnet, S., L'Helguen, S., Malien, F., 2014. Contrasted Saharan dust events in LNLC environments: impact on nutrient dynamics and primary production. Biogeosciences 11, 4783–4800. https://doi.org/10.5194/bg-11-4783-2014.
Rollins, A.W., Browne, E.C., Min, K.E., Pusede, S.E., Wooldridge, P.J., Gentner, D.R., Goldstein, A.H., Liu, S., Day, D.A., Russell, L.M., Cohen, R.C., 2012. Evidence for NOx control over nighttime SOA formation. Science (80-.). 337, 1210–1212. https://doi.org/10.1126/science.1221520.
Ruacho, A., Richon, C., Whitby, H., Bundy, R.M., 2022. Sources, Sinks, and Cycling of Dissolved Organic Copper Binding Ligands in the Ocean. Earth Environ, Commun. https://doi.org/10.1038/s43247-022-00597-1.
Rubin, M., Berman-Frank, I., Shaked, Y., 2011. Dust-and mineral-iron utilization by the marine dinitrogen-fixer Trichodesmium. Nat. Geosci. 4, 529–534. https://doi.org/10.1038/ngeo1181.
Saini, A., Harner, T., Chinnadhurai, S., Schuster, J.K., Yates, A., Sweetman, A., Aristizabal-Zuluaga, B.H., Jiménez, B., Manzano, C.A., Gaga, E.O., Stevenson, G., Falandysz, J., Ma, J., Miglioranza, K.S.B., Kannan, K., Tominaga, M., Jariyasopit, N., Rojas, N.Y., Amador-Muñoz, O., Sinha, R., Alani, R., Suresh, R., Nishino, T., Shoeib, T., 2020. GAPS-megacities: a new global platform for investigating persistent organic pollutants and chemicals of emerging concern in urban air. Environ. Pollut. 267, 115416 https://doi.org/10.1016/j.envpol.2020.115416.
Schoffman, H., Lis, H., Shaked, Y., Keren, N., 2016. Iron-nutrient interactions within phytoplankton. Front. Plant Sci. 7, 196214 https://doi.org/10.3389/fpls.2016.01223.
Sebastián, M., Arístegui, J., Montero, M.F., Escanez, J., Xavier Niell, F., 2004. Alkaline phosphatase activity and its relationship to inorganic phosphorus in the transition zone of the north-western African upwelling system. Prog. Oceanogr. 62, 131–150. https://doi.org/10.1016/j.pocean.2004.07.007.
Sedwick, P.N., Bernhardt, P.W., Mulholland, M.R., Najjar, R.G., Blumen, L.M., Sohst, B. M., Sookhdeo, C., Widner, B., 2018. Assessing phytoplankton nutritional status and potential impact of wet deposition in seasonally oligotrophic waters of the mid-Atlantic bight. Geophys. Res. Lett. 45, 3203–3211. https://doi.org/10.1002/2017GL075361.
Seinfeld, J.H., Pandis, S.N., 2016. Atmospheric Chemistry and Physics : From Air Pollution to Climate Change, 3rd ed. John Wiley & Sons.
Sepehri, A., Sarrafzadeh, M.H., 2018. Effect of nitrifiers community on fouling mitigation and nitrification efficiency in a membrane bioreactor. Chem. Eng. Process. - Process Intensif. 128, 10–18. https://doi.org/10.1016/j.cep.2018.04.006.
Sepehri, A., Sarrafzadeh, M.H., 2019. Activity enhancement of ammonia-oxidizing bacteria and nitrite-oxidizing bacteria in activated sludge process: metabolite reduction and CO2 mitigation intensification process. Appl Water Sci 9, 1–12. https://doi.org/10.1007/s13201-019-1017-6.
Sepehri, A., Sarrafzadeh, M.H., Avateffazeli, M., 2020. Interaction between Chlorella vulgaris and nitrifying-enriched activated sludge in the treatment of wastewater with low C/N ratio. J. Clean. Prod. 247, 119164 https://doi.org/10.1016/j.jclepro.2019.119164.
Shaked, Y., Xu, Y., Leblanc, K., Morel, F.M.M., 2006. Zinc availability and alkaline phosphatase activity in Emiliania huxleyi: implications for Zn-P co-limitation in the ocean. Limnol. Oceanogr. 51, 299–309. https://doi.org/10.4319/lo.2006.51.1.0299.
Sharma, D., Biswas, H., Panda, P.P., Chowdhury, M., Silori, S., Pandey, M., Kaushik, A., Kumar, A., 2022. Atmospheric dust addition under elevated CO2 restructured phytoplankton community from the Arabian Sea: a microcosm approach. Mar. Chem. 247, 104183 https://doi.org/10.1016/j.marchem.2022.104183.
Sheesley, R.J., Schauer, J.J., Hemming, J.D., Geis, S., Barman, M.A., 2005. Seasonal and spatial relationship of chemistry and toxicity in atmospheric particulate matter using aquatic bioassays. Environ. Sci. Technol. 39, 999–1010. https://doi.org/10.1021/es049873+.
Sheibley, R.W., Enache, M., Swarzenski, P.W., Moran, P.W., Foreman, J.R., 2014. Nitrogen deposition effects on diatom communities in lakes from three national parks in Washington state. Water Air Soil Pollut. 225, 1–23. https://doi.org/10.1007/s11270-013-1857-x.
Shi, J.H., Gao, H.W., Zhang, J., Tan, S.C., Ren, J.L., Liu, C.G., Liu, Y., Yao, X., 2012. Examination of causative link between a spring bloom and dry/wet deposition of Asian dust in the Yellow Sea. China. J. Geophys. Res. Atmos. 117 https://doi.org/10.1029/2012JD017983.
Silva, V., Pereira, J.L., Campos, I., Keizer, J.J., Gonçalves, F., Abrantes, N., 2015. Toxicity assessment of aqueous extracts of ash from forest fires. CATENA 135, 401–408. doi: https://doi.org/10.1016/J.CATENA.2014.06.021.
Simon, N., Cras, A.L., Foulon, E., Lemée, R., 2009. Diversity and evolution of marine phytoplankton. Comptes Rendus - Biol. https://doi.org/10.1016/j.crvi.2008.09.009.
Sinoir, M., Ellwood, M.J., Butler, E.C.V., Bowie, A.R., Mongin, M., Hassler, C.S., 2016. Zinc cycling in the Tasman Sea: distribution, speciation and relation to phytoplankton community. Mar. Chem. 182, 25–37. https://doi.org/10.1016/j.marchem.2016.03.006.
Song, W., Wang, Y.L., Yang, W., Sun, X.C., Tong, Y.D., Wang, X.M., Liu, C.Q., Bai, Z.P., Liu, X.Y., 2019. Isotopic evaluation on relative contributions of major NOx sources to nitrate of PM2.5 in Beijing. Environ. Pollut. 248, 183–190. https://doi.org/10.1016/j.envpol.2019.01.081.
Srinivas, B., Sarin, M.M., 2013. Atmospheric dry-deposition of mineral dust and anthropogenic trace metals to the bay of Bengal. J. Mar. Syst. 126, 56–68. https://doi.org/10.1016/j.jmarsys.2012.11.004.
Srinivas, B., Sarin, M.M., Sarma, V.V.S.S., 2011. Atmospheric dry deposition of inorganic and organic nitrogen to the bay of Bengal: impact of continental outflow. Mar. Chem. 127, 170–179. https://doi.org/10.1016/j.marchem.2011.09.002.
Stuart, R.K., Dupont, C.L., Johnson, D.A., Paulsen, I.T., Palenik, B., 2009. Coastal strains of marine Synechococcus species exhibit increased tolerance to copper shock and a distinctive transcriptional response relative to those of open-ocean strains. Appl. Environ. Microbiol. 75, 5047–5057. https://doi.org/10.1128/AEM.00271-09.
Sutak, R., Botebol, H., Blaiseau, P.L., Léger, T., Bouget, F.Y., Camadro, J.M., Lesuisse, E., 2012. A comparative study of iron uptake mechanisms in marine microalgae: Iron binding at the cell surface is a critical step. Plant Physiol. 160, 2271–2284. https://doi.org/10.1104/pp.112.204156.
Sutherland, J.W., Acker, F.W., Bloomfield, J.A., Boylen, C.W., Charles, D.F., Daniels, R. A., Eichler, L.W., Farrell, J.L., Feranec, R.S., Hare, M.P., Kanfoush, S.L., Preall, R.J., Quinn, S.O., Rowell, H.C., Schoch, W.F., Shaw, W.H., Siegfried, C.A., Sullivan, T.J., Winkler, D.A., Nierzwicki-Bauer, S.A., 2015. Brooktrout Lake case study: biotic recovery from acid deposition 20 years after the 1990 clean air act amendments. Environ. Sci. Technol. 49, 2665–2674. https://doi.org/10.1021/es5036865.
Suzumura, M., Hashihama, F., Yamada, N., Kinouchi, S., 2012. Dissolved phosphorus pools and alkaline phosphatase activity in the euphotic zone of the western North Pacific Ocean. Front. Microbiol. 3, 19995. https://doi.org/10.3389/fmicb.2012.00099.
Swackhamer, Paerl, H., Eisenreich, S., Hurley, J., Hornbuckle, K., McLachlan, M., Mount, D., Muir, D., Schindler, D., 2004. Impacts of atmospheric pollutant on aquatic ecosystems. Issues Ecol. 12.
Tan, S., Cheung, S., Ho, T.Y., Liu, H., 2019. Metatranscriptomics of the bacterial community in response to atmospheric deposition in the Western North Pacific Ocean. Mar. Genomics 45, 57–63. https://doi.org/10.1016/j.margen.2019.01.008.
Tao, Y., Murphy, J.G., 2019. The mechanisms responsible for the interactions among oxalate, pH, and Fe dissolution in PM2.5. ACS Earth Sp. Chem. 3, 2259–2265. https://doi.org/10.1021/acsearthspacechem.9b00172.
Te Chien, C., Mackey, K.R.M., Dutkiewicz, S., Mahowald, N.M., Prospero, J.M., Paytan, A., 2016. Effects of African dust deposition on phytoplankton in the western tropical Atlantic Ocean off Barbados. Global Biogeochem. Cycles 30, 716–734. https://doi.org/10.1002/2015GB005334.
Thomas, S.A., Cebrian, J., 2008. Ecosystem patterns and processes. In: Encyclopedia of Ecology, Five-Volume Set. Elsevier Inc., pp. 1139–1148. https://doi.org/10.1016/B978-008045405-4.00308-6
Thorpe, A., Harrison, R.M., 2008. Sources and properties of non-exhaust particulate matter from road traffic: a review. Sci. Total Environ. 400, 270–282. https://doi.org/10.1016/j.scitotenv.2008.06.007.
Timmermans, K.R., Davey, M.S., Van der Wagt, B., Snoek, J., Geider, R.J., Veldhuis, M.J. W., Gerringa, L.J.A., De Baar, H.J.W., 2001. Co-limitation by iron and light of Chaetoceros brevis, C. Dichaeta and C. Calcitrans (Bacillariophyceae). Mar. Ecol. Prog. Ser. 217, 287–297. https://doi.org/10.3354/MEPS217287.
Tovar, A., Moreno, C., Mánuel-Vez, M.P., García-Vargas, M., 2002. A simple automated method for the speciation of dissolved inorganic nitrogen in seawater. Anal. Chim. Acta 469, 235–242. https://doi.org/10.1016/S0003-2670(02)00752-3.

Uematsu, M., Duce, R.A., Prospero, J.M., 1985. Deposition of atmospheric mineral particles in the North Pacific Ocean. J. Atmos. Chem. 3, 123–138. https://doi.org/10.1007/BF00049372.

Uematsu, M., Toratani, M., Kajino, M., Narita, Y., Senga, Y., Kimoto, T., 2004. Enhancement of primary productivity in the western North Pacific caused by the eruption of the Miyake-jima volcano. Geophys. Res. Lett. 31 https://doi.org/10.1029/2003GL018790.

Van Damme, M., Clarisse, L., Franco, B., Sutton, M.A., Erisman, J.W., Wichink Kruit, R., Van Zanten, M., Whitburn, S., Hadji-Lazaro, J., Hurtmans, D., Clerbaux, C., Coheur, P.F. ois, 2021. Global, regional and national trends of atmospheric ammonia derived from a decadal (2008-2018) satellite record. Environ. Res. Lett. doi:https://doi.org/10.1088/1748-9326/abd5e0.

Veres, P.R., Andrew Neuman, J., Bertram, T.H., Assaf, E., Wolfe, G.M., Williamson, C.J., Weinzierl, B., Tilmes, S., Thompson, C.R., Thames, A.B., Schroder, J.C., Saiz-Lopez, A., Rollins, A.W., Roberts, J.M., Price, D., Peischl, J., Nault, B.A., Møller, K.H., Miller, D.O., Meinardi, S., Li, Q., Lamarque, J.F., Kupc, A., Kjaergaard, H.G., Kinnison, D., Jimenez, J.L., Jernigan, C.M., Hornbrook, R.S., Hills, A., Dollner, M., Day, D.A., Cuevas, C.A., Campuzano-Jost, P., Burkholder, J., Paul Bui, T., Brune, W. H., Brown, S.S., Brock, C.A., Bourgeois, I., Blake, D.R., Apel, E.C., Ryerson, T.B., 2020. Global airborne sampling reveals a previously unobserved dimethyl sulfide oxidation mechanism in the marine atmosphere. Proc. Natl. Acad. Sci. U. S. A. 117, 4505–4510. https://doi.org/10.1073/pnas.1919344117.

Vicars, W.C., Sickman, J.O., Ziemann, P.J., 2010. Atmospheric phosphorus deposition at a montane site: size distribution, effects of wildfire, and ecological implications. Atmos. Environ. 44, 2813–2821. https://doi.org/10.1016/j.atmosenv.2010.04.055.

Violaki, K., Bourrin, F., Aubert, D., Kouvarakis, G., Delsaut, N., Mihalopoulos, N., 2018. Organic phosphorus in atmospheric deposition over the Mediterranean Sea: An important missing piece of the phosphorus cycle. Prog. Oceanogr. 163, 50–58. https://doi.org/10.1016/j.pocean.2017.07.009.

Visser, F., Gerringa, L.J.A., Van Der Gaast, S.J., De Baar, H.J.W., Timmermans, K.R., 2003. The role of the reactivity and content of iron of aerosol dust on growth rates of two Antarctic diatom species. J. Phycol. 39, 1085–1094. https://doi.org/10.1111/j.0022-3646.2003.03-023.x.

Volta, A., Sforzini, S., Camurati, C., Teoldi, F., Maiorana, S., Croce, A., Benfenati, E., Perricone, G., Lodi, M., Viarengo, A., 2020. Ecotoxicological effects of atmospheric particulate produced by braking systems on aquatic and edaphic organisms. Environ. Int. 137, 105564 https://doi.org/10.1016/j.envint.2020.105564.

Wang, R., Balkanski, Y., Boucher, O., Bopp, L., Chappell, A., Ciais, P., Hauglustaine, D., Peñuelas, J., Tao, S., 2015a. Sources, transport and deposition of iron in the global atmosphere. Atmos. Chem. Phys. 15, 6247–6270. https://doi.org/10.5194/acp-15-6247-2015.

Wang, Rong, Balkanski, Y., Boucher, O., Ciais, P., Peñuelas, J., Tao, S., 2015b. Significant contribution of combustion-related emissions to the atmospheric phosphorus budget. Nat. Geosci. 8, 48–54. https://doi.org/10.1038/ngeo2324.

Wang, F.J., Chen, Y., Guo, Z.G., Gao, H.W., Mackey, K.R., Yao, X.H., Zhuang, G.S., Paytan, A., 2017. Combined effects of iron and copper from atmospheric dry deposition on ocean productivity. Geophys. Res. Lett. 44, 2546–2555. https://doi.org/10.1002/2016GL072349.

Wang, W., Yu, J., Cui, Y., He, J., Xue, P., Cao, W., Ying, H., Gao, W., Yan, Y., Hu, B., Xin, J., Wang, L., Liu, Z., Sun, Y., Ji, D., Wang, Y., 2018. Characteristics of fine particulate matter and its sources in an industrialized coastal city, Ningbo, Yangtze River Delta. China. Atmos. Res. 203, 105–117. https://doi.org/10.1016/j.atmosres.2017.11.033.

Wang, W., Zhang, H., Chen, H., Zhuang, Y., Huang, Y., Liu, G., 2019. Effects of Asian dust input on eukaryotic phytoplankton community structure in the open areas in the northwestern Pacific Ocean. Mar. Biol. Res. 15, 49–60. https://doi.org/10.1080/17451000.2019.1588981.

Wang, Yonghong, Gao, W., Wang, S., Song, T., Gong, Z., Ji, D., Wang, L., Liu, Z., Tang, G., Huo, Y., Tian, S., Li, J., Li, M., Yang, Y., Chu, B., Petäjä, T., Kerminen, V.M., He, H., Hao, J., Kulmala, M., Wang, Yuesi, Zhang, Y., 2020. Contrasting trends of PM2.5and surface-ozone concentrations in China from 2013 to 2017. Natl. Sci. Rev. 7, 1331–1339. https://doi.org/10.1093/nsr/nwaa032.

Wang, Q., Zhang, C., Jin, H., Chen, Y., Yao, X., Gao, H., 2022. Effect of anthropogenic aerosol addition on phytoplankton growth in coastal waters: role of enhanced phosphorus bioavailability. Front. Microbiol. 13, 2029. https://doi.org/10.3389/fmicb.2022.915255.

Weathers, K.C., Ponette-González, A.G., 2011. Atmospheric Deposition. Springer, Dordrecht, pp. 357–370. https://doi.org/10.1007/978-94-007-1363-5_17.

Wik, A., Nilsson, E., Källqvist, T., Tobiesen, A., Dave, G., 2009. Toxicity assessment of sequential leachates of tire powder using a battery of toxicity tests and toxicity identification evaluations. Chemosphere 77, 922–927. https://doi.org/10.1016/j.chemosphere.2009.08.034.

Wright, L.P., Zhang, L., Cheng, I., Aherne, J., Wentworth, G.R., 2018. Impacts and Effects Indicators of Atmospheric Deposition of Major Pollutants to Various Ecosystems-a Review. Res, Aerosol Air Qual. https://doi.org/10.4209/aaqr.2018.03.0107.

Wu, C., Wang, G., Li, Jin, Li, Jianjun, Cao, C., Ge, S., Xie, Y., Chen, J., Liu, S., Du, W., Zhao, Z., Cao, F., 2020. Non-agricultural sources dominate the atmospheric NH3 in Xi'an, a megacity in the semi-arid region of China. Sci. Total Environ. 722, 137756 https://doi.org/10.1016/j.scitotenv.2020.137756.

Xie, X., Hu, J., Qin, M., Guo, S., Hu, M., Wang, H., Lou, S., Li, J., Sun, J., Li, X., Sheng, L., Zhu, J., Chen, G., Yin, J., Fu, W., Huang, C., Zhang, Y., 2022. Modeling particulate nitrate in China: current findings and future directions. Environ. Int. https://doi.org/10.1016/j.envint.2022.107369.

Xin, X., Huang, G., An, C., Weger, H., Cheng, G., Shen, J., Rosendahl, S., 2019. Analyzing the biochemical alteration of Green algae during chronic exposure to Triclosan based on synchrotron-based Fourier transform infrared Spectromicroscopy. Anal. Chem. 91, 7798–7806. https://doi.org/10.1021/acs.analchem.9b01417.

Xin, X., Chen, B., Péquin, B., Song, P., Yang, M., Song, X., Zhang, B., 2022. Binary toxicity of polystyrene nanoplastics and polybrominated diphenyl ethers to Arctic Cyanobacteria under ambient and future climates. Water Res. 226, 119188 https://doi.org/10.1016/j.watres.2022.119188.

Xin, K., Chen, J., Soyol-Erdene, T.O., 2023. Formation mechanism and source apportionment of nitrate in atmospheric aerosols. APN Sci. Bull. 2023, 102–111. https://doi.org/10.30852/SB.2023.2225.

Yadav, K., Sarma, V.V.S.S., Rao, D.B., Kumar, M.D., 2016. Influence of atmospheric dry deposition of inorganic nutrients on phytoplankton biomass in the coastal bay of Bengal. Mar. Chem. 187, 25–34. https://doi.org/10.1016/j.marchem.2016.10.004.

Yang, T., Chen, Y., Zhou, S., Li, H., 2019. Impacts of aerosol copper on marine phytoplankton: a review. Atmosphere (Basel). https://doi.org/10.3390/atmos10070414.

Yang, J., Ma, L., He, X., Au, W.C., Miao, Y., Wang, W.X., Nah, T., 2023. Measurement report: abundance and fractional solubilities of aerosol metals in urban Hong Kong - insights into factors that control aerosol metal dissolution in an urban site in South China. Atmos. Chem. Phys. 23, 1403–1419. https://doi.org/10.5194/acp-23-1403-2023.

Ye, Y., Zhan, H., Yu, X., Li, J., Wang, X., Xie, Z., 2021. Detection of organosulfates and nitrooxy-organosulfates in Arctic and Antarctic atmospheric aerosols, using ultra-high resolution FT-ICR mass spectrometry. Sci. Total Environ. 767, 144339 https://doi.org/10.1016/j.scitotenv.2020.144339.

Ye, C., Lu, K., Song, H., Mu, Y., Chen, J., Zhang, Y., 2023. A critical review of sulfate aerosol formation mechanisms during winter polluted periods. J. Environ. Sci. 123, 387–399. https://doi.org/10.1016/J.JES.2022.07.011.

Yong, S.C., Roversi, P., Lillington, J., Rodriguez, F., Krehenbrink, M., Zeldin, O.B., Garman, E.F., Lea, S.M., Berks, B.C., 2014. A complex iron-calcium cofactor catalyzing phosphotransfer chemistry. Science 80-.). 345, 1170–1173. https://doi.org/10.1126/science.1254237.

Yung, M.M.N., Wong, S.W.Y., Kwok, K.W.H., Liu, F.Z., Leung, Y.H., Chan, W.T., Li, X.Y., Djurišić, A.B., Leung, K.M.Y., 2015. Salinity-dependent toxicities of zinc oxide nanoparticles to the marine diatom Thalassiosira pseudonana. Aquat. Toxicol. 165, 31–40. https://doi.org/10.1016/j.aquatox.2015.05.015.

Zaghloul, A., Saber, M., Gadow, S., Awad, F., 2020. Biological indicators for pollution detection in terrestrial and aquatic ecosystems. Bull. Natl. Res. Cent. 44, 1–11. https://doi.org/10.1186/s42269-020-00385-x.

Zak, D., Hupfer, M., Cabezas, A., Jurasinski, G., Audet, J., Kleeberg, A., McInnes, R., Kristiansen, S.M., Petersen, R.J., Liu, H., Goldhammer, T., 2021. Sulphate in freshwater ecosystems: a review of sources, biogeochemical cycles, ecotoxicological effects and bioremediation. Earth-Science Rev. https://doi.org/10.1016/j.earscirev.2020.103446.

Zeb, B., Alam, K., Ditta, A., Ullah, S., Ali, H.M., Ibrahim, M., Salem, M.Z.M., 2022. Variation in coarse particulate matter (PM10) and its characterization at multiple locations in the semiarid region. Front. Environ. Sci. 10, 36. https://doi.org/10.3389/fenvs.2022.843582.

Zhai, S., Yang, L., Hu, W., 2009. Observations of atmospheric nitrogen and phosphorus deposition during the period of algal bloom formation in northern lake taihu. China. Environ. Manage. 44, 542–551. https://doi.org/10.1007/s00267-009-9334-4.

Zhang, Q., Jimenez, J.L., Canagaratna, M.R., Allan, J.D., Coe, H., Ulbrich, I., Alfarra, M. R., Takami, A., Middlebrook, A.M., Sun, Y.L., Dzepina, K., Dunlea, E., Docherty, K., DeCarlo, P.F., Salcedo, D., Onasch, T., Jayne, J.T., Miyoshi, T., Shimono, A., Hatakeyama, S., Takegawa, N., Kondo, Y., Schneider, J., Drewnick, F., Borrmann, S., Weimer, S., Demerjian, K., Williams, P., Bower, K., Bahreini, R., Cottrell, L., Griffin, R.J., Rautiainen, J., Sun, J.Y., Zhang, Y.M., Worsnop, D.R., 2007. Ubiquity and dominance of oxygenated species in organic aerosols in anthropogenically-influenced northern hemisphere midlatitudes. Geophys. Res. Lett. 34 https://doi.org/10.1029/2007GL029979.

Zhang, Y., Mahowald, N., Scanza, R.A., Journet, E., Desboeufs, K., Albani, S., Kok, J.F., Zhuang, G., Chen, Y., Cohen, D.D., Paytan, A., Patey, M.D., Achterberg, E.P., Engelbrecht, J.P., Fomba, K.W., 2015. Modeling the global emission, transport and deposition of trace elements associated with mineral dust. Biogeosciences 12, 5771–5792. https://doi.org/10.5194/bg-12-5771-2015.

Zhang, C., Gao, H., Yao, X., Shi, Z., Shi, J., Yu, Y., Meng, L., Guo, X., 2018. Phytoplankton growth response to Asian dust addition in the Northwest Pacific Ocean versus the Yellow Sea. Biogeosciences 15, 749–765. https://doi.org/10.5194/bg-15-749-2018.

Zhang, C., Ito, A., Shi, Z., Aita, M.N., Yao, X., Chu, Q., Shi, J., Gong, X., Gao, H., 2019a. Fertilization of the Northwest Pacific Ocean by East Asia air pollutants. Global Biogeochem. Cycles 33, 690–702. https://doi.org/10.1029/2018GB006146.

Zhang, C., Yao, X., Chen, Y., Chu, Q., Yu, Y., Shi, J., Gao, H., 2019b. Variations in the phytoplankton community due to dust additions in eutrophication, LNLC and HNLC oceanic zones. Sci. Total Environ. 669, 282–293. https://doi.org/10.1016/j.scitotenv.2019.02.068.

Zhang, J., Peng, J., Song, C., Ma, C., Men, Z., Wu, J., Wu, L., Wang, T., Zhang, X., Tao, S., Gao, S., Hopke, P.K., Mao, H., 2020. Vehicular non-exhaust particulate emissions in Chinese megacities: source profiles, real-world emission factors, and inventories. Environ. Pollut. 266, 115268 https://doi.org/10.1016/j.envpol.2020.115268.

Zhang, C., Chu, Q., Yingchun, M., Yao, X., Gao, H., 2022. Weakened fertilization impact of anthropogenic aerosols on marine phytoplankton—a comparative analysis of dust and haze particles. Ecotoxicol. Environ. Saf. 230, 113162 https://doi.org/10.1016/J.ECOENV.2022.113162.

Zhong, Q., Shen, H., Yun, X., Chen, Y., Ren, Y., Xu, H., Shen, G., Du, W., Meng, J., Li, W., Ma, J., Tao, S., 2020. Global sulfur dioxide emissions and the driving forces. Environ. Sci. Technol. 54, 6508–6517. https://doi.org/10.1021/acs.est.9b07696.

Zhou, W., Li, Q.P., Wu, Z., 2021a. Coastal phytoplankton responses to atmospheric deposition during summer. Limnol. Oceanogr. 66, 1298–1315. https://doi.org/10.1002/lno.11683.

Zhou, Y., Yang, X., Wang, Y., Li, F., Wang, J., Tan, L., 2021b. Exogenous nutrient inputs restructure phytoplankton community and ecological stoichiometry of eastern Indian Ocean. Ecol. Indic. 127, 107801 https://doi.org/10.1016/j.ecolind.2021.107801.

Zhu, H., Chen, Y., Zhao, Y., Zhang, L., Zhang, X., Zheng, B., Liu, L., Pan, Y., Xu, W., Liu, X., 2022. The response of nitrogen deposition in China to recent and future changes in anthropogenic emissions. J. Geophys. Res. Atmos. 127, e2022JD037437 https://doi.org/10.1029/2022JD037437.

Zou, J., Liu, Z., Hu, B., Huang, X., Wen, T., Ji, D., Liu, J., Yang, Y., Yao, Q., Wang, Y., 2018. Aerosol chemical compositions in the North China plain and the impact on the visibility in Beijing and Tianjin. Atmos. Res. 201, 235–246. https://doi.org/10.1016/j.atmosres.2017.09.014.

Zhu, Z.L., Wang, S.C., Zhao, F.F., Wang, S.G., Liu, F.F., Liu, G.Z., 2019. Joint toxicity of microplastics with triclosan to marine microalgae Skeletonema costatum. Environ. Pollut. 246, 509–517. https://doi.org/10.1016/j.envpol.2018.12.044.